2-20-1970

Volcanic Rocks Associated with the Western Part of the Mogollon Plateau Volcano-tectonic Complex, Southwestern New Mexico

Rodney Charles Rhodes

Recommended Citation

Rhodes, Rodney Charles. "Volcanic Rocks Associated with the Western Part of the Mogollon Plateau Volcano-tectonic Complex, Southwestern New Mexico." (1970). https://digitalrepository.unm.edu/eps_etds/265

VOLCANIC ROCKS
OF THE
MOGOLLON
PLATEAU

RHODES

THE UNIVERSITY OF NEW MEXICO
ALBUQUERQUE, NEW MEXICO 87106

Policy on Use of Theses and Dissertations

Unpublished theses and dissertations accepted for master's and doctor's degrees and deposited in the University of New Mexico Library are open to the public for inspection and reference work. *They are to be used only with due regard to the rights of the authors.* The work of other authors should always be given full credit. Avoid quoting in amounts, over and beyond scholarly needs, such as might impair or destroy the property rights and financial benefits of another author.

To afford reasonable safeguards to authors, and consistent with the above principles, anyone quoting from theses and dissertations must observe the following conditions:

1. Direct quotations during the first two years after completion may be made only with the written permission of the author.
2. After a lapse of two years, theses and dissertations may be quoted without specific prior permission in works of original scholarship provided appropriate credit is given in the case of each quotation.
3. Quotations that are complete units in themselves (e.g., complete chapters or sections) in whatever form they may be reproduced and quotations of whatever length presented as primary material for their own sake (as in anthologies or books of readings) ALWAYS require consent of the authors.
4. The quoting author is responsible for determining "fair use" of material he uses.

This thesis/dissertation by Rodney Charles Rhodes has been used by the following persons whose signatures attest their acceptance of the above conditions. (A library which borrows this thesis/dissertation for use by its patrons is expected to secure the signature of each user.)

NAME AND ADDRESS	DATE
E. L. Du Bois, Jr. Box 159 De Vargas Hall, UNM	10/19/70
Richard L. Burroughs, Geol. Dept Adams State College Alamosa, Colo	9/2/71
Durga Rimal, Nord Resources, ALBQ NM	3/15/72
Randol L. Arnold. Geol. Dept UTEP - El Paso Tex.	11/15/73
Jacquelin Backer, NMSU Las Cruces	12/29/73
[illegible] Connerdi, Waterloo	3/6/75
Allen Dart, Museum of New Mexico, Santa Fe	4/4/77

Oct. 1968—1,000—GS

This dissertation, directed and approved by the candidate's committee, has been accepted by the Graduate Committee of The University of New Mexico in partial fulfillment of the requirements for the degree of

DOCTOR OF PHILOSOPHY

Title
VOLCANIC ROCKS ASSOCIATED WITH THE WESTERN
PART OF THE MOGOLLON PLATEAU VOLCANO-
TECTONIC COMPLEX, SOUTHWESTERN NEW MEXICO

RODNEY CHARLES RHODES
Candidate

GEOLOGY
Department

David T. Benedetti
Dean

20 February 1970
Date

Committee

Wolfgang E. Elston
Chairman

Lee A. Woodward

Albert M. Kudo

VOLCANIC ROCKS ASSOCIATED WITH THE WESTERN PART OF THE MOGOLLON PLATEAU VOLCANO-TECTONIC COMPLEX, SOUTHWESTERN NEW MEXICO

BY
RODNEY CHARLES RHODES
B.Sc.(Hons.), University of Natal, 1964
M.Sc., University of Natal, 1966

DISSERTATION

Submitted in Partial Fulfillment of the
Requirements for the Degree of
Doctor of Philosophy in Geology
in the Graduate School of
The University of New Mexico
Albuquerque, New Mexico
January, 1970

4

VOLCANIC ROCKS ASSOCIATED WITH THE WESTERN PART OF THE MOGOLLON PLATEAU VOLCANO-TECTONIC COMPLEX, SOUTHWESTERN NEW MEXICO

BY
RODNEY CHARLES RHODES

ABSTRACT OF DISSERTATION

Submitted in Partial Fulfillment of the
Requirements for the Degree of
Doctor of Philosophy in Geology
in the Graduate School of
The University of New Mexico
Albuquerque, New Mexico
January, 1970

5

ABSTRACT

An area of approximately 450 square miles was mapped on a reconnaissance basis, covering part of the western half of the Mogollon Plateau volcano-tectonic complex. This report deals with the geology of the area and its relationship to the regional volcano-tectonic structure of the Mogollon Plateau.

Over 10,000 feet of Tertiary volcanic rocks crop out and have been grouped into the Lower, Middle, and Upper Volcanic Groups. The oldest rocks comprise the Lower Volcanic Group and consist of quartz latite ash-flow tuffs and basaltic andesite lava flows. Flow direction studies indicate that these rocks flowed in a northeasterly direction from a source area lying southwest of the Mogollon Plateau. The Middle Volcanic Group includes two major ash-flow sheets and associated rhyolite lava flows. Within the mapped area the ash flows are restricted to their source cauldrons where they are very thick and display vertical compositional zoning. Quartz latite lava flows were extruded around the margins of one of the cauldrons and appear to represent defluidized residue of the ash-flow magma. Large arcuate bodies of rhyolite lavas are genetically related to the ash-flow tuffs and in part outline the Mogollon Plateau volcano-tectonic structure. Unconformably overlying the Middle Volcanic Group are rocks of the Upper Volcanic Group, including felsic

ash-flow and ash-fall tuffs, and lava flows ranging in composition from latite to basaltic andesite. Three eruptive centers were recognized in the mapped area, forming vents for much of the younger lava flows.

Rocks in general become progressively younger from the rim to the center of the volcano-tectonic depression. The rim is uplifted into a broad anticlinorium and several transverse warps, radial to the central depression, were found. Mineralization is controlled by post-volcanic warping and faulting. The rim of the Mogollon Plateau is flanked by an outer graben filled with late Tertiary sediments derived from uplifted areas. The basinward side of the rim consists of deeply incised pediment surfaces sloping toward the center of the volcano-tectonic depression and blanketed with pediment gravels.

7

CONTENTS

CONTENTS (contd.)

ILLUSTRATIONS

FIGURES

page

10

FIGURES (contd.)

TABLES

TABLES (contd.)

PLATES

PLATES (contd.)

B1

PLATES (contd.)

VOLCANIC ROCKS ASSOCIATED WITH THE WESTERN PART OF THE MOGOLLON PLATEAU VOLCANO-TECTONIC COMPLEX, SOUTHWESTERN NEW MEXICO

INTRODUCTION

PURPOSE AND SCOPE

This study was undertaken to determine the stratigraphy and structure of the volcanic rocks forming part of the western rim of the Mogollon Plateau, and to investigate their relationship with the rocks occupying the central part of the Mogollon Plateau volcano-tectonic depression.

METHODS OF INVESTIGATION

Approximately 450 square miles were mapped on a reconnaissance basis during the summers of 1967 and 1968. As most of the area lies within the Gila Wilderness, field work was done on foot and occasionally on horseback. Mapping was done on advance proofs of 1:24000 U.S.G.S. topographic maps which were subsequently reduced to 1:72000 in order to compile the final geologic map.

Laboratory studies include petrographic examination of about 240 thin sections, universal stage measurements on twinned plagioclase crystals, X-ray diffraction of heat-treated sanidine, statistical analysis of parameters of zircon crystals, and flow direction studies using microscopic techniques.

LOCATION AND ACCESSIBILITY

The area mapped lies within the Gila National Forest in Catron and Grant Counties, southwestern New Mexico, between longitudes 108°20'W and 109°00'W and latitudes 33°10'N and 33°25'N (Plate 1). Population is centered in the villages of Glenwood and Pleasanton, and a few ranches are located in the San Francisco Valley. U. S. Highway 180 follows the San Francisco Valley, and New Mexico Highway 78 runs in an easterly direction close to the northern border of the area. Other roads in the San Francisco Valley are of graded dirt and include a few unimproved jeep tracks which frequently become impassable in wet weather.

Forest service cabins are located within the Gila Wilderness at Holt Mountain, Apache Spring, Little Creek, and White Creek, and cabins with fire-lookout towers on Grouse Mountain and Mogollon Baldy. A few privately owned cabins lie within the wilderness.

CLIMATE AND VEGETATION

The climate of the San Francisco Valley is semi-arid, with average precipitation increasing with elevation from approximately 12 to 28 inches per year, the maximum falling in summer. High peaks of the Mogollon Range are snow-covered during winter. Vegetation is typical of life zones between Upper Sonoran and Hudsonian.

PREVIOUS GEOLOGIC WORK

Prior to the present investigation the area was mapped by Weber and Willard (1959a) and Willard, Weber, and Kuellmer (1961) as part of thirty-minute quadrangle reconnaissance surveys. The resulting maps adequately show the distribution of volcanic and sedimentary rocks, and subdivide the volcanics into broad lithologic groups, but no attempt was made to establish a formational stratigraphic column or to delineate volcano-tectonic structures. As a result the geologic map of New Mexico (Dane and Bachman, 1965) that is based on this and other reconnaissance work presents an inadequate representation of the geology of the Mogollon Plateau (Elston, 1968).

The Mogollon mining district was mapped by Ferguson (1927) who established and described the volcanic stratigraphy of the area. Subsequent work has shown this stratigraphic column to be incomplete, lacking both the major ash-flow sheets present in the Bursum and Gila Cliff Dwellings cauldrons. Recent work in the western part of the Mogollon Plateau has been done mainly by Peter J. Coney (personal communication and unpublished data) who mapped a narrow strip along Highway 78 from Mogollon to Willow Creek. Coney extended many of Ferguson's units across the Mogollon Range, and recognized several additional formations not represented in the Mogollon mining district. Reconnaissance traverses through many parts of the Mogollon Plateau by Wolfgang E. Elston enabled him to interpret the broad volcano-tectonic framework of the complex. The results of his work were summarized in a series of publications

(Elston, 1960a; 1960b; 1965a; 1965b; 1965c; 1968). In addition a brief summary of the stratigraphy of the Mogollon Range was published (Rhodes, 1968). A preliminary report on the geologic structure and petrology of the Mogollon Plateau province, with a geologic cross-section from the San Francisco Valley to Black Mountain, was given by Elston, Coney, and Rhodes (1968).

Some areas outside the Mogollon Plateau complex have been studied in detail and a summary of the literature is given by Elston (1968). Maps with accompanying geologic reports include those of Jicha (1954), Kuellmer (1954), and Elston (1957) in the Mimbres Valley and Black Range to the south, Jones, Hernon, and Moore (1967) at Santa Rita, Stearns (1962) in the San Augustin Plains to the north, Givens (1957) and Tonking (1957) in the Datil province north of the San Augustin Plains, and Wargo (1959a) to the west of the Mogollon Plateau.

Mining claims in northwestern Grant County were described by Gillerman (1964) and some aspects of the Gila Conglomerate in the San Francisco Valley were discussed by Heindl (1962). General stratigraphic relations between volcanic rocks in southwestern New Mexico were discussed by Wargo (1959b).

ACKNOWLEDGMENTS

I wish to thank my advisor, Prof. Wolfgang E. Elston, who suggested the topic and guided the project from its inception. Field and laboratory work was financed by Prof. Elston through NASA Grant NGL-32-004-011 and aid was also

obtained during the academic year 1968-69 in the form of a University of New Mexico Fellowship.

Thanks are due to the faculty and students of the Department of Geology, University of New Mexico, who offered encouragement and criticism during the research. Grateful acknowledgment is made especially to Prof. A. M. Kudo for his invaluable assistance in many aspects of the laboratory work; to Prof. L. A. Woodward for his constructive criticism of the manuscript; to Mr. Thomas R. Fisher, field assistant during the summer of 1967; to Mr. Wayne R. Sigleo, field assistant in 1968; and to Mr. Ronald P. Geitgey and Dr. Peter J. Coney, with whom many pleasant days were spent in the field. I would like to thank also Messrs. J. C. Rattė and D. R. Gaskill of the U. S. Geological Survey for valuable suggestions concerning stratigraphy and structure of the Mogollon Range.

Technical assistance in the laboratory was rendered by Mr. Don Power and Mr. Joe Sanchez. Finally, special thanks are due to my wife who typed the manuscript and helped in many ways.

PHYSIOGRAPHY AND GEOMORPHOLOGY

ALTITUDE AND RELIEF

Elevations in the Mogollon Range are the highest in southwestern New Mexico. Individual peaks include Whitewater Baldy (10,892 ft.), Willow Mountain (10,780 ft.), Mogollon Baldy (10,778 ft.), and Grouse Mountain (10,132 ft.). Elevations in the Jerky and Diablo Mountains are lower, with only Lilley Mountain and Granite Peak exceeding 9,000 feet. Brushy Mountain, west of Glenwood, is 7,400 feet high. Lowest elevations are in the San Francisco Valley which descends to 4,600 feet in the south of the area.

Relief is considerable as rivers draining the Mogollon Range have cut canyons over 2,000 feet below adjacent mountain tops. In contrast to the rugged western side the eastern slopes descend in a series of smooth pediment surfaces toward the center of the Gila Basin. River valleys have incised several hundred feet below these pediments whereas the Jerky and Diablo Mountains rise abruptly above them (Plate 2). Relief is subdued in the San Francisco Valley west of the Mogollon Range, but Brushy Mountain rises steeply from the western side of the valley.

DRAINAGE

The area mapped lies west of the continental divide and is drained by the headwaters of the Gila River and its

tributary, the San Francisco. The San Francisco River flows in a southerly direction through a structural valley on the west side of the Mogollon Range, then turns sharply toward the west at a point just north of the Catron-Grant county line, and enters Arizona. Short intermittent mountain streams flowing in deep, steep-sided canyons drain into the San Francisco from the steep western flanks of the Mogollon Range, the chief among them being Whitewater, Big Dry, and Mogollon Creeks. Drainage east of the Mogollon Range is by the headwaters of the Gila River which are incised up to 800 feet below a flat pediment surface. The drainage divide between the eastward-flowing headwaters of the Gila and the westward-flowing tributaries of the San Francisco follows the crest of the Mogollon and Diablo Mountains.

Structural control over drainage patterns is well marked in the Mogollon Range. The most prominent structural feature in the area is the Mogollon Range fault separating the uplifted block of the Mogollon Range from the outer sediment-filled graben, and several streams (e.g. Whitewater and Big Dry Creeks) flow through spectacular box-canyons at the mountain front. Mogollon Creek changes direction abruptly as it approaches the border-fault and flows in a southeasterly direction parallel to the front of the range.

PEDIMENTS AND TERRACES

The San Francisco Valley west of the Mogollon Range is

characterized by at least three well-developed pediment surfaces cut into Gila Conglomerate and covered with a veneer of Pleistocene gravel, the highest surface giving rise to Whitewater and Sacaton Mesas. A similar pattern of three graded surfaces sloping toward the centers of valleys has been reported from southeastern Arizona (Heindl, 1952, p. 114). Similar gravel-covered pediments slope gently eastward from the Mogollon Range toward the center of the Gila Basin. West Fork Gila River is incised several hundred feet below this surface and a bedrock terrace is intermittently developed along the river about 20 feet above the present river level.

A well-defined erosion bench occurs at an altitude of approximately 7,000 feet in the Mogollon mining district and was described by Ferguson (1927, p. 4). It becomes indistinct south of Whitewater Creek but surfaces at a comparable elevation occur on the north flanks of Sheridan Mountain and between Rain and Mogollon Creeks. These may be equivalent in age to the erosional bench around Mogollon.

TOPOGRAPHIC EXPRESSION OF THE MOGOLLON PLATEAU

The physiographic entity of the Mogollon Plateau was first recognized by Gilbert (1875, p. 530) who described a central basin surrounded by an arcuate mountain range on the west side. Recently Trauger (1965) gave the name "Gila Sag" to this central depression, and Elston (1965a, p. 823) described the Mogollon Plateau as "... a volcano-tectonic basin with a

raised rim, roughly circular in plan, and 90 miles in diameter." The central depression forms the drainage basin of the headwaters of the Gila River which flows westward through a deep canyon cut into the southwest rim of the structure.

Is the topography of the Mogollon Plateau a result of Quaternary river erosion or is it a reflection of the underlying geology and not merely an erosional feature? In order to reconstruct the original physiography by erasing the effects of Quaternary valley incision, a topographic envelope with a contour interval of 1,000 feet has been drawn for the Mogollon Plateau (Fig. 1), having control points spaced six miles apart. The resulting map shows the arcuate mountain ranges forming the rim and the central closed basin around Gila Hot Springs. The outer graben is defined in the west and northwest, and the San Augustin Plains cut across the northern rim of the structure. A subsidiary, partly enclosed basin is present in the northeast, just north of the Catron-Sierra county line.

Known and inferred late Tertiary basaltic centers have been plotted on Fig. 1 to establish their relationship to the volcano-tectonic structure. These basaltic centers correspond to the highest parts of the rim in several places in the north and west and also form the central peak of the volcano-tectonic complex. Highest parts of the rim often consist of basaltic centers superimposed upon flow-banded rhyolite domes.

11

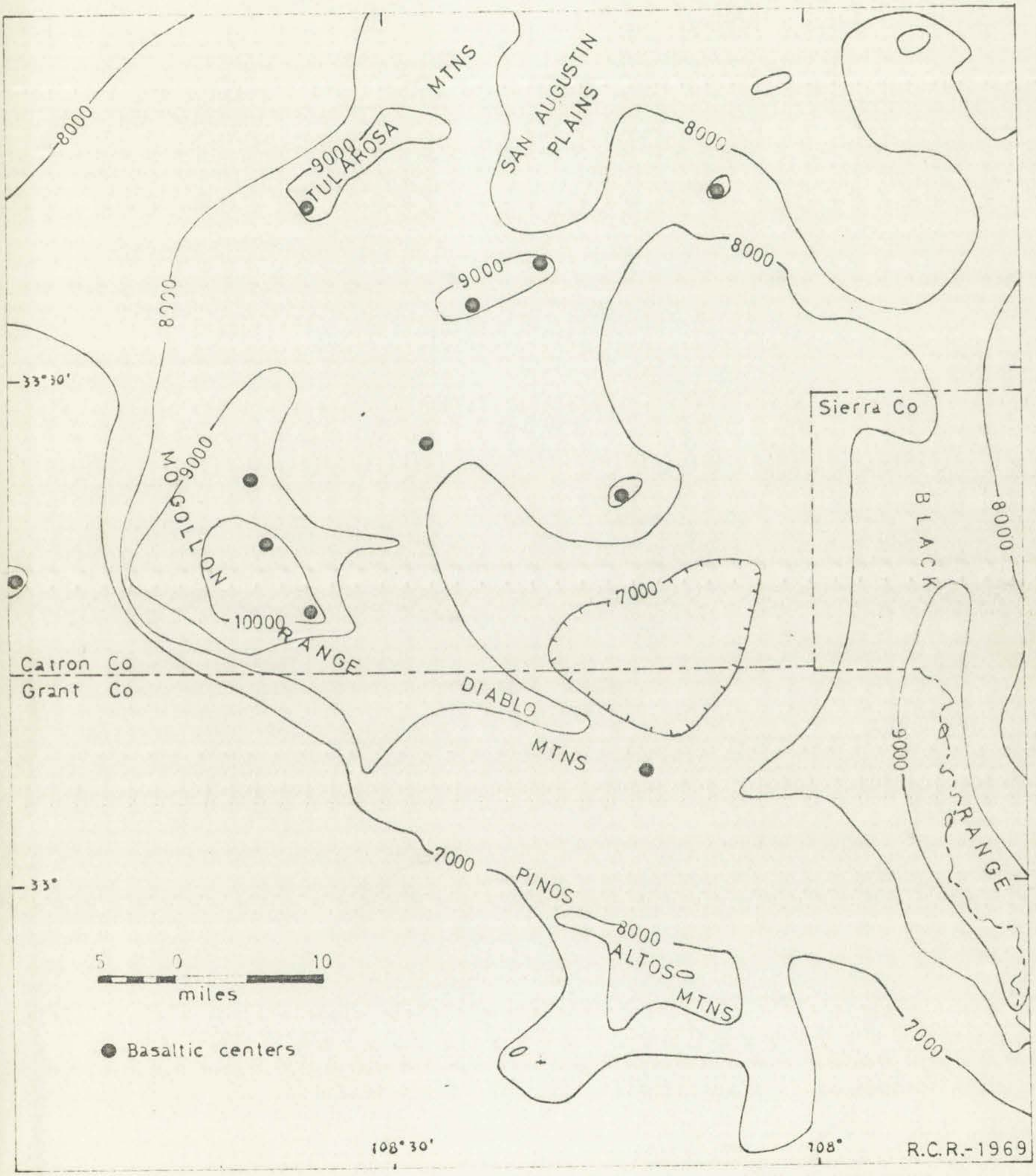

Fig. 1. Topographic envelope on the Mogollon Plateau volcano-tectonic complex with a six-mile spacing of control points.

Subsequent faulting follows the earlier structural trends established by the flow-banded rhyolites.

Prior to the present cycle of canyon cutting initiated by regional late Cenozoic uplift and rejuvenation of the southern Rocky Mountains, the topography of the Mogollon Plateau was probably relatively subdued and basin- or crater-like in form. The central depression was floored with basalt, above which some of the rhyolite domes may have protruded as topographic highs (e.g. the Diablo Mountains). Faulting that followed pre-existing structural trends accentuated the crater-like physiography, even though the central depression was partially filled in by several hundred feet of Gila Conglomerate. As with the San Juan Mountains in Colorado (Steven, 1968) the present physiography of the Mogollon Plateau in general reflects the shape of the ancient volcanic surface (Fig. 1) and has been modified only slightly by Quaternary erosion.

STRATIGRAPHY AND PETROGRAPHY OF THE VOLCANIC ROCKS

GENERAL STATEMENT

The mapped area covers the southwestern part of the Mogollon Plateau volcanic complex (Plate 1). Tertiary volcanic rocks crop out over most of the area but are overlain in places by late Tertiary Gila Conglomerate and pediment gravels; no pre-Tertiary rocks were identified. Division of the volcanic rocks into Upper, Middle, and Lower Volcanic Groups should be regarded as tentative until more detailed information on the volcano-tectonic complex is available.

A composite stratigraphic section shows the total maximum thickness of volcanic rocks to be in the order of 15,000 feet (Table 1). This maximum thickness is probably never attained at any locality, however, due to changes in thickness of individual volcanic units across cauldron walls, domal extrusions of flow-banded rhyolite, and localized centers of basaltic eruption. An estimated figure of less than 10,000 feet is probably closer to the actual thickness of post-Whitewater Creek volcanic rocks in the mapped area. No radiometric dates are available for rocks within the mapped area but several of the units that extend outside the area have been dated (Elston, Bikerman, and Damon, 1968).

Table 1. Composite stratigraphic column for the western part of the Mogollon Plateau volcano-tectonic complex

Formation	Lithology	Maximum thickness (in feet)
Alluvium	Unconsolidated sands and gravels	
UNCONFORMITY		
Gila Conglomerate	Fanglomerates, sandstones, and pediment gravels	700+
UNCONFORMITY		
Bearwallow Mountain Formation	Basaltic andesite, andesite and latite flows, breccias and agglomerates	2,000
Mogollon Andesite	Andesite flows, breccias, and agglomerates	400
DISCONFORMITY		
Deadwood Gulch Rhyolite	Ash-flow and ash-fall tuffs, tuffaceous sandstones, and volcanic conglomerates	1,100
UNCONFORMITY		
Double Spring Andesite	Basaltic andesite flows	150+
Latite at Turkeyfeather Creek	Latite and quartz latite ash-flow tuffs	1,000+
UNCONFORMITY		
Jerky Mountain Rhyolite	Rhyolite lava flows	1,500+
Bloodgood Canyon Rhyolite	Rhyolite ash-flow tuffs	800+
Last Chance Andesite	Andesite flows and breccias	100
Quartz Latite at Nabours Mountain	Quartz latite lava flows	400
Fanney Rhyolite	Rhyolite lava flows	2,000+
Mineral Creek Andesite	Andesite flows and breccias	1,000
Sacaton Quartz Latite	Quartz latite lava flows	1,500
Apache Spring Quartz Latite	Quartz latite ash-flow tuffs	2,500+
UNCONFORMITY		
Cranktown Sandstone and Houston Andesite	Sandstones, breccias, volcanic mudflows, and andesite lava flows	700
UNCONFORMITY		
Cooney Formation	Quartz latite and dacite ash-flow tuffs, tuffaceous sandstones, and andesite lava flows	2,000+
Whitewater Creek Rhyolite	Rhyolite tuff	600+

LABORATORY TECHNIQUES

About 240 thin sections were examined and compositions of plagioclase phenocrysts were determined with a universal stage, applying the Rittmann zone method and curves for high-temperature plagioclase (Rittmann and El-Hinnawi, 1961). Alkali feldspar compositions were determined by means of X-ray diffraction techniques (Tuttle and Bowen, 1958) using powdered samples that were made homogeneous by heating to 850°C for 20-30 minutes. Modal analyses of more than 30 representative specimens were made using a Swift point counter and about 1,000 points per thin section were counted.

Nine wet chemical analyses of rocks from the mapped area, and calculated C.I.P.W. norms, are given. The analyses were made by K. Aoki, Tohoku University, Sendai, Japan and J. R. Muysson, McMaster University, Ontario, Canada. Representatives of the important rock series were selected for analysis to indicate differentiation trends that are reflected in the petrography and mineralogy of the rocks.

WHITEWATER CREEK RHYOLITE

The oldest volcanic rock in the Mogollon Range is the Whitewater Creek Rhyolite (Ferguson, 1927, p. 6-7) which crops out only in the lower reaches of Whitewater and Mineral Creeks in the northwestern part of the area. Although no base is exposed, outcrops exceed 700 feet in thickness. The rock contains numerous inclusions of andesite and dacite, indicating

the existence at lower depths of older andesitic volcanics. No petrographic work was done on this unit.

COONEY FORMATION

Overlying Whitewater Creek Rhyolite in Whitewater Creek are ash-flow tuffs belonging to the Cooney Formation. These rocks were named the Cooney Quartz Latite by Ferguson (1927, p. 7-9) and a partial chemical analysis shows them to correspond to a soda rhyolite in composition (Table 2). Petrographically the tuffs range from dacite to quartz latite in composition and future work will possibly delineate individual members.

The Cooney Formation is 700 feet thick in Mineral Creek (Ferguson, 1927, p. 7), but thickens southward to at least 1,500 feet in Whitewater Creek, where it consists of purple, red, and white ash-flow tuffs interbedded with thin, discontinuous lenses of red sandstone. The uppermost unit in Whitewater Canyon is a purple dacitic ash-flow tuff characterized by strongly zoned plagioclase phenocrysts. The Cooney Formation extends southward along the front of the Mogollon Range, faulted in the west and east against younger Gila Conglomerate and Fanney Rhyolite respectively, but disappears beneath younger rocks south of Holt Gulch. In Sacaton Creek beds possibly equivalent to the Cooney Formation crop out and extend southward into Mogollon Creek. The rocks in this southern outcrop area are more varied than the type section in Whitewater Creek and include andesites and volcanically-derived

Table 2. Partial chemical analyses of rocks from the Lower Volcanic Group at Mogollon compared with Nockolds' averages.

	1	2	3	4	5
SiO_2	67.83	48.00	51.43	66.88	51.86
CaO	2.10	7.72	8.78	3.56	8.40
Na_2O	3.30	1.95	3.18	3.84	3.36
K_2O	5.46	3.28	1.04	3.07	1.33

1) Cooney Quartz Latite from canyon above Cooney (from Ferguson, 1927, p. 8; W. T. Schaller, analyst).

2) Mineral Creek Andesite from Cooney mine (from Ferguson, 1927, p. 14; W. T. Schaller, analyst).

3) Average of 26 tholeiitic andesites (from Nockolds, 1954).

4) Average of 137 granodiorites (from Nockolds, 1954).

5) Average of 50 diorites (from Nockolds, 1954).

sediments. In the lower reaches of Rain and Mogollon Creeks is an altered greenish ash-flow tuff that is overlain by a complex sequence of volcanic mudflows, bedded sandstones, andesite lavas, and cliff-forming purple ash-flow tuffs. On a regional scale the apparent southward thickening of the Cooney Formation from 700 feet north of Mogollon to over 2,000 feet in Mogollon Creek may indicate thickening toward a source area lying to the south or southwest, and flow-direction studies support this hypothesis. There remains some uncertainty, however, regarding correlation of the Cooney at its type locality near Mogollon with the rocks in the southern part of the area.

The Cooney Formation consists mainly of crystal-rich ash-flow tuffs containing numerous pumice fragments and some devitrified glass shards. Granophyric and micrographic texture is common in the devitrified groundmass and spherulites are developed in places. Evidence for vapor-phase crystallization is usually lacking owing to effects of regional hydrothermal alteration in the mineralized mining districts, but tridymite was identified as a vapor-phase constituent in a purple ash-flow tuff from near Mogollon Creek. Lithic inclusions of andesite and rhyolite are ubiquitous.

Modal analyses of five specimens of welded tuff from Whitewater Creek show that the phenocryst content varies between 25-50 percent (Table 3). Plagioclase is dominant in the northern exposure belt, where quartz and sanidine are rarely present as phenocrysts. In the southern part of the

Table 3. Modal analyses of welded tuffs from the Cooney Formation in Whitewater Creek determined using a Swift point counter.

	1	2	3	4	5
Groundmass [a]	61	72	61	50	50
Plagioclase [b]	25	22	27	40	31
Sanidine	-	-	1	-	-
Quartz	tr	tr	6	tr	tr
Biotite [c]	4	3	1	3	3
Pyroxene	-	tr	3[e]	-	-
Opaque oxides	2	1	1	5	3
Accessories [d]	tr	tr	tr	tr	tr
Inclusions	8	2	-	2	13
Total	100	100	100	100	100
Points counted	1286	1169	928	1070	1427
Plagioclase composition	An_{27-36}	An_{27-32}	An_{22-36}	An_{24-47}	An_{24-47}

a) groundmass largely devitrified
b) including alteration products - calcite and sericite
c) including alteration products - chlorite and magnetite
d) including sphene, apatite, and zircon
e) altered to antigorite and magnetite
tr=trace

Specimens 1 and 2 are white tuff from lower part of section separated from one another by thin red sandstone; 3 is red welded tuff from middle of section; 4 and 5 are porphyritic welded tuffs from uppermost unit.

area, however, quartz and sanidine are common phenocryst minerals and may exceed plagioclase in abundance. The lithological differences between the rocks in the two outcrop areas suggest that they represent two separate members that erupted in the same general area at about the same time. Their exact relative stratigraphic position remains unknown, and alteration has precluded radiometric dating.

Plagioclase constitutes up to 40 percent of some flows in the northern part of the area and is usually normally zoned and twinned according to the albite, Carlsbad, and pericline laws. Compositions are usually oligoclase-andesine, but individual crystals in the upper purple, porphyritic member are zoned from An_{13} to An_{57}. Many phenocrysts display optically discontinuous rims. Alteration to calcite and kaolinite is invariably present. In the southern part of the area sanidine occurs as subhedral phenocrysts that are usually kaolinized. Perthitic texture is highly developed in some places. Quartz, likewise, is an important phenocryst mineral in the south and occurs as rounded and sometimes highly embayed crystals. Both quartz and sanidine are major constituents of the groundmass of the tuffs throughout the area, and are often intergrown in micrographic or granophyric texture. X-ray diffraction of heat-treated samples of tuff from the type section in Whitewater Creek indicate a sanidine composition of Or_{60}-Or_{70}.

Ferromagnesian minerals are usually oxidized and in some cases have been almost obliterated by deuteric crystallization of the welded tuffs. Biotite is most abundant but is commonly

chloritized and always oxidized. In areas of intense hydrothermal alteration it is replaced by green chlorite displaying the anomalous blue interference colors of penninite. Hornblende, pleochroic from yellowish-green to greenish-brown, is sparsely present and clinopyroxene (usually augite) occurs in minor amounts in some specimens. Olivine altered to iddingsite occurs in andesite flows in the southern part of the area. Accessory minerals include apatite, zircon, opaque oxides, and sphene.

The Cooney Formation generally displays evidence of hydrothermal alteration. Plagioclase phenocrysts are commonly replaced by calcite. kaolinite, and less frequently, sericite. Chlorite is common as a secondary alteration product and may be associated with calcite, antigorite, and epidote. Zeolites were noted in thin sections from the southern part of the area and green clay (montmorillonite?) is present in some specimens. Chlorite is present in veinlets near Mogollon Creek and secondary quartz, fluorite, and calcite were found in the southern part of the area.

CRANKTOWN SANDSTONE AND HOUSTON ANDESITE

Overlying the Cooney Formation at Mogollon with a marked unconformity are several hundred feet of clastic sediments of andesitic derivation, named the Cranktown Sandstone by Ferguson (1927). Thickness and distribution of the formation are highly irregular, but Ferguson (1927, p. 9) reports

general thinning to the east and south from the type locality at the mouth of Silver Creek where it is 500 feet thick. Sandstones typical of this formation are rare south of Whitewater Creek. Lying near the base of Cranktown Sandstone at Mogollon is the Houston Andesite, approximately 40 feet thick, which at different localities may represent different flows tonguing into Cranktown Sandstone.

Over 400 feet of interbedded sandstones, breccias, and andesite flows crop out in Holt Gulch, whereas in Sheridan Creek the sequence consists of over 500 feet of andesite flows with few interbedded andesite breccias. The increasing predominance of andesite at the expense of Cranktown Sandstone in a southward direction is suggestive of a progressive facies change, with Houston Andesite at Mogollon representing the feather-edge of a sequence of flows lapping on to older rocks in a northeasterly direction. At least 600 feet of andesite crops out in Little Dry Creek but intense hydrothermal alteration in the Wilcox mining district around Sacaton Creek makes determination of thickness and extent of the unit in this area difficult. Southeast of Sacaton Creek the Houston Andesite was not separately mapped but was included within the Cooney Formation and possibly represents interfingering with upper parts of the Cooney. Like the Cooney Formation, Cranktown Sandstone and Houston Andesite crop out only along the front of the Mogollon Range where they are cut off in the west by the San Francisco graben and are overlain by Sacaton Quartz Latite.

Cranktown Sandstone in Holt Gulch consists of clastic sediments and breccias of volcanic derivation, containing angular to subangular fragments from 5-10 mm in diameter. The sediments are poorly sorted and have irregular and indistinct bedding. Plagioclase predominates over quartz and sanidine and minor amounts of opaque oxides, biotite (commonly chloritized), muscovite, sphene, and zircon. Rock fragments in the breccias include andesite, recrystallized rhyolite, and spherulitic glass. Green clay (montmorillonite?) and hematite occur as interstitial cement. Alteration of plagioclase to calcite is common and veinlets of calcite are abundant.

Houston Andesite usually has porphyritic, holocrystalline to hypocrystalline texture and is sometimes amygdaloidal. Plagioclase having the composition An_{34}-An_{47} is the dominant mineral but is extensively altered to calcite, sericite, and kaolinite. Minute grains of clinopyroxene occur in the groundmass of some specimens but ferromagnesian minerals, for the most part, have been replaced by iddingsite, fibrous antigorite, or chlorite, having anomalous blue interference colors of penninite, that is intergrown with magnetite and calcite. Aggregates and veinlets of epidote are prominent in the Wilcox mining district. Oxidized and chloritized biotite occurs sporadically and opaque oxides, apatite, and rare zircon are accessory minerals. Vesicles are filled with fibrous zeolites and highly embayed and resorbed quartz grains occur rarely as xenocrysts. Veinlets of secondary calcite and quartz are common.

APACHE SPRING QUARTZ LATITE

Apache Spring Quartz Latite is the major ash-flow sheet in the western part of the Mogollon Plateau and was named after a locality near Black Mountain (sec. 36, T.11 S., R.18 W.). The formation occurs principally within the Bursum cauldron where exposures are over 2,500 feet thick, with the base not exposed (Rhodes, 1968, p. 260). No attempt was made during reconnaissance mapping to subdivide the formation into separate flows or cooling units, but it is compositionally zoned from rhyolite at the base to quartz latite at the top. The Apache Spring is a red to grayish-purple, crystal-rich, welded tuff with eutaxitic texture. In the Bursum cauldron it consists of several cooling units and is generally densely welded. Some flows contain numerous xenoliths up to a few centimeters in diameter.

Near the margins of the Bursum cauldron the formation includes spectacular breccia deposits containing foreign rock fragments up to several tens of feet in size, and probably emplaced as volcanic mudflows from the caldera wall (Plate 3). These deposits are unsorted and poorly bedded and have been interpreted by J. C. Rattè (personal communication) as avalanche material derived from the cauldron walls during eruption of the ash-flow tuff. These avalanche or mudflow breccias crop out in Whitewater, Big Dry, Sacaton, Rain, and West Fork Mogollon Creeks.

Pore space was generally obliterated by welding and vapor-phase crystallization in densely welded Apache Spring Quartz

Latite. The groundmass is pervasively devitrified to variolites and spherulites, but glassy vitroclastic texture is preserved near the bottom of the section. Glass shards are abundant and usually display axiolitic texture under crossed nicols. Ubiquitous pumice fragments have collapsed into fibrous, lenticular lenses and abundant coarse-grained granophyric quartz and alkali feldspar may represent vapor-phase crystallization localized by pumice fragments (Ross and Smith, 1960, p. 37). Many of these coarse-grained aggregates consist of minute, inward-pointing euhedral to subhedral crystals of alkali feldspar accompanied by larger anhedral, poikilitic grains of quartz, attesting to the efficiency of vapor-phase activity. The recrystallized groundmass consists of a fine-grained granophyric aggregate of quartz, alkali feldspar, and opaque oxides.

Phenocrysts consist of quartz, plagioclase, sanidine, biotite, and subordinate clinopyroxene and hornblende. Quartz is generally rounded and embayed but may retain relict crystal faces. Sanidine is subhedral, commonly kaolinized, and displays Carlsbad twins. Fine exsolution lamellae are usually discernable and X-ray studies confirm that the mineral is micro- or cryptoperthitic. Plagioclase is abundant as subhedral laths with albite, pericline, and Carlsbad twins, and crystals usually display normal and oscillatory zoning. Overgrowths of sanidine or graphic intergrowths of sanidine and quartz are common. Few sanidine phenocrysts are rimmed by, or intergrown with, quartz (Plate 4). Biotite is pleochroic, X = pale brown or yellowish-brown, Y = reddish-brown, Z = dark brown or

Table 4. Modal analyses of the Apache Spring Quartz Latite showing vertical compositional zoning in the ash-flow sheet (recalculated xenolith-free)

	1	2	3	4	5	6	7	8	9	10
Groundmass	84.0	72.8	75.9	64.3	57.0	50.8	63.2	56.4	58.1	63.1
Quartz	2.9	6.9	7.7	4.9	12.9	4.0	3.3	2.8	3.0	2.6
Sanidine	11.5	18.3	11.8	26.5	23.5	36.9	32.6	33.9	30.8	27.3
Plagioclase	1.1	1.1	2.5	2.8	4.4	5.2	0.7	3.4	5.6	2.7
Biotite	0.1	0.1	1.6	tr	1.3	1.8	0.1	2.0	0.9	1.9
Hornblende	-	-	-	-	-	-	-	tr	-	-
Clinopyroxene	-	-	-	-	-	-	-	-	0.3	1.3
Opaque ores	0.3	0.8	0.5	1.4	0.8	1.3	0.1	1.4	1.4	1.0
Accessories	tr	tr	tr	tr	0.1	tr	tr	0.1	tr	0.1
Total	99.9	100.0	100.0	99.9	100.0	100.0	100.0	100.0	100.0	100.0
No. of points counted	961	1127	865	1360	959	1092	863	1080	1183	829
Original % xenoliths	(6.1)	(26.2)	(34.2)	(43.1)	(0.9)	(1.8)	(3.9)	-	-	(6.0)
Height above exposed base (feet)	0	300	700	900	1200	1400	1600	1700	1900	2100
Plagioclase (An%)	22-33	25-30	25-27	26-31	32	24-36	20-29	24-34	20-34	28-36
Sanidine (Or%)	78	82	67	82	67	60	55	63	51	50

tr = trace

reddish-brown, although much of it is oxidized and chloritized. Hornblende, pleochroic from pale yellowish-green or yellowish-red to reddish-brown, occurs rarely and has characteristic oxidized rims of granular opaque oxides. Pale green augite is prominent near the top of the section. Accessory minerals include opaque oxides, apatite, zircon, and rare sphene. Green clay (montmorillonite?) occurs in the groundmass of some specimens.

The ultimate extent of the ash-flow sheet is unknown and the outline of the Bursum cauldron also has not been completely delineated, but preliminary calculations of the volume of the Apache Spring Quartz Latite indicate that it is in the region of 700 km^3, corresponding to magnitude 6 in the classification of Smith (1960, p. 819).

Lava flows of Fanney Rhyolite overlie Apache Spring Quartz Latite in the western part of the Bursum cauldron and the base of the Fanney rises in an eastward direction toward the center of the cauldron. Likewise, lava flows of Sacaton Quartz Latite overlie Apache Spring in the southern part of the cauldron and the base of the Sacaton rises progressively northward. These relationships indicate resurgent doming of Apache Spring Quartz Latite in the center of the Bursum cauldron.

Modal analyses of 10 specimens of Apache Spring Quartz Latite are given (Table 4) and two chemical analyses are included (Table 5, nos. 1 and 2).

Table 5. New chemical analyses for the Bearwallow Mountain Formation and the Middle Volcanic Group from the mapped area.

Chemical Analyses (oxide percentages)

	1	2	3	4	5	6	7	8	9
SiO_2	69.10	73.63	74.93	75.63	75.99	75.74	50.29	62.49	65.92
TiO_2	0.44	0.27	0.11	0.24	0.24	0.17	1.73	0.81	0.61
Al_2O_3	15.11	12.00	13.25	12.57	12.51	12.78	16.09	17.28	17.33
Fe_2O_3	2.19	2.23	0.88	1.23	1.23	0.97	4.66	4.01	2.41
FeO	0.79	1.10	0.60	0.70	0.50	0.32	6.41	0.98	0.69
MnO	0.07	0.01	0.01	0.06	0.06	0.05	0.16	0.05	0.11
MgO	0.29	0.12	0.08	0.11	0.09	0.09	5.78	1.72	0.62
CaO	0.73	0.44	0.46	0.29	0.30	0.18	7.81	4.53	1.28
Na_2O	3.68	2.07	3.49	3.67	3.82	3.65	3.35	4.27	5.24
K_2O	5.97	5.76	5.00	5.09	5.00	4.96	1.58	2.37	4.93
P_2O_5	0.05	0.03	0.04	0.02	0.02	0.01	0.44	0.22	0.17
H_2O+	1.13	1.91	0.90	0.24	0.12	0.45	0.39	0.41	0.36
H_2O-	0.21	0.43	0.14	0.08	0.02	0.35	0.61	0.38	0.25
CO_2	n.d.	n.d.	n.d.	0.00	0.00	0.01	0.17	0.00	0.00
Total	99.76	100.00	99.89	99.93	99.90	99.73	99.47	99.52	99.92

C.I.P.W. norms

	1	2	3	4	5	6	7	8	9
Q	23.16	38.58	34.50	34.08	33.78	34.86	0.90	16.56	12.90
Or	35.03	33.92	29.47	30.02	29.47	29.47	9.45	13.90	28.91
Ab	30.92	17.29	29.34	30.92	32.49	30.92	28.30	36.16	44.54
An	3.61	2.22	2.22	1.39	1.39	0.83	24.19	21.13	6.39
Cor	1.43	1.63	1.31	0.51	0.31	1.02	-	-	1.02
En	0.70	0.30	0.20	0.30	0.20	0.20	14.30	4.30	1.50
Fs	-	-	0.13	-	-	-	5.28	-	-
Wo	-	-	-	-	-	-	4.52	0.58	-
Mt	1.39	2.78	1.39	1.86	1.16	0.93	6.73	1.16	0.93
Il	0.91	0.46	0.15	0.46	0.46	0.30	3.34	1.52	1.22
Hm	1.28	0.32	-	-	0.48	0.32	-	3.20	1.76
Ap	-	-	-	-	-	-	1.01	-	-
C	-	-	-	-	-	-	0.40	-	-

1. Apache Spring Quartz Latite from top of ash-flow sheet on Black Mountain (sec. 35, T.11 S., R.18 W.). Analyst: K. Aoki, Japan.

2. Apache Spring Quartz Latite from bottom of ash-flow sheet in Big Dry Creek (sec. 3, T.12 S., R.18 W.). Analyst: K. Aoki, Japan.

3. Fanney Rhyolite overlying Apache Spring in Bursum cauldron, on north side of Whitewater Creek (sec. 15, T.11 S., R.18 W.). Analyst: K. Aoki, Japan.

4. Bloodgood Canyon Rhyolite from top of ash-flow sheet in Middle Fork Gila River (sec. 30, T.11 S., R.14 W.). Analyst: J. Muysson, Ontario.

5. Bloodgood Canyon Rhyolite from bottom of ash-flow sheet in Middle Fork Gila River (sec. 30, T.11 S., R.14 W.). Analyst: J. Muysson, Ontario.

6. Jerky Mountain Rhyolite from Rawmeat Canyon (sec. 15, T.12 S., R.16 W.). Analyst: J. Muysson, Ontario.

7. Type I, olivine-clinopyroxene basalt from Bearwallow Mountain Formation near White Creek cabin (sec. 12, T.12 S., R.16 W.). Analyst: J. Muysson, Ontario.

8. Type III, amphibole-orthopyroxene latite from Bearwallow Mountain Formation near Iron Creek (sec. 9, T.11 S., R.17 W.). Analyst: J. Muysson, Ontario.

9. Type V, biotite-clinopyroxene latite from Bearwallow Mountain Formation on north flank of Mogollon Baldy (probably late-stage intrusive dike) (sec. 10, T.12 S., R.17 W.). Analyst: J. Muysson, Ontario.

SACATON QUARTZ LATITE

The Sacaton Quartz Latite was named after Sacaton Mountain, a prominent peak in the Mogollon Range. It is probably equivalent to the Pacific Quartz Latite near the mouths of Silver and Copper Creeks at Mogollon (Ferguson, 1927, p. 11-12) but the presence in the Houston Canyon area of the Mogollon mining district of tuffs and breccias of Cooney lithology intruded by dikes of Sacaton-Pacific lithology, suggests that some of the Pacific Quartz Latite as mapped by Ferguson is a melange of Cooney fragments intruded by Sacaton Quartz Latite (W. E. Elston, unpublished data). At the type locality on Sacaton Mountain the Sacaton Quartz Latite consists of massive porphyritic rock with blocky jointing and a paucity of megascopic planar structures. Phenocrysts of euhedral feldspar and rounded quartz impart a granitoid texture in hand specimen. Vitrophyres occur in the formation and probably represent chilled flow margins. Quartz phenocrysts are usually prominent but are sparse or absent in some flows. A coarsely porphyritic quartz latite lava flow crops out near the base of the formation in Holt Gulch and on the divides above Rain Creek. The Sacaton usually forms steep slopes mantled by talus slides.

Sacaton Quartz Latite consists of porphyritic, crystal-rich lava flows in which the groundmass is invariably recrystallized. Euhedral phenocrysts up to 8 mm in size are characteristic and are associated with a highly devitrified groundmass that commonly contains granophyric patches and rare

spherulites. Euhedral to subhedral phenocrysts of plagioclase are normally zoned, sometimes with discontinuous turbid rims and relatively clear cores. Alteration to kaolinite, sericite, and calcite is common and crystals are sometimes embayed. Compositions are An_{22}-An_{46} and individual crystals are commonly zoned throughout this range. Sanidine is present as subhedral phenocrysts with microperthitic exsolution lamellae and rare Carlsbad or spindle-shaped twins. It occurs intergrown with plagioclase and in a few specimens it mantles euhedral crystals of well-twinned plagioclase. Compositions of heat-treated sanidine range from Or_{62}-Or_{77}. Where present quartz occurs as large rounded phenocrysts that are highly resorbed and embayed. Biotite is the chief ferromagnesian mineral and is usually oxidized and chloritized. In places it is completely replaced by chlorite (locally penninite) and in some specimens is associated with muscovite and hematite. Prismatic hornblende, pleochroic from yellowish-brown to reddish-brown, was found in one specimen from Holt Gulch. Accessory minerals include apatite, opaque oxides, sphene, and zircon. Epidote, zeolites, and intergrown calcite and chlorite are present as secondary alteration products in areas of intense hydrothermal alteration.

The formation is approximately 1,000 to 1,500 feet thick and lies upon Apache Spring Quartz Latite in the Bursum cauldron, whereas outside the cauldron it overlies Houston Andesite. About 800 feet of Sacaton is present in Sheridan and Holt Gulches where it is overlain by Fanney Rhyolite with

no intervening Mineral Creek Andesite. Ferguson (1927, p. 11-12) reported 500-600 feet of Pacific Quartz Latite along the western edge of the Mogollon mining district, thinning rapidly eastward to 50-100 feet within a distance of one mile. Southeast of Sacaton Creek the formation is several hundred feet thick and is overlain unconformably by Deadwood Gulch Rhyolite and, in Mogollon Creek, by Mineral Creek Andesite.

Lithological similarity between Sacaton and Apache Spring Quartz Latite makes delineation of their mutual contact difficult, and detailed field work is required to determine the complex relationship between the two rock units. The arcuate outcrop pattern of Pacific-Sacaton Quartz Latite and its marked lateral thinning suggests several local vents from which the lava was extruded, aligned along the western and southern margins of the Bursum cauldron. Intrusive contacts of Pacific Quartz Latite were recognized in the Houston-Silver Creek area of the Mogollon mining district (W. E. Elston, unpublished data), and the absence of overlying Mineral Creek Andesite in the Holt Mountain area indicates the possible existence there of an extrusive dome forming a topographic high in Sacaton time (see section on flow direction studies).

MINERAL CREEK ANDESITE

Following accumulation of Sacaton Quartz Latite another widespread outpouring of andesite lava occurred, giving rise to the Mineral Creek Andesite lying upon an uneven surface cut into older rocks (Ferguson, 1927, p. 12-14). The formation

consists of andesite lava flows, volcanic breccias, and minor volcanic sediments. Many lava flows are vesicular and amygdaloidal and they vary in color from grayish-black to reddish-purple. The andesite is very susceptible to hydrothermal alteration and fresh outcrops are rare.

Mineral Creek Andesite is holocrystalline to hypocrystalline and tends to be coarsely porphyritic and vesicular. Phenocrysts 1-3 mm in size lie in a groundmass of felty, elongated feldspar laths, granular pyroxene, and opaque oxides. Devitrification of glass and hydrothermal alteration are extensive, especially in the Mogollon mining district, where the rock is laced with veinlets of secondary quartz. A distinctive and widespread flow contains elongated feldspar laths up to 10 mm long and aligned parallel to the direction of flow. Plagioclase, the dominant mineral, is generally zoned normally, but oscillatory zoning with more than 40 reversals occurs. Average composition is An_{50} although some crystals are zoned throughout the range An_{26}-An_{63}. Kaolinite and sericite are alteration products. Clinopyroxene is ubiquitous and olivine, altered to iddingsite, is common. Chlorite and green fibrous antigorite are alteration products of primary ferromagnesian minerals. Accessory minerals include opaque oxides.

Within the Mogollon mining district, thickness of the formation varies from zero to a maximum of 700 feet in Mineral Creek, but farther south in North Fork of Whitewater Creek it is at least 800 feet thick and the base is not exposed. The

formation is absent in Holt Gulch, where Fanney Rhyolite lies directly upon Sacaton Quartz Latite, and in Sheridan Gulch where only a few andesite fragments were found as float. Mineral Creek Andesite crops out again near Big Dry Creek and the thickness increases from 300 feet at Sheridan Mountain to over 600 feet two miles farther south. In Spider Creek over 600 feet of Mineral Creek Andesite crop out, overlain by Fanney Rhyolite. West of the San Francisco River the oldest exposed rock in the volcanic section is andesite, overlain and intruded by Fanney Rhyolite, that is correlated with Mineral Creek. It is over 800 feet thick in the southwestern corner of the mapped area with the base not exposed (Plate 1). It is 1,000 feet thick in Mogollon Creek and overlies Sacaton Quartz Latite.

It is not known to what extent the present thickness and distribution of Mineral Creek Andesite is a result of post-depositional erosion, especially in pre-Deadwood Gulch time, but the absence of the formation between Whitewater Creek and Sheridan Gulch probably reflects the existence there of a dome of Sacaton Quartz Latite forming a topographic high around which the andesites flowed (see section on flow direction studies). Thickening of the formation toward the south and southwest may indicate an extrusive andesite vent in this direction, an interpretation supported by flow direction studies. Abrupt thinning of the formation from nearly 1,000 feet in Mogollon Creek to zero in West Fork Mogollon Creek

possibly reflects the presence of another dome of Sacaton Quartz Latite, but may be due to pre-Deadwood Gulch faulting and erosion. Structural details of this area are not known.

FANNEY RHYOLITE

A thick sequence of flow-banded and spherulitic rhyolite lavas around Mogollon was named Fanney Rhyolite by Ferguson (1927, p. 14-16) and is continuous with lithologically similar rocks forming the bulk of the Mogollon Range north of Big Dry Creek. Fanney Rhyolite varies in lithology and probably consists of numerous flows with different depositional and cooling histories. The most widespread and characteristic type is stony, flow-banded rhyolite that shows linear orientation of phenocrysts and inclusions in flow bands 1-10 mm wide. Spherulites are common and attain diameters of several centimeters. West of Glenwood and on Holt Mountain lustrous black vitrophyre is studded with brilliant red spherulites up to 10 mm in size. Interbedded with flow-banded rhyolite are brecciated rhyolite, perlite zones, rare tuffaceous beds, and cavernous rhyolites characterized by numerous lithophysae lined with drusy quartz. The rock varies in color through white, gray, pale purple, red, and black.

The rock in thin section varies from vitrophyre to completely devitrified rhyolite containing sparse phenocrysts up to 2 mm in size. Phenocrysts seldom constitute more than 5 percent by volume of the rock. Graphically intergrown quartz and euhedral sanidine are sparsely present in the groundmass and

lithophysal cavities are lined with vuggy quartz. Phenocrysts are quartz, usually rounded and embayed, and subhedral microperthitic sanidine of composition Or_{50}-Or_{60}. Sanidine may be intergrown with quartz in phenocrysts or may form rims around subhedral plagioclase (Plate 5). Phenocrysts of oligoclase (An_{20}-An_{25}) are slightly zoned and display albite, pericline, and Carlsbad twins. Sparse biotite is oxidized and slightly chloritized and is pleochroic from light to dark brown. Accessories include opaque oxides, apatite, zircon, and rare sphene, while tridymite was identified in one specimen. Banding is conspicuous and may be due to alternating layers of coarse- and fine-grained devitrification, alternating bands of granophyre and spherulites, or differential oxidation of iron in adjacent layers. Rare interbedded tuffs contain devitrified pumice fragments and andesite xenoliths. Rhyolite dikes along the front of the Mogollon Range have similar mineralogy but are usually altered to sericite, kaolinite, and chlorite.

The main body of Fanney Rhyolite along the front of the Mogollon Range is in fault contact with Cooney Formation in the west and Apache Spring Quartz Latite in the south. Throughout this area the formation is 1,000-2,000 feet thick but thins east and southeast to approximately 400 feet near Willow Mountain and 50 feet at Center Baldy. It is absent at Mogollon Baldy. West of the San Francisco River, Fanney Rhyolite thins southwestward from nearly 600 feet west of Glenwood to zero at the confluence of Big Dry Creek and the San Francisco River. In the Mogollon mining district Ferguson (1927, p. 15)

Table 6. Modal analyses of Fanney Rhyolite determined using a Swift point counter

	1	2	3	4
Groundmass	99.4	97.1	97.7	95.2
Quartz	0.4	0.9	0.6	0.3
Sanidine	tr	1.1	1.3	1.8
Plagioclase	0.2	0.5	0.4	2.4
Biotite	tr	0.3	tr	0.3
Opaque oxides	tr	0.1	tr	tr
Accessories	tr	tr	tr	tr
Total	100.0	100.0	100.0	100.0
Points counted	928	1,449	1,418	1,413
Plagioclase (An%)	An_{22-25}	An_{22-25}	n.d.	An_{20-24}
Sanidine (Or%)	Or_{60}	Or_{51}	n.d.	Or_{54}

tr = trace n.d. = not determined

Location of samples: (1) Holt Mountain (sec. 2, T.12 S., R.19 W.); (2) Whitewater Creek (sec. 15, T.11 S., R.18 W.) (chemical analysis Table 5, no. 3); (3) near Grouse Mountain (sec. 27, T.11 S., R.18 W.); (4) Whitewater Creek (sec. 12, T.11 S., R.19 W.).

described northward thinning of the formation from 1,000-1,200 feet at Whitewater Creek to less than 10 feet north of Mineral Creek.

In the area of thickest accumulation, flow banding is highly contorted and commonly vertical (Plate 6); toward the margins of the body it tends to be horizontal and regular. Structurally, Fanney Rhyolite has the form of a large mushroom-shaped domal extrusion, elongated northwesterly, with a surrounding apron of subhorizontal lava flows. Evidence for a complex depositional history of the marginal flow lobes is provided by fragmental tuffs (Ferguson, 1927, p. 15) and vitrophyres, the latter being prominent west of Glenwood. A widespread basal, bedded pumiceous tuff indicates initial explosive eruption of ash, whereas interbedded breccias and tuffs indicate repeated fragmentation of flow carapaces and intermittent explosive volcanism.

Flows of Fanney Rhyolite were not found south of Big Dry Creek but numerous rhyolite dikes in the southern part of the mapped area indicate wider lateral extent of the formation in former times. Dikes intrude Mineral Creek Andesite and older formations but do not cut Deadwood Gulch Rhyolite. They vary from a few inches to tens of feet wide and are generally aligned northwestward, parallel to the Mogollon Range border fault.

Modal analyses of 4 specimens of Fanney Rhyolite are given (Table 6) and a chemical analysis is included in Table 5, no. 3.

QUARTZ LATITE AT NABOURS MOUNTAIN

Lava flows of quartz latite crop out on the crest of the Mogollon Range between Holt and Nabours Mountains, and at Grouse Mountain. Previously I incorrectly correlated these flows with Apache Spring Quartz Latite, thereby misinterpreting and unnecessarily complicating the volcanic stratigraphy in the Mogollon Range (Rhodes, 1968; Elston, Coney, and Rhodes, 1968). I now regard these rocks as being post-Fanney lava flows genetically related, but not equivalent, to Apache Spring Quartz Latite.

These quartz latite lava flows are 200-300 feet thick and are overlain by Deadwood Gulch Rhyolite near Holt Mountain (Plate 1). On the north side of the mountain they crop out about 100 feet below the crest and dip steeply northward, suggesting that the lava filled an ancient channel cut into Fanney Rhyolite (Rhodes, 1968, p. 261).

The rock is crystal-rich and contains phenocrysts of quartz, sanidine (Or_{49}-Or_{55}), plagioclase (An_{26}-An_{36}), biotite, amphibole, and clinopyroxene in a recrystallized granophyric to spherulitic groundmass. Sparse reaction pairs of biotite rimmed with hornblende and augite possibly indicate abrupt decrease in vapor pressure during final crystallization in the magma chamber.

LAST CHANCE ANDESITE

Last Chance Andesite was recognized in the Mogollon

mining district by Ferguson (1927), where it consists of thin interbedded andesite flows, breccias, agglomerates, and local reworked sandstones. The formation thins southward from 600 feet north of Mineral Creek to less than 300 feet at Whitewater Creek as "...the andesite flows and breccias lapped against the great mound of Fanney rhyolite" (Ferguson, 1927, p. 17). Rocks correlated with Last Chance Andesite at Mogollon crop out only around Whitewater Creek in the northwestern part of the mapped area, where thin andesite flows and breccias lie beneath Deadwood Gulch Rhyolite. The unit thins eastward, suggesting that it may have been derived from a source lying west of the Mogollon Plateau.

No petrographic work was done on this unit.

BLOODGOOD CANYON RHYOLITE

Bloodgood Canyon Rhyolite consists of gray to grayish-purple ash-flow tuffs that were named by Elston (1968) after Bloodgood Canyon, a few miles south of the mapped area. K/Ar dates on Bloodgood Canyon Rhyolite from outside the Mogollon Plateau range from 23.2-26.3 m.y. (Elston, Bikerman, and Damon, 1968, p. 266) but some of these rocks are probably not strictly equivalent to Bloodgood Canyon at its type locality. In the mapped area the Bloodgood Canyon Rhyolite is densely to moderately welded and consists of several cooling units marked by slight breaks in slope (Plate 7). Lithologically the formation is characterized by phenocrysts of iridescent blue moonstone (sanidine cryptoperthite), rounded quartz, and sparse

biotite. Abundant pumice fragments are commonly obscured by post-depositional recrystallization. Xenoliths are sparse, except in a poorly welded zone at the bottom of Middle Fork Gila River, just north of the mapped area.

Phenocrysts make up 12-35 percent of the rock and lie in a recrystallized granophyric groundmass in which shards and pumice fragments are scarcely resolvable, although shards with axiolitic texture may be seen under crossed nicols. Spherulites occur rarely. Granophyric patches of poikilitic euhedral alkali feldspar and anhedral quartz probably represent vapor-phase crystallization localized by pre-existing pumice fragments, and rare micrographic intergrowths of quartz and alkali feldspar in the groundmass also may be due to vapor-phase crystallization. Tridymite was identified as a vapor-phase mineral in a few thin sections. Rounded and embayed phenocrysts of quartz, commonly retaining relict crystal faces, and subhedral crystals of cryptoperthitic sanidine, are ubiquitous. X-ray diffraction of heat-treated samples indicate sanidine compositions of Or_{47}-Or_{58}. A strong peak corresponding to soda feldspar is also obtained by X-ray diffraction, suggesting that albite or anorthoclase is an important constituent of the recrystallized groundmass. Oxidized biotite, pleochroic from reddish-yellow to reddish-brown, is the chief ferromagnesian mineral, although oxidized hornblende occurs sporadically near the top of the section. Accessory minerals include abundant sphene, opaque oxides, and subordinate apatite and zircon. Chlorite and possibly sericite are rare alteration

Table 7. Modal analyses of a vertical sequence of Bloodgood Canyon Rhyolite from Middle Fork Gila River, just north of the mapped area (sec. 30, T.11 S., R.14 W.)

	1	(*)	2	3	4	5
Height above exposed base (feet)	10		150	400	600	800
Groundmass	76.2	(87.5)	66.2	73.2	82.2	73.7
Xenoliths	13.0	(-)	-	-	-	-
Quartz	3.9	(4.5)	10.6	10.7	3.7	6.3
Sanidine	6.0	(6.9)	21.7	15.1	13.6	18.9
Biotite	tr	(tr)	1.2	0.7	0.2	tr
Hornblende	-	(-)	-	-	-	0.6
Opaque oxides	0.9	(1.1)	0.3	0.1	0.2	0.5
Sphene	tr	(tr)	tr	0.2	tr	tr
Total	100.0	(100.0)	100.0	100.0	99.9	100.0
Points counted	1,195		1,019	1,678	1,261	1,485

(*) totals in parentheses are calculated xenocryst-free

tr = trace

products.

The source for Bloodgood Canyon Rhyolite is the Gila Cliff Dwellings cauldron where the unit is over 800 feet thick with the base exposed only at the southern edge of the cauldron. Within the mapped area the formation crops out east of the Ring Canyon fault which seems to be near the western margin of the cauldron. The ash-flow tuffs are faulted against Deadwood Gulch and Jerky Mountain Rhyolites, and nowhere within the mapped area was an unfaulted contact found between Bloodgood Canyon and Jerky Mountain Rhyolites. In Middle Fork Gila River, however, W. E. Elston and P. J. Coney (personal communication) found Jerky Mountain flow-banded lavas overlying Bloodgood Canyon ash-flow tuffs. Deadwood Gulch and Jerky Mountain Rhyolites lie unconformably upon pre-Bloodgood Canyon formations in the western part of the mapped area, suggesting that the tuffs did not overflow the western rim of the Mogollon Plateau volcano-tectonic depression.

Modal analyses of 5 specimens of Bloodgood Canyon Rhyolite are given in Table 7 and two chemical analyses are included in Table 5, nos. 4 and 5.

JERKY MOUNTAIN RHYOLITE

Jerky Mountain Rhyolite was named after the Jerky Mountains in the eastern part of the mapped area (Elston, 1968, p. 237). Texturally the formation is similar to Fanney Rhyolite but mineralogically the two are distinct. Jerky Mountain Rhyolite overlies Bloodgood Canyon ash-flow tuff in

the Gila Cliff Dwellings cauldron but in some areas of the Diablo Mountains it may in part be older than Bloodgood Canyon Rhyolite (Elston, Coney, and Rhodes, 1968, p. 271).

Flow-banded lava with flow bands 1-10 mm wide predominates. Flow banding varies from vertical to subhorizontal and flow folds range in amplitude from a few millimeters to tens of meters. Breccias and fragmental tuffs occur at several localities and spherulitic lavas are common. Jerky Mountain Rhyolite is porphyritic and contains 3-12 percent phenocrysts up to 3 mm in diameter in aphanitic glassy to devitrified groundmass. Flow banding consists of alternating layers of fine- and coarse-grained devitrification, sometimes accentuated by preferential alignment of phenocrysts. Granophyric and micrographic quartz and sanidine are common and cavities in the rock are generally lined with drusy quartz.

Phenocrysts of rounded, embayed quartz and subhedral microperthitic sanidine are present. Some phenocrysts display cuneiform type of graphic intergrowth between sanidine and quartz. Euhedral oxidized hornblende, pleochroic from yellowish-brown to reddish-brown or dark brown, is the chief ferromagnesian mineral. Subordinate biotite is pleochroic from yellowish-brown to dark reddish-brown. X-ray diffraction shows the presence of quartz, sanidine (Or_{39}-Or_{47}), and sodium feldspar (albite or anorthoclase) in the groundmass. Accessory minerals include euhedral sphene, opaque oxides, and zircon. Rounded aggregates of plagioclase were noted as xenoliths in one thin section.

Table 8. Modal analyses of Jerky Mountain Rhyolite determined using a Swift point counter.

	1	2	3	4
Groundmass	96.5	88.9	90.9	93.0
Quartz	1.8	4.9	2.8	3.5
Sanidine	1.6	6.2	6.3	3.5
Hornblende	0.1	tr	tr	tr
Biotite	tr	tr	tr	-
Accessories	tr	tr	tr	tr
Total	100.0	100.0	100.0	100.0
Points counted	974	1,106	1,187	1,147
Sanidine composition	Or_{40}	Or_{39}	Or_{45}	Or_{47}

tr = trace

Location of samples: (1) West Fork Gila River (sec. 1, T.12 S., R.16 W.); (2) Rawmeat Canyon (sec. 29, T.12 S., R.16 W.); (3) Rawmeat Canyon (sec. 15, T.12 S., R.16 W.) (chemical analysis - Table 5, column 6); (4) Trail Creek (sec. 30, T.12 S., R.16 W.)

The base of Jerky Mountain Rhyolite was observed only in Mogollon Creek where it overlies Mineral Creek Andesite and is 1,000-1,500 feet thick. In the Jerky and northern part of the Diablo Mountains between 800-1,000 feet of rhyolite are exposed, but the formation was not found in the Gila Cliff Dwellings cauldron east of the Ring Canyon fault. Jerky Mountain Rhyolite was probably extruded as large dome-like masses, similar in morphology to the Fanney Rhyolite domes, elongated in a northwesterly direction. Extrusive centers seem to have been located along the margin of the Gila Cliff Dwellings cauldron.

Modal analyses of 4 specimens of Jerky Mountain Rhyolite are given in Table 8 and a chemical analysis is included in Table 5, no. 6.

QUARTZ LATITE AT TURKEYFEATHER CREEK

Quartz latite ash-flow tuffs crop out locally in Turkeyfeather Creek and along West Fork Gila River (Plate 1). They are overlain by Deadwood Gulch Rhyolite and, near White Creek, are in fault contact with Jerky Mountain Rhyolite. The base of the formation was not found in the mapped area but approximately 400 feet are exposed in Turkeyfeather Creek and over 1,000 feet in West Fork Gila River. A similar clinopyroxene-bearing welded tuff, possibly correlative with this unit, crops out in Mogollon Creek. The stratigraphic relationship of the formation with Double Spring Andesite is not known from field data.

The quartz latite consists of crystal-rich ash-flow tuffs

with phenocrysts up to 6 mm in diameter in a glassy to recrystallized groundmass containing abundant shards and pumice fragments. Graphically intergrown quartz and sanidine and granophyric quartz in vesicles of pumice fragments indicate vapor-phase crystallization. Xenoliths of andesite, rhyolite, and perlite are present. Phenocrysts of euhedral to subhedral sanidine, zoned plagioclase (oligoclase-andesine), oxidized and partially chloritized biotite, and clinopyroxene are common. Phenocrysts of quartz and oxyhornblende occur sporadically. Accessory minerals include opaque oxides, zircon, apatite, and sphene while calcite, chlorite, and possibly antigorite are alteration products.

DOUBLE SPRING ANDESITE

This is a new formational name proposed by W. E. Elston (personal communication) to supersede Last Chance(?) Andesite used previously (Elston, Coney, and Rhodes, 1968). Within the mapped area, Double Spring Andesite crops out only in West Fork Gila River where it is 100-150 feet thick, with no base exposed. It is porphyritic, containing phenocrysts up to 4 mm in length of labradorite and clinopyroxene. Iddingsite and antigorite are alteration products of olivine, and accessory minerals include opaque oxides and apatite. The rock is in fault contact with quartz latite and Jerky Mountain Rhyolite to east and west respectively, and is overlain by Deadwood Gulch Rhyolite.

DEADWOOD GULCH RHYOLITE

The youngest rhyolitic rock in the mapped area consists of interbedded ash-flow, ash-fall, and waterlain tuffs, tuffaceous sandstones, and volcanic conglomerates which lie on a regional unconformity that truncates older units. First recognized and described from the Mogollon mining district by Ferguson (1927, p. 18-19), Deadwood Gulch Rhyolite has subsequently been found over large parts of the Mogollon Plateau. No vent for Deadwood Gulch Rhyolite has yet been found. Ash flows are subordinate but abundant pumiceous ash-fall and lapilli tuffs indicate explosive eruption.

Deadwood Gulch Rhyolite is usually white to buff and is extremely porous and poorly welded. Locally it is stained pink or red by hydrothermal fluids, especially in fault zones, and is silicified and recrystallized in mineralized areas. The formation is vitric and vesicular in thin section although incipient alteration of the groundmass to green clay (montmorillonite?) is common. Vapor-phase crystallization (commonly tridymite) ranges from vuggy coatings to complete filling of vesicular cavities. Glass shards and pumice fragments are abundant and phenocrysts of sanidine, plagioclase, quartz, and biotite up to 5 mm in size usually make up 10 percent of the rock. Xenoliths of altered andesite, rhyolite, and sometimes perlite are ubiquitous. Spherulites are rare.

Phenocrysts of subhedral, micrographic sanidine, commonly zoned and embayed, subhedral plagioclase (An_{17}-An_{27}), and rounded, embayed quartz are common. Oxidized and partially

chloritized biotite is pleochroic, X = yellowish-brown, Y = brown, Z = dark brown or reddish-brown. Prismatic crystals of brownish-green hornblende ($c \wedge Z = 15^\circ$) were found in a specimen from West Fork Gila River, and accessory minerals include opaque oxides, sphene, apatite, and zircon. Green clay, sericite, and kaolinite occur as alteration products. In areas of intense hydrothermal alteration close to the Mogollon Range fault, calcite and fluorite replace some feldspathic xenoliths in the rock.

An isopach map was drawn to illustrate the distribution and thickness of Deadwood Gulch Rhyolite in the western part of the Mogollon Plateau (Fig. 2). The major features are the Dry Creek and Hell's Hole structural basins filled with tuffs and tuffaceous sediments of Deadwood Gulch Rhyolite. Positive areas apparently not covered by Deadwood Gulch extend along the northern, northwestern, and western margins of the Dry Creek basin, and a ridge of positive ground extends northward from the northern part of the Diablo Mountains to include the Jerky Mountains. The Hell's Hole basin is apparently bordered on the west by fault blocks, whereas the Dry Creek basin is a structural sag developed by warping rather than faulting (see section on structure). Deadwood Gulch Rhyolite is approximately 1,000 feet thick in each of these basins, and thins to zero at the basin margins.

Two general facies can be recognized within the formation. The central part of the Dry Creek basin consists of massive, vesicular tuffs, whereas north of Whitewater Creek both massive

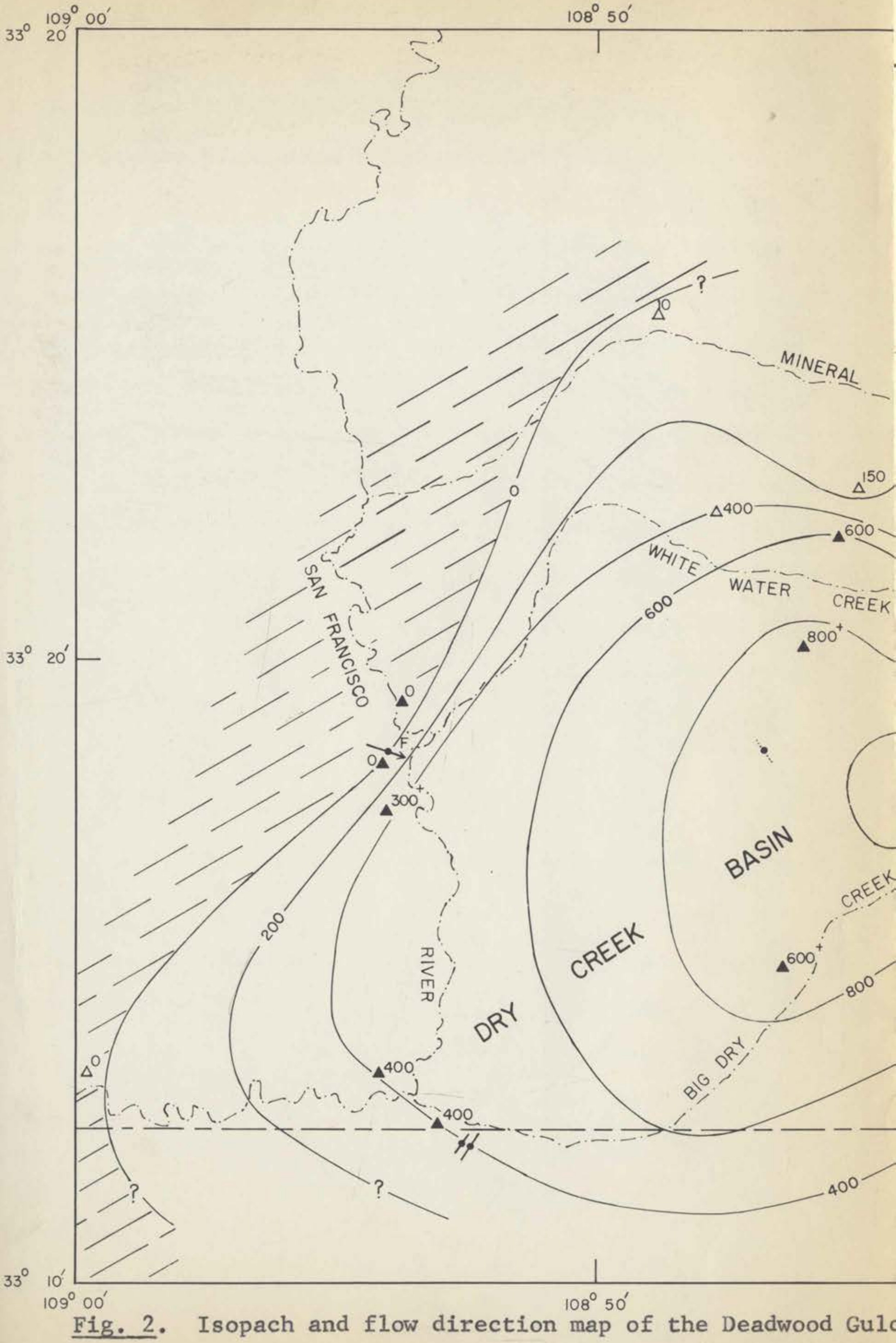

Fig. 2. Isopach and flow direction map of the Deadwood Gulc

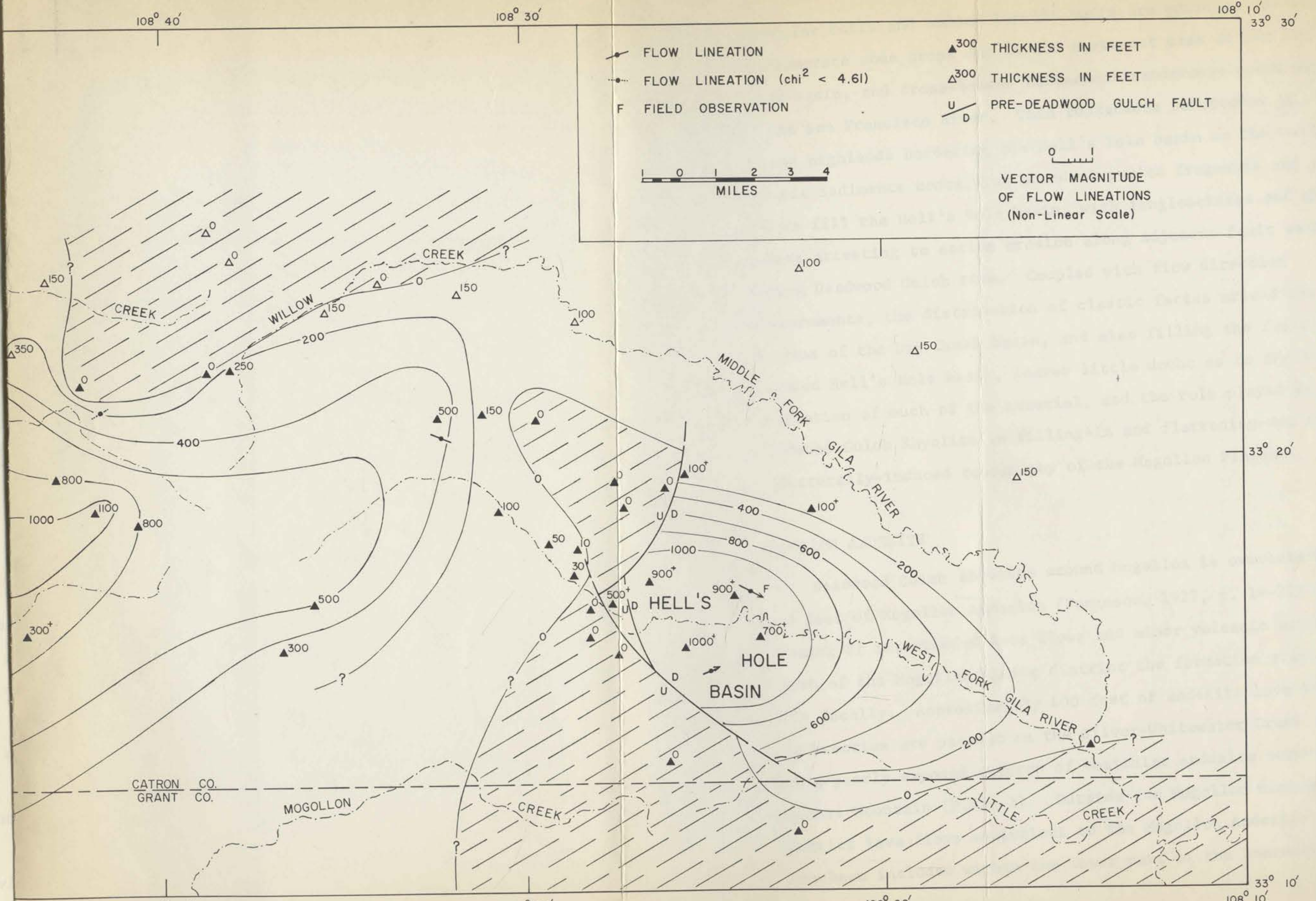
108° 40'
108° 30'
108° 10'
33° 30'
33° 20'
33° 10'
108° 20'
FLOW LINEATION
FLOW LINEATION (chi² < 4.61)
F FIELD OBSERVATION
▲300 THICKNESS IN FEET
△300 THICKNESS IN FEET
U D PRE-DEADWOOD GULCH FAULT
1 0 1 2 3 4
MILES
VECTOR MAGNITUDE OF FLOW LINEATIONS (Non-Linear Scale)
WILLOW CREEK
MIDDLE FORK GILA RIVER
WEST FORK GILA RIVER
HELL'S HOLE BASIN
CATRON CO.
GRANT CO.
MOGOLLON CREEK
LITTLE CREEK
0
50
100
150
200
250
300
350
400
500
600
700
800
900
1000
1100
?

h Rhyolite.

vesicular tuffs and bedded lapilli tuffs are present. An upper conglomerate zone crops out in the northeast part of the Dry Creek basin, and cross-bedded tuffaceous sandstones occur west of the San Francisco River. Thin tuffaceous sandstones lap on to the highlands bordering the Hell's Hole basin on the west. Clastic sediments containing abundant pumice fragments and glass shards fill the Hell's Hole basin, with fanglomerates and gravel washes attesting to active erosion along adjacent fault scarps during Deadwood Gulch time. Coupled with flow direction measurements, the distribution of clastic facies around the margins of the Dry Creek basin, and also filling the fault-bounded Hell's Hole basin, leaves little doubt as to the local derivation of much of the material, and the role played by Deadwood Gulch Rhyolite in filling-in and flattening-out the structurally-induced topography of the Mogollon Plateau.

MOGOLLON ANDESITE

Deadwood Gulch Rhyolite around Mogollon is overlain by 250-600 feet of Mogollon Andesite (Ferguson, 1927, p. 19-21) consisting of interbedded lava flows and minor volcanic breccias. South of the Mogollon mining district the formation crops out only locally. Approximately 400 feet of andesite lava flows and breccias are present on the Silver-Whitewater Creek divide and a poorly exposed outcrop of vesicular andesite occurs near Nabours Mountain (Plate 1). Outside the Mogollon mining district lava flows equivalent to the Mogollon Andesite may have been included within the lower part of the Bearwallow

Mountain Formation, from which they cannot always be distinguished on lithological grounds.

Mogollon Andesite is holocrystalline and porphyritic and contains phenocrysts up to 3 mm in size in a groundmass of felty, elongated plagioclase laths. Plagioclase phenocrysts (An_{25}-An_{60}) are commonly zoned from andesine to labradorite. Augite occurs as small grains in the groundmass whereas orthopyroxene forms larger phenocrysts. Iddingsite occurs sporadically and may be associated with hematite and green antigorite, probably pseudomorphous after olivine (Sun, 1957). Rare primary interstitial quartz is present and accessory minerals include opaque oxides and apatite.

BEARWALLOW MOUNTAIN FORMATION

The youngest volcanic rocks in the western part of the Mogollon Plateau consist of dark-colored lavas, breccias, and agglomerates ranging in composition from basaltic andesite to quartz latite, collectively mapped as the Bearwallow Mountain Formation which was named after a probable eruptive center on Bearwallow Mountain, a prominent peak north of the mapped area (Elston, 1968). Porphyritic vesicular and amygdaloidal lavas predominate, frequently oxidized and scoriaceous near extrusive vents. Volcanic basaltic bombs with twisted teardrop shapes were found in White Creek in a cinder bed interbedded with lava flows, and the flanks of Mogollon Baldy are littered with fragments of bombs.

Three basaltic vents were tentatively identified within the mapped area (Fig. 3), all of which are topographically expressed by the local drainage patterns. Willow Creek and its tributaries apparently outline a caldera approximately 3 miles in diameter. The Mogollon Baldy caldera is outlined by West Fork Mogollon Creek and Gobbler Canyon, and is breached on the south by Lookout Canyon. A small circular vent filled with basaltic agglomerate and lava is situated about 1 mile west of Glenwood. The vent is approximately 1 mile in diameter, and basaltic andesite forming its southern rim has a near-vertical contact with Mineral Creek Andesite and Fanney Rhyolite. Over 1,000 feet of basaltic lava crops out at each volcanic center, but elsewhere the Bearwallow Mountain Formation is substantially thinner.

Considerable variation in texture, mineralogy, and composition exists within the Bearwallow Mountain Formation and five distinct petrographic types were recognized. Each type appears to be associated with a specific volcanic center.

Type I. Olivine-clinopyroxene basaltic andesite: Olivine- or iddingsite-bearing basaltic andesite crops out on Mogollon Baldy and to the east of the Mogollon Range, and appears to be associated primarily with the Mogollon Baldy center. Similar rocks occur also outside the mapped area on Black Mountain. Olivine-clinopyroxene basaltic andesites are usually holocrystalline, vesicular, equigranular, and medium-grained. Abundant subhedral plagioclase laths having compositions An_{54}-

An_{75} are commonly strongly zoned and twinned according to Carlsbad, albite, and pericline laws. Flakes of reddish-brown iddingsite are prominent and commonly surround relict cores of olivine (Plate 8). Pale green anhedral grains of clinopyroxene are common whereas orthopyroxene is rare. Partially chloritized biotite occurs in trace amounts associated with clinopyroxene, and is pleochroic, X = yellowish-brown, Y = brown, Z = dark brown. Accessory minerals include opaque oxides, apatite, and zircon. Amygdales of calcite, chlorite, and zeolites are present and veinlets of alkali feldspar(?) occur in basaltic andesite from Lilley Mountain. Rare xenocrysts of quartz, rimmed with calcite and clinopyroxene, are present.

A chemical analysis of olivine-clinopyroxene basaltic andesite is given in Table 5, no. 7, and a modal analysis of the same rock is given in Table 9.

Type II. Orthopyroxene-clinopyroxene andesite: Andesitic rocks of Type II are distinguished from Type I by the relative proportions of olivine (or iddingsite) and orthopyroxene. They crop out west of the San Francisco River and around the Willow Mountain caldera (Fig. 3). Iddingsite-bearing Type II andesite, intermediate with Type I, was found on Mogollon Baldy, and Type II orthopyroxene-clinopyroxene andesites crop out on Black Mountain, outside the mapped area.

Type II andesites vary from holocrystalline equigranular to porphyritic with plagioclase and pyroxene phenocrysts up to 3 mm in an aphanitic groundmass. A characteristic variety

Table 9. Modal analyses of representative specimens from the Bearwallow Mountain Formation determined using a Swift point counter.

	1	2	3	4
	Type I	Type II	Type III	Type V
Groundmass	1.6	90.3	56.6	79.1
Plagioclase	59.1	7.4	30.5	15.5
Olivine (incl. iddingsite)	17.5	-	-	-
Orthopyroxene	0.8	2.1	0.9	-
Clinopyroxene	17.5	0.2	0.2	0.6
Oxyhornblende	-	-	11.8*	-
Biotite	-	-	-	3.6
Opaque oxides	3.5	tr	tr	1.2
Accessories	tr	tr	tr	tr
Total	100.0	100.0	100.0	100.0
Points counted	1,008	1,065	1,165	1,164
Plagioclase composition	An_{75-56}	An_{65-47}	An_{56-41}	An_{40-25}

(*) includes opaque oxides
tr = trace

Location of samples: (1) West Fork Gila River near White Creek cabin (sec. 12, T.12 S., R.16 W.) (chemical analysis in Table 5, column 7); (2) Willow Mountain (sec. 11, T.11 S., R.18 W.); (3) Iron Creek (sec. 9, T.11 S., R.17 W.) (chemical analysis in Table 5, column 8); (4) Mogollon Baldy (sec. 10, T.12 S., R.17 W.) (chemical analysis in Table 5, column 9).

contains phenocrysts set in microlitic groundmass with strong flow orientation (Plate 9). Vesicular andesites commonly contain amygdales of calcite and zeolites. Phenocrysts and microlites of plagioclase (An_{42}-An_{66}) are twinned according to albite, pericline, and Carlsbad laws and display normal and oscillatory zoning. Phenocrysts of orthopyroxene predominate and are pleochroic from pale green to pale red. Less abundant, slightly zoned clinopyroxene occurs in the groundmass and forms rims around orthopyroxene phenocrysts. Iddingsite, with rare relict cores of olivine, is sparse but increases in abundance as Type II andesites grade into Type I basaltic andesites. Biotite occurs in traces and accessory minerals include opaque oxides and apatite. Calcite and sericite are alteration products of plagioclase. Highly embayed and resorbed xenocrysts of quartz with reaction rims of calcite, clinopyroxene, and subordinate zeolites are rare.

A modal analysis of porphyritic Type II andesite from Willow Mountain is given (Table 9).

Type III. Hornblende-orthopyroxene latite: Melanocratic reddish-black latites crop out east of Willow Mountain where they are in fault contact with Type II andesites, and a faulted outlier of hornblende-orthopyroxene latite crops out in the Diablo Mountains, overlying Jerky Mountain Rhyolite. Hornblende-bearing latites are porphyritic, with phenocrysts of plagioclase and oxyhornblende up to 5 mm long in aphanitic groundmass (Plate 10). Phenocrysts and microlites of

plagioclase (An_{34}-An_{56}) usually have strong normal and oscillatory zoning and have rare optically discontinuous rims or anti-perthitic texture. Oxidized oxyhornblende is the dominant ferromagnesian mineral and is pleochroic, X = yellowish-brown, Y = reddish-brown, Z = dark reddish-brown. Pale green phenocrysts of orthopyroxene are common and are commonly rimmed with oxyhornblende. Pale green clinopyroxene is less abundant and usually occurs in the groundmass. Rare oxidized biotite is pleochroic from yellowish-brown to dark brown. Rounded quartz grains without reaction rims occur in several thin sections and in the groundmass of some specimens. Staining techniques failed to indicate the presence of potassium feldspar, possibly due to the aphanitic nature of the groundmass. Accessory minerals include opaque oxides, chlorite, and apatite while secondary calcite and zeolites are present.

A chemical analysis of hornblende-orthopyroxene latite is given in Table 5, no. 8, and a modal analysis of the same rock is given in Table 9.

Type IV. Biotite-orthopyroxene-clinopyroxene latite: This rock type was not found in the mapped area but corresponds to the Pelona Latite of Elston (1968, p. 239), and the specimen examined was provided by W. E. Elston from the central plug at Pelona Mountain in the northern part of the Mogollon Plateau. In view of its petrographic and mineralogic continuity with other members of the Bearwallow Mountain suite, I consider this rock to represent part of the Bearwallow Mountain petrologic

series. The rock is holocrystalline, equigranular, and hypidiomorphic. Plagioclase (An_{26}-An_{47}) is usually strongly zoned and twinned according to albite, pericline, and Carlsbad laws. Biotite is the dominant ferromagnesian mineral and is pleochroic from pale to dark brown. Orthopyroxene occurs as large crystals and is commonly rimmed with clinopyroxene, which occurs also as small grains in the groundmass. Anhedral quartz and sanidine (confirmed by staining techniques) are present in the groundmass, and sanidine forms rims around some plagioclase crystals.

Type V. Biotite-clinopyroxene quartz latite: This rock was found as a small dike on the flanks of Mogollon Baldy and is distinguished from Type IV latite by the absence of orthopyroxene. It is holocrystalline and porphyritic with phenocrysts up to 5 mm in an aphanitic groundmass (Plate 11). Plagioclase (An_{25}-An_{40}) occurs as phenocrysts and microlites that display strong normal zoning and are twinned according to albite, pericline, and Carlsbad laws. Biotite, pleochroic X = pale yellowish-brown, Y = brown, Z = dark brown, is the dominant ferromagnesian mineral. Phenocrysts of pale green clinopyroxene are usually associated with opaque oxides. Quartz and sanidine (identified by staining techniques) occur in the groundmass but individual crystals are too small to be optically resolved. Accessory minerals include opaque oxides, apatite, and zircon.

A chemical analysis of biotite-clinopyroxene quartz latite

is given (Table 5, no. 9), and a modal analysis of the same rock is given in Table 9.

REGIONAL STRATIGRAPHIC CORRELATIONS

Reconnaissance geologic mapping in southwestern New Mexico has resulted in the extension of the Datil Formation (or Datil Group) from its type locality north of the San Augustin Plains to include almost all pre-Bearwallow Mountain volcanic rocks in the Mogollon Plateau region. A recent discussion of Tertiary volcanic stratigraphy and the "Datil" problem was given by Elston (1968), who concluded that the "Datil" consists of at least three eruptive cycles. Elston distinguished between Datil (restricted sense), the oldest cycle encompassing rocks approximately 38-29 m.y. old, and Datil (broad sense), including rocks as young as 20 m.y.. In the western part of the Mogollon Plateau, I have recognized a three-fold subdivision of the volcanic rocks into Lower, Middle, and Upper Volcanic Groups, a subdivision that can probably be extended to cover most of the Mogollon Plateau complex (Elston, 1968, p. 238). The Lower Volcanic Group corresponds to Datil (restricted sense) of Elston (1968) whereas the other two groups are included within Datil (broad sense). Additional field work and radiometric dating are required before the "Datil" problem can be resolved on a regional scale and consequently terminology and regional correlations employed in this section are tentative.

Rocks of at least three volcanic provinces are included within Datil (restricted sense). These are (1) the Mimbres Valley and southern Black Range province in the southeastern part of the Mogollon Plateau; (2) the Tadpole Ridge-Cooney province in the southwestern part of the Mogollon Plateau; and (3) the type-Datil province in the northern part of the Mogollon Plateau. The best known of these is the Mimbres Valley and southern Black Range province which was studied by Jicha (1954), Kuellmer (1954), and Elston (1957). These rocks range from 29.8 m.y. for Caballo Blanco Rhyolite to 33.4 m.y. for Kneeling Nun Rhyolite, but the underlying Sugarlump Rhyolite and Rubio Peak Formation are as yet undated (Elston, Bikerman, and Damon, 1968). A vent for Kneeling Nun Rhyolite occurs in the southern Black Range (Kuellmer, 1954). Rocks of the Mimbres Valley province are separated from the Tadpole Ridge-Cooney province by the Santa Rita-Hanover topographical and structural high (Elston, Coney, and Rhodes, 1968). The Cooney Formation in the Mogollon Range is of unknown age but is lithologically similar to Tadpole Ridge Quartz Latite (31.2 m.y.) with which it is tentatively correlated (Fig. 4). Flow direction studies on both these units indicate derivation from the southwest. Similar southwesterly flow lineations were obtained for the Mineral Creek and Houston Andesites in the Mogollon Range (see section on flow direction studies) and for the lower andesite units (Tda_1) around Reserve and the San Augustin Plains (G. A. Krimsky, personal communication). These

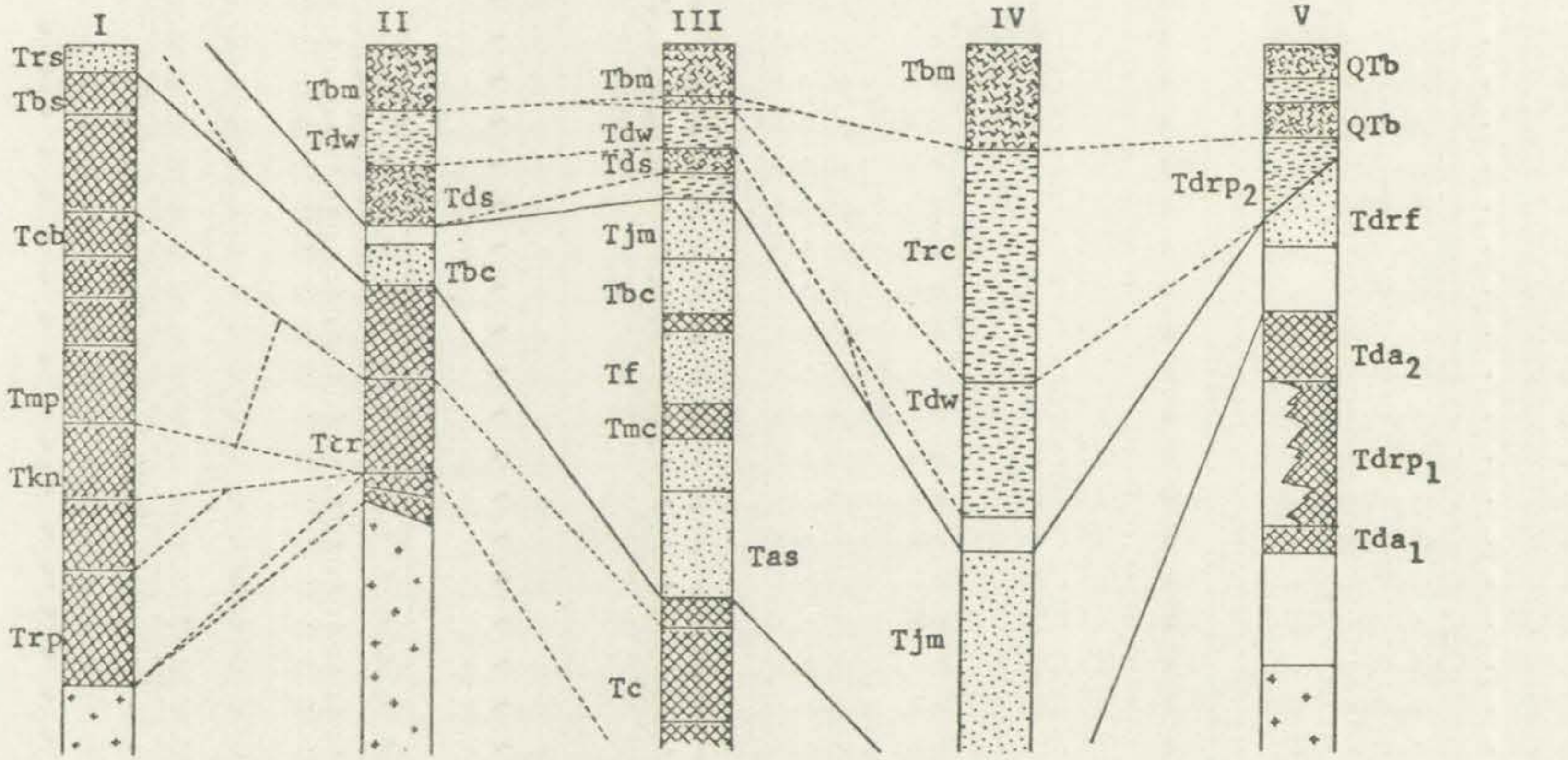

I. Dwyer Quadrangle (Elston, 1957); II. Pinos Altos Range (Elston, Coney, and Rhodes, 1968); III. Mogollon Range (this report); IV. O-Bar-O Mountain Quadrangle (Rhodes, unpublished data); V. Pelona Quadrangle (Stearns, 1962).

Trs-Swartz Rhyolite; Tbs-Bear Springs Basalt; Tcb-Caballo Blanco Rhyolite; Tmp-Mimbres Peak Rhyolite; Tkn-Kneeling Nun Rhyolite; Trp-Rubio Peak Andesite; Tbm-Bearwallow Mountain Formation; Tdw-Deadwood Gulch Rhyolite; Tds-Double Spring Andesite; Tbc-Bloodgood Canyon Rhyolite; Ttr-Tadpole Ridge Quartz Latite; Tjm-Jerky Mountain Rhyolite; Tf-Fanney Rhyolite; Tmc-Mineral Creek Andesite; Tas-Apache Spring Quartz Latite; Tc-Cooney Formation; Trc-Railroad Canyon Rhyolite; Tda-andesites; Tdrp-felsic ash-flows; Tdrf-rhyolite lavas.

░ **Felsic Suite** Upper Volcanic Group	▒ Mafic Suite Upper Volcanic Suite	☐ Sedimentary rocks
▤ Middle Volcanic Group	▩ Lower Volcanic Group	⁘ Basement rocks

Fig. 4. Regional correlation chart for the northern, western and southern parts of the Mogollon Plateau volcanic complex.

are all interpreted as belonging to the Tadpole Ridge-Cooney province. Volcanic rocks north of the San Augustin Plains, including the Hell's Mesa member of the Datil (Tonking, 1957), and the lower rhyolite ($Tdrp_1$) and upper andesite (Tda_2) around the San Augustin Plains (Stearns, 1962), belong to the type-Datil province, from which G. A. Krimsky (personal communication) obtained northwesterly flow lineations.

Rocks of the Middle Volcanic Group are separated from the Lower Volcanic Group by a regional unconformity. The Middle Volcanic Group consists of two major ash-flow sheets, the Apache Spring Quartz Latite and Bloodgood Canyon Rhyolite, and related bodies of Fanney and Jerky Mountain flow-banded rhyolite lavas. The middle rhyolite unit ($Tdrp_2$) around the San Augustin Plains (Stearns, 1962) probably represents, in part, the distal ends of Apache Spring and Bloodgood Canyon ash-flow sheets. The Last Chance Andesite at Mogollon (Ferguson, 1927) is interpreted as part of the Tadpole Ridge-Cooney province that is interfingered with the base of the Middle Volcanic Group.

The extensive Upper Volcanic Group includes several felsic and mafic rock units which lie unconformably upon older formations. In the western part of the Mogollon Plateau volcanic complex the group includes felsic rocks such as Deadwood Gulch Rhyolite, quartz latite at Turkeyfeather Creek, latite domes at Willow Creek and John Kerr Peak, and moonstone-bearing rhyolite tuff (Railroad Canyon Rhyolite?) in the O-Bar-O Mountain area

(R. C. Rhodes, unpublished data). Mafic rocks include Double Spring Andesite and the Bearwallow Mountain Formation. Tentative regional correlation between rocks of the Upper Volcanic Group is given in Fig. 5.

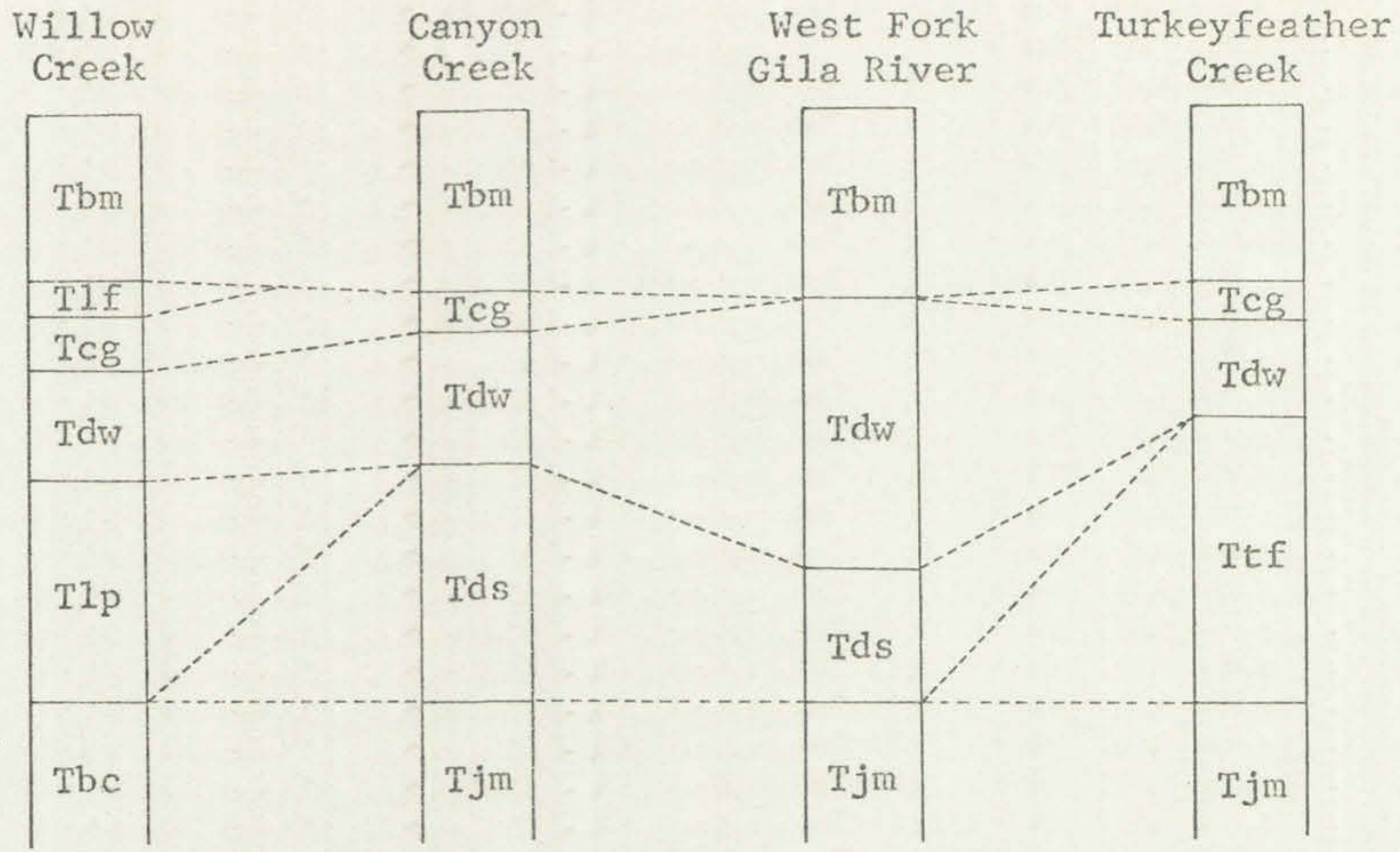

Tbm-Bearwallow Mountain Formation; Tlf-latite flows; Tcg-conglomerate; Tdw-Deadwood Gulch Rhyolite; Tlp-porphyritic latite flows; Ttf-quartz latite at Turkeyfeather Creek; Tds-Double Spring Andesite; Tjm-Jerky Mountain Rhyolite; Tbc-Bloodgood Canyon Rhyolite.
Willow Creek and Canyon Creek sections from P. J. Coney (unpublished data).

Fig. 5. Regional correlation chart for the Upper Volcanic Group in the western part of the Mogollon Plateau complex.

INTRUSIVE ROCKS

Numerous dikes of rhyolite and diabase along the front of the Mogollon Range are aligned parallel to the Mogollon Range fault, and rhyolite dikes are intruded also nearer the margin of the Bursum cauldron and west of the San Francisco graben. They vary from a few inches to tens of feet wide. Rhyolite dikes appear to be equivalent in age to Fanney Rhyolite, as they intrude all pre-Fanney formations but not younger rocks. Diabase dikes are intrusive into the Cooney Formation and Houston Andesite. Most rhyolite intrusives are probably feeder dikes for Fanney lava flows. Alteration is extensive and the granophyric groundmass is usually coarser-grained than in extrusive Fanney Rhyolite. Altered diabase dikes are less common and are holocrystalline, equigranular, and medium-grained. Calcitized and sericitized plagioclase, chlorite associated with relict biotite or pseudomorphous after pyroxene, and aggregates of anhedral quartz are the dominant minerals. Kaolinized sanidine is rare and accessory minerals include opaque oxides and zircon.

Quartz porphyry dikes resembling Sacaton Quartz Latite intrude Houston Andesite in the Sacaton Creek area. Prominent phenocrysts of zoned plagioclase are partially altered to calcite while quartz and sanidine occur in the groundmass. Chloritized biotite and fibrous zeolites are present.

GILA CONGLOMERATE

The term "Gila Conglomerate" was applied to alluvial sediments in the San Francisco Valley by Gilbert (1875) and is used today to include "...poorly- to well-consolidated alluvial materials that are deposited in the structural valleys of the Gila River and some of its tributaries" (Heindl, 1952, p. 113). Description of stratigraphic sections in the upper San Francisco Valley was given by Heindl (1962, p. 79-81). Over 700 feet of Gila Conglomerate crop out and are interbedded with thin basalt flows near the foot of Glenwood Brushy Mountain. Contacts between valley fill and Tertiary volcanics on each side of the San Francisco Valley are generally faulted but, where sediment overlaps on to the volcanics, fresh basalt grades upward into weathered rubbly regolith and finally into typical Gila Conglomerate. Dips of the Gila are generally a few degrees toward the center of the graben.

Three interfingering sedimentary facies are present in the Gila Conglomerate (Fig. 6), becoming finer-grained toward the center of the basin. Fanglomerates flank each side of the valley, forming facies belts a few hundred yards wide in the west and up to a mile in the east. Fanglomerates grade laterally into a coarse sandstone facies which consists of cross-bedded sandstones and gravels with numerous scour-and-fill channels. Pebbles of basalt, rhyolite, and locally-derived mud pellets are common. Toward the center of the

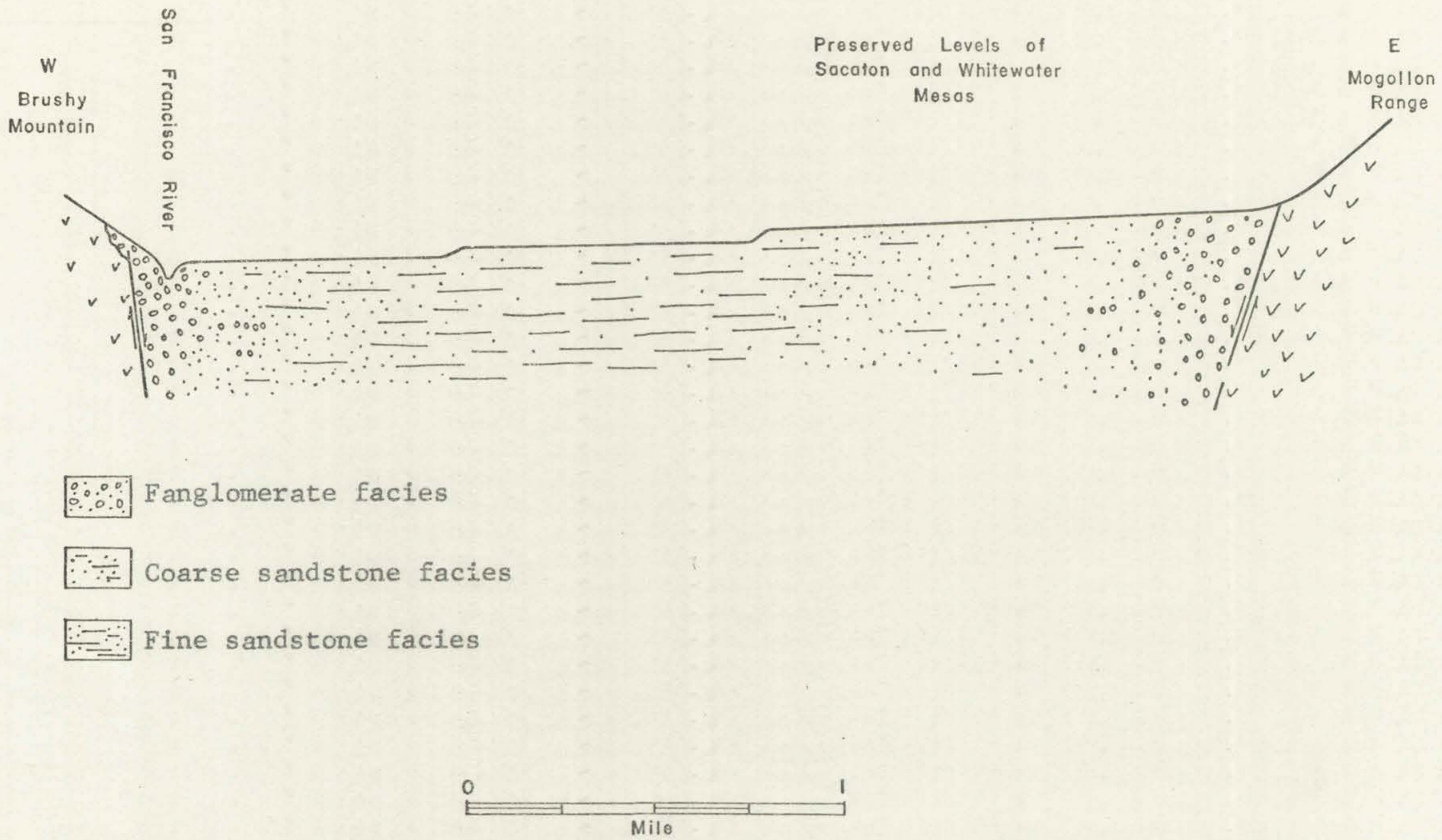

Fig. 6. Diagrammatic cross-section through the San Francisco Valley showing lateral facies changes in the Gila Conglomerate.

valley, the coarse sandstone facies passes into a fine sandstone facies, characterized by evenly-bedded, fine-grained sandstones and mudstones, an absence of cross-beds, and a paucity of gravel washes. Mud pellets are common.

SURFICIAL DEPOSITS

PEDIMENT AND TERRACE GRAVELS

Unconsolidated pediment gravels lie upon flat surfaces cut across Gila Conglomerate in the San Francisco Valley, but were not mapped separately from older Gila sediments. Likewise, pediment surfaces east of the Mogollon and Jerky Mountains are veneered with several feet of gravel containing rounded boulders of basalt and rhyolite.

High level terrace gravels were found west of Glenwood where they probably occupy an old meander channel of the San Francisco River.

ALLUVIUM

Alluvium is found in the beds of larger creeks in the area and forms the floor of an incipient floodplain along the San Francisco River. Rounded pebbles and boulders of locally-derived volcanic rocks are associated with alluvial sand and silt.

TALUS

Talus blankets many steep slopes but was not mapped separately from underlying bedrock. Large rock slides several hundred yards long and tens of yards wide are common in the Mogollon Range, and consist of poorly-rounded boulders.

STRUCTURAL GEOLOGY

VOLCANO-TECTONIC STRUCTURES

Two volcano-tectonic ash-flow cauldrons were recognized in the mapped area but the reconnaissance nature of field work prevented anything but rudimentary investigation of them. Apache Spring Quartz Latite in the Mogollon Range is confined to the Bursum cauldron (Elston, Coney, and Rhodes, 1968), which I interpret as a large collapse cauldron related to extrusion of hundreds of cubic kilometers of Apache Spring ash-flow tuffs. Only the southern margin of the cauldron is fully exposed. The western margin is concealed beneath younger formations downthrown by faults, and the eastern margin is buried beneath Bloodgood Canyon and Jerky Mountain Rhyolites. It is not known whether the eastern rim is present in the subsurface, perhaps overlapped by the younger Gila Cliff Dwellings cauldron, or whether the cauldron is asymmetrically developed with the northern and eastern sides simply merging into the larger volcano-tectonic basin (Elston, Coney, and Rhodes, 1968, p. 283). Volcano-tectonic collapse of the Bursum cauldron may have taken place concurrently with extrusion of the ash flows. Distribution of the Sacaton Quartz Latite and Fanney Rhyolite lava flows, described earlier, suggest late-stage resurgent doming of Apache Spring Quartz Latite in the Bursum cauldron.

Within the mapped area, Bloodgood Canyon Rhyolite is confined to the Gila Cliff Dwellings cauldron, which is also

incompletely delineated (Elston, Coney, and Rhodes, 1968). Zones of hematite staining and closely spaced cleavage planes occur in Little Creek close to the postulated cauldron margin. Faulting has obscured the western side of the Gila Cliff Dwellings cauldron.

FAULTING AND WARPING

Widespread faulting followed cessation of Bearwallow Mountain volcanism and continued intermittently during, and after, deposition of the Gila Conglomerate. Faults are of the high-angle, tensional type and generally follow pre-existing structural trends resulting, in the mapped area, in a north-northwesterly alignment with a subordinate set at right angles.

The late Tertiary structure of the mapped area is dominated by two grabens separated by a horst that forms the core of the Mogollon Mountains (Plate 12). The San Francisco graben in the west is a deep, asymmetrical trough, trending approximately north-northwest, bordered by the Mogollon Range and San Francisco faults on the east and west side respectively. The graben is filled to unknown depth with Gila Conglomerate and throw on the Mogollon Range fault is estimated at 5,000-10,000 feet. The San Francisco fault is downthrown approximately 1,000 feet on the east and the fault plane dips 75^{o}-85^{o}E. Subordinate fractures on the western side of the graben are probably related to the major San Francisco fault, and the Frisco Hot Springs may be located on one of these secondary fractures. The Turkeyfeather graben is a local structure and is floored with

Bearwallow Mountain basaltic andesite and a thin veneer of pediment gravel. It trends north-northwest and is delineated on the west and east sides by the Whitewater Baldy and Jerky Mountain faults respectively, both of which cause more than 2,000 feet of stratigraphic separation. The graben is cut off in the south by cross-fractures and is finally terminated against masses of flow-banded rhyolite in the Diablo Mountains.

Fanney Rhyolite in the Mogollon Range is truncated on the west and south sides by the Nabours Mountain and Indian Peak faults respectively (Plate 12), which outline a crescent-shaped block hinged near Sheridan Mountain. Displacement ranges from over 1,000 feet on the northern and eastern ends of the two faults to a few hundred feet at the hinge.

The Ring Canyon fault is the most important fracture in the eastern part of the mapped area. Displacement appears to have been several thousand feet, downthrown to the west, and the fault probably follows in part the pre-existing structural trends along the western margin of the Gila Cliff Dwellings cauldron. The area between the Ring Canyon and Jerky Mountain faults contains several horsts and grabens which may be related to fractures pre-dating Deadwood Gulch Rhyolite.

An isopach map of Deadwood Gulch Rhyolite shows two structural basins in the mapped area (Fig. 2). The Dry Creek basin is a closed synclinal structure elongated east-northeast and centered on the Mogollon Range, with the axis of the syncline radial to the central Gila Basin. The Hell's Hole basin farther east was bounded on the west by uplifted fault

blocks now represented by the Jerky and Diablo Mountains.

REGIONAL TECTONIC SYNTHESIS

In order to explain the structure of the mapped area and to relate it to the overall structure of the Mogollon Plateau volcanic complex, a regional tectonic map of the Mogollon Plateau and its environs was compiled (Plate 13). This map supersedes an older, schematic tectonic compilation given by Elston, Coney, and Rhodes (1968, Plate 1). Data are generally scanty and were derived mainly from the geologic map of New Mexico (Dane and Bachman, 1965) with details of structure taken directly from published original sources. Additional information was obtained from unpublished data of P. J. Coney and W. E. Elston, while details in the San Mateo Mountains were obtained from unpublished reports (Farkas, 1968; Furlow, 1965). General discussions on regional tectonics of parts of southern New Mexico were given by Kelley (1955), Trauger (1965), and Elston (1958).

Mapping of Tertiary volcanics in southwestern New Mexico has not yet advanced sufficiently past the reconnaissance stage to enable detailed tectonic interpretations to be made, although certain conclusions regarding first-order structural relationships can be put forward. Elston, Coney, and Rhodes (1968, p. 277) pointed out that the Mogollon Plateau is not associated with a geosynclinal-orogenic cycle, but is situated about 75 miles north of the Mexican and Sonoran geosynclines and also falls between the Laramide and Cascadian orogenies in

age. Calc-alkalic volcanism of the Mogollon Plateau is associated with a relatively stable continental platform characterized by vertical basin-and-swell tectonics. Elston (1960b) showed that andesites thicken and thin in response to regional tectonic control, and two basins in which thick andesite sections are preserved have been recognized in the Dwyer and Virden Quadrangles (Plate 13). Elston (1960b, p. 58) suggested that andesites filling these structural basins represent collapsed volcanoes, and recent flow direction studies tend to support this hypothesis. A thick accumulation of volcanically-derived clastic sediments northwest of the Mogollon Plateau has been named the Datil sedimentary basin (Plate 13) but little is known of the paleotectonics of this area.

Preliminary data, therefore, indicate that prior to eruption of Apache Spring Quartz Latite, the Mogollon Plateau was flanked on the south, west, and northwest by peripheral subsiding structural basins, some of which were the sites of andesitic volcanic centers. The central area later became the site of large-scale ash-flow eruptions and volcano-tectonic collapse. A similar pattern of volcanism and tectonism was described from Sumatra by van Bemmelen (1961, p. 402):

> "...the ignimbrite eruptions cause volcano-tectonic collapses on the crest of rising anticlines or tumors, whereas the andesitic volcanoes form protruberances on the back of subsiding geanticlines or tumors."

The significance of intrusive-extrusive complexes of flow-banded rhyolite as indicators of regional geologic

structure was discussed by Elston (1965b, p. 173-174). The locations of extrusive rhyolite lavas forming the structural framework of the Mogollon Plateau complex, are shown (Plate 13). Extrusions of this nature are not known from north of the San Augustin Plains nor from the Blue Mountains in Arizona, except near the Red Mountain caldera (Ratté _et_ _al_., 1969) and they appear to be restricted to volcanic vents associated with regional fracture systems. Elston (1965c) pointed out the relationship between surface extrusions of flow-banded rhyolite and sub-volcanic ring dikes in more deeply eroded terrains.

Volcano-tectonic collapse of the Mogollon Plateau can be likened to structural evolution of a sedimentary basin and will be discussed in relation to the basin-development concepts of Dallmus (1958). In three-dimensional consideration, the area of subsidence forms the base of a cone-shaped solid having its apex at the center of the Earth. The base of the cone has the curved shape of a segment of a sphere and its outer rim corresponds to the intersection of the sides of the cone with the surface of a sphere. This outer rim is comparable to a series of inflexion points. The apical angle of the cone at the center of the Earth subtends a chord connecting opposing inflection points, and also the arc corresponding to the curved shape of the spherical segment. Subsidence of the circular sector involves vertical translation of the arc toward the position of the chord resulting in crowding of the arc into the area of the chord and consequently shortening the length of the arc. This crowding of the spherical segment into a

cone generates lateral compression which gives rise to characteristic structural elements in the upper parts of the crust.

The most prominent structural feature of the Mogollon Plateau is the central depressed basin, named the Gila Sag by Trauger (1965), enclosed within a mountainous raised rim. The mountains forming the rim tend to be faulted asymmetric anticlinoria (Plate 13) and the overall structure of the Mogollon Plateau is that of a saucer-shaped central depression surrounded by a raised anticlinal rim. Superimposed upon the raised rim in the west and southwest are culminations and depressions radial to the central basin (Plate 13) but it awaits further detailed mapping of other parts of the rim to determine whether radial folds occur along the entire circumference of the structure.

Volcano-tectonic subsidence of the central Gila Basin probably began in pre-Deadwood Gulch time. Double Spring Andesite appears to be restricted to the central parts of the basin and Deadwood Gulch Rhyolite is 100-400 feet thick over much of the northern part of the Mogollon Plateau. During this time the volcano-tectonic complex responded as a structural entity to collapse of the upper crust, possibly brought about by withdrawal of magma at depth. The uplifted peripheral rim of the complex lies outside the inflection points of the central area of subsidence and, if the crust behaves as a unit, then it follows that the inflection points are points of rotation, and negative movement on the basinward side should be countered by positive movement on the outward side. Such a system can be

compared with a simple lever pivoting about a fulcrum (the points of inflection). This view, however, is oversimplified as the crust is continuous beyond the limits of the peripheral rim and creates drag on the uplifted segment. Accordingly, a more realistic analog would be that of a beam of three spans, fixed at either end and with a load applied to the center. The western half of such a system (Fig. 7) has the supporting or inflection point located in the vicinity of the Jerky Mountains. Continued subsidence of the central basin probably caused tensional forces to build up until fracturing was initiated, allowing the basin to collapse further along faults located on the basinward side of the inflection point, thereby accounting for the development of the Hell's Hole basin in pre-Deadwood Gulch time. Continued post-volcanic subsidence of the central basin may have caused arching of a peripheral anticline. The region between the fixed end and the inflection point was bowed upward and became a zone of tensional faulting bordered on the west by a peripheral fault system. Major displacement occurred on the Mogollon Range fault as a result of stress compensation between the uplifted Mogollon Range arch and the fixed end of the beam system (Fig. 7) and the San Francisco fault probably developed in response to secondary stress brought about by this displacement, thereby forming the asymmetrical San Francisco graben. The smaller Turkeyfeather graben may have developed by a similar mechanism due to stress differences between the Mogollon Range arch and the inflection point.

An application of the concept of spurs and sags in basin compared with a simple lever pivoting about a fulcrum (the point of inflection). This view, however, is oversimplified as the crust is continuous beyond the limits of the peripheral thrust and thrust belt to a tilted segment. Accordingly, a more realistic analog would be that of a beam of three spans, fixed at either end and with a load applied to the center. The western half of such a system (Fig. 7) has the properties of inflection point located in the vicinity of the early thrusts. Continued subsidence of the central basin probably caused tensional forces to build up until the faulting was initiated, allowing the basin to collapse further along faults located on the eastward side of the inflection point, thereby accounting for the development of the Hall's Hole basin in pre-Oakland time. Continued post-volcanic subsidence of the central basin may have caused arching of a peripheral anticline. The strata between the flank and the inflection point was bowed upward and became a zone of tensional faulting bordered on the west by a peripheral fault system. Major displacement occurred on the Hagerman Range fault as a result of stress concentration between the uplifted Hagerman Range arch and the fixed end of the beam system (Fig. 7) and the San Francisco fault probably developed in response to secondary stress brought about by this displacement, thereby forming the Hagerman-San Francisco graben. The smaller fault and grabens may have developed by a similar mechanism due to stress differences between the peripheral faults and the inflection point.

The significance of the passage of sorts and sigs in basin

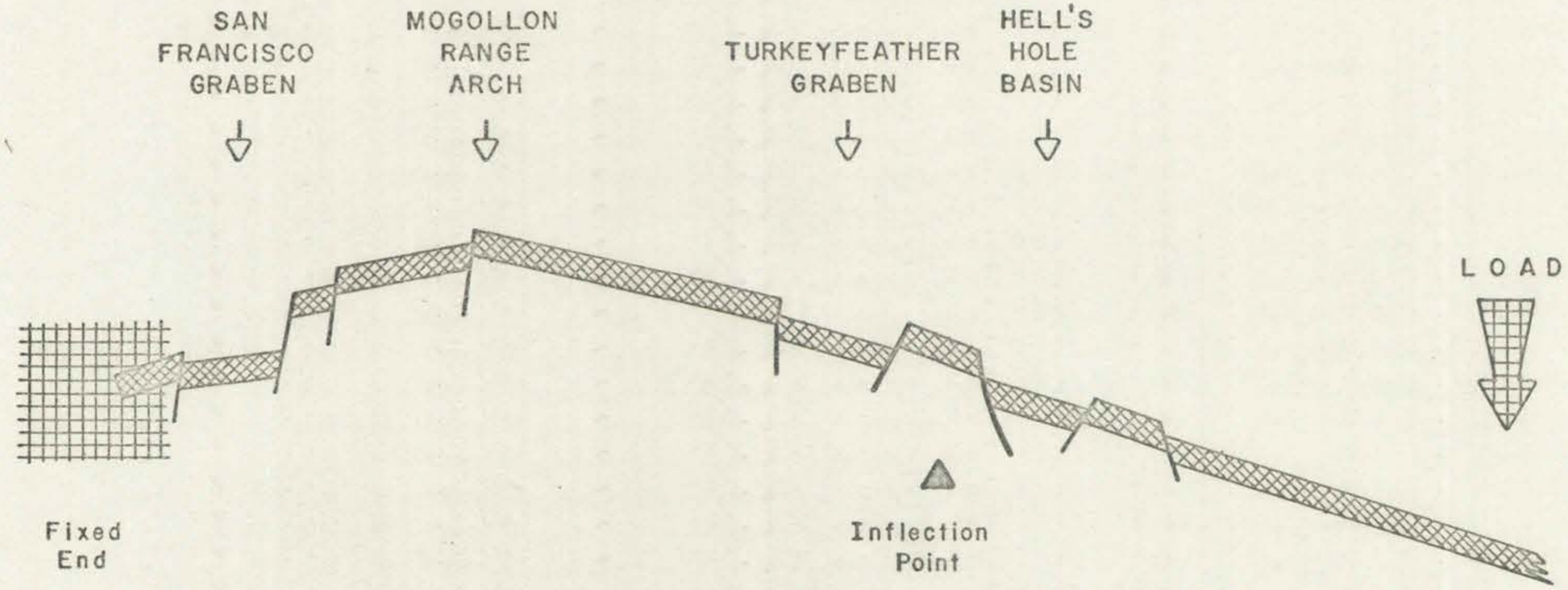

Fig. 7. Diagrammatic representation of the structure of the western rim of the Mogollon Plateau volcano-tectonic depression.

genesis (Wengard, 1962) is provided by radial folds in the rim of the Mogollon Plateau (Plate 13). As described previously, subsidence of the central part of the basin involves crowding of a spherical segment into a conical figure, with resultant crustal shortening and lateral compression. This can be accommodated by vertical warping into a series of radial folds. Szabo (1968, p. 123) described a simple experimental model of this type of folding associated with basin genesis:

> "If a sheet of paper is laid over an oval cutout representing the hingeline of a subsiding area and a load is applied near the center of the cutout, the central area subsides and a series of radial ridges form. The ridges extend toward the center as plunging anticlinal noses separated by synclinal sags. Height and width of the ridges increase toward the peripheral uplift, where they merge into the bordering uplift, resulting in an undulating peripheral profile".

This model fits the essential features of the Mogollon Plateau, accounting for the central basin of subsidence, the raised anticlinal rim, and the radiating spurs and sags giving rise to an undulating peripheral profile, well developed in the southwestern part of the rim.

STRUCTURAL CONTROL OF ORE DEPOSITS

Although a comprehensive study of the economic geology of the mapped area lies outside the scope of this report, some observations can be made concerning the regional structural setting of the ore deposits. A detailed description of the Mogollon gold-silver mining district was given by Ferguson

(1927) and the Wilcox tellurium and Rain Creek fluorspar districts were discussed by Gillerman (1964, p. 177-180).

Wisser (1960, p. 91-94) showed that the Mogollon district lies upon the west flank of a north-striking anticline (Mogollon Range arch) that was subsequently warped along an east-striking anticlinal axis (Mogollon anticline) (Plate 12). Early mineralization occurred along north-south longitudinal fractures named by Ferguson (1927) the Queen, Pacific, and Great Western faults, none of which are known to extend into the mapped area. A second set of tensional faults, striking approximately east-west, apparently formed in response to warping of the Mogollon anticline and resulted in a graben on the crest of the anticline. The east-west fractures carry most of the productive mineralization of the Mogollon mining district which, structurally, is located on the top of an uplifted dome produced by the crossing of two anticlinal warps.

In a similar way the Rain Creek fluorspar district is located on the Rain Creek anticline near where it crosses the Mogollon Range arch, although details of mineralization and fracturing in this area are not known. The Wilcox district lies on the Mogollon Range arch midway between the Dry Creek syncline and the Rain Creek anticline (Plate 12) and, south of the mapped area, the Gila fluorspar district (Gillerman, 1964, p. 170-175) lies approximately on the crest of a third culmination at the mouth of the Gila River. Hydrothermal alteration and mineralization, apparently related to the Mogollon Range arch, are intensified where the secondary set

of anticlines, radiating outward from the central Gila Basin, are superimposed as culminations upon the peripheral arch.

Warping of the rim of the Mogollon Plateau into culminations and depressions began in pre-Deadwood Gulch time and resulted in thick accumulation of Deadwood Gulch Rhyolite in the Dry Creek basin. In the Mogollon mining district the Deadwood Gulch Rhyolite forms the hanging wall in the Fanney mine, showing that mineralization was post-Deadwood Gulch in age. It is known also to be older than the Mogollon Range fault which probably reflects the main episode of late Tertiary faulting. Warping occurred throughout, and probably continued after, Deadwood Gulch time, until tensional forces that were initiated finally resulted in fracturing and block-faulting, these fractures becoming the sites of penecontemporaneous mineralization.

PALEOMAGNETISM

About 60 oriented specimens from volcanic units in the western part of the Mogollon Plateau were tested by Dr. David Strangway (University of Toronto) to determine their direction of magnetism, whether normal or reversed. The results are presented in Table 10. Approximately 20 percent of the specimens gave inconclusive readings owing to extremely weak magnetism or to excessive overprinting of a magnetic field due to lightning strikes.

Whitewater Creek Rhyolite: This formation has reversed magnetism.

Cooney Formation: Nine specimens were tested, including a vertical sequence from Whitewater Creek (7 specimens) and 2 samples of ash-flow tuff from Mogollon Creek. Consistently reversed magnetic readings were obtained, although both samples from Mogollon Creek were only weakly magnetized. The paleomagnetic data available are in accordance, therefore, with tentative stratigraphic correlation between these two outcrop areas.

Houston Andesite: One sample of andesite from Sacaton Creek was found to have reversed magnetism.

Apache Spring Quartz Latite: Eleven specimens of Apache Spring from the Bursum cauldron, including a vertical sequence in Whitewater Creek, gave reversed magnetic readings. One specimen from the Rain Creek divide was normally magnetized but may have

Table 10. Paleomagnetism of the volcanic rocks from the mapped area.

	MAGNETISM	
	NORMAL	REVERSED
Bearwallow Mountain Formation	*	*
Mogollon Andesite	*	
Deadwood Gulch Rhyolite	*	
Double Spring Andesite	*	
Latite at Turkeyfeather Creek		*
Jerky Mountain Rhyolite		*
Bloodgood Canyon Rhyolite		*
Last Chance Andesite	*	
Fanney Rhyolite	*	
Mineral Creek Andesite	*	
Sacaton (and Pacific) Quartz Latite		*
Apache Spring Quartz Latite		*
Houston Andesite		*
Cooney Formation		*
Whitewater Creek Rhyolite		*

been lightning struck. Five specimens gave inconclusive readings.

Sacaton Quartz Latite: Six specimens of Sacaton Quartz Latite from Little Dry Creek, Sacaton Mountain, and Big Dry Creek, and Pacific Quartz Latite (Ferguson, 1927) from Mogollon were tested, of which one gave inconclusive results. The remainder had weak reversed magnetism.

Mineral Creek Andesite: Six specimens of andesite from scattered localities throughout the area were all normally magnetized.

Fanney Rhyolite: One specimen of Fanney Rhyolite from Holt Mountain was normally magnetized.

Last Chance Andesite: This unit is normally magnetized.

Bloodgood Canyon Rhyolite: Four specimens from the Gila Cliff Dwellings cauldron, one sample from the San Augustin Plains, and one from the Blue Range in Arizona all gave reversed magnetic readings. A specimen from near the top of the section at Prior Creek in the Gila Cliff Dwellings cauldron was normally magnetized.

Jerky Mountain Rhyolite: This unit has reversed magnetism.

Quartz Latite at Turkeyfeather Creek: Two specimens gave reversed magnetic readings.

Double Spring Andesite: One specimen from West Fork Gila River was normally magnetized.

Deadwood Gulch Rhyolite: Two specimens had normal, although

very weak, magnetism.

Mogollon Andesite: One specimen was normally magnetized.

Bearwallow Mountain Formation: Both normal and reversed magnetic readings were obtained from this unit.

FLOW DIRECTION STUDIES

GENERAL STATEMENT

The importance of linear fluidal textures in tracing volcanic flows back to their vent areas in relatively old or deformed terrains was stated by Smith and Elston (1967). Together with chemical and petrographic data, they can be used also to distinguish volcanic rocks that may be closely associated in space and time yet were derived from different volcanic centers. Until recently, however, the study of vector properties of volcanic rocks has received little attention, with the notable exception of Waters (1960), Christiansen and Lipman (1966), Schmincke (1967), Schmincke and Swanson (1967), and Smith (1967).

Criteria for determination of flow directions of volcanic rocks, developed by Smith (1967), were applied to flows associated with known vents in the Jemez Mountains and Mount Taylor, New Mexico. The present study is their first application to a large, complex, and virtually unknown volcanic terrain. Results have indicated the source areas for many volcanic units and have proved the usefulness of the technique.

Some lineations were measured in the field, but most measurements were made microscopically using thin sections from oriented specimens cut parallel to the dip of the formation. Wherever possible about 200 grains per thin section were measured. The terminology used is defined here

according to the usage of Smith (1967):

Flow lineation: Preferred orientation of megascopic or microscopic components resulting from primary flow in volcanic rocks.

Flow azimuth: Absolute direction of movement at any point in a flow.

Flow direction: The sum of all directions of flow lineation and flow azimuth plotted for a particular flow. The term thus indicates the pattern of movement of the entire flow over a given area.

Criteria used to determine flow azimuth are as follows:

Fork-shaped shards: Fork-shaped glass shards in ash-flow tuff tend to be oriented with one prong parallel to flow lineation and pointing away from the source.

Imbrication effect: Phenocrysts in lava and ash-flow tuff are sometimes imbricated and dip toward the source.

Block effect: Small particles in lava and ash-flow tuff frequently pile up behind larger, slow-moving fragments, thereby indicating direction of flow.

Penetration effect: Pumice fragments in ash-flow tuff may be deformed by collision of a more rapidly moving phenocryst oriented in the direction of flow.

Spindle-shaped objects: Spindle-shaped phenocrysts aligned parallel to the flow tend to be oriented with their blunt ends facing toward the source.

Eddy effect: Although not found in ash-flow tuffs by Smith (1967) similar effects were reported from rhyolite lava flows by Cummings (1964) and were seen in a few specimens of Apache

Spring Quartz Latite. Relatively large phenocrysts cause minor eddy currents to develop on their leeward sides.

Elongated phenocrysts (especially feldspar laths) were used most frequently, although glass shards and elongated pumice fragments in ash-flow tuffs were counted when found in sufficient abundance. Following measurement and computation of the flow lineation of each specimen using a Fortran IV computer program (Smith, 1967; Appendix I of this report) the thin section was re-examined for petrographic criteria by which flow azimuth could be determined. Statistical values for flow lineations are tabulated in Appendix II.

RESULTS

Cooney Formation: Flow lineation measurements were made on 16 specimens of the Cooney Formation including 6 samples from the southern part of the area, totalling almost 3,000 grain measurements (Appendix II). All but two specimens produced significant results above the 90 percent confidence level (Tukey Chi-square with two degrees of freedom $\geq$ 4.61) and vector magnitudes range from 0.07-0.61. Flow lineations are southwest-northeast and range between 184° and 300°, with a mean of 238° (Fig. 8). Azimuths for two specimens indicate flow from the southwest and it is concluded that the source area for the Cooney Formation was southwest of the Mogollon Plateau. No significant differences were found between flow lineations of Cooney around Whitewater Creek and the rocks from the southern part of the area.

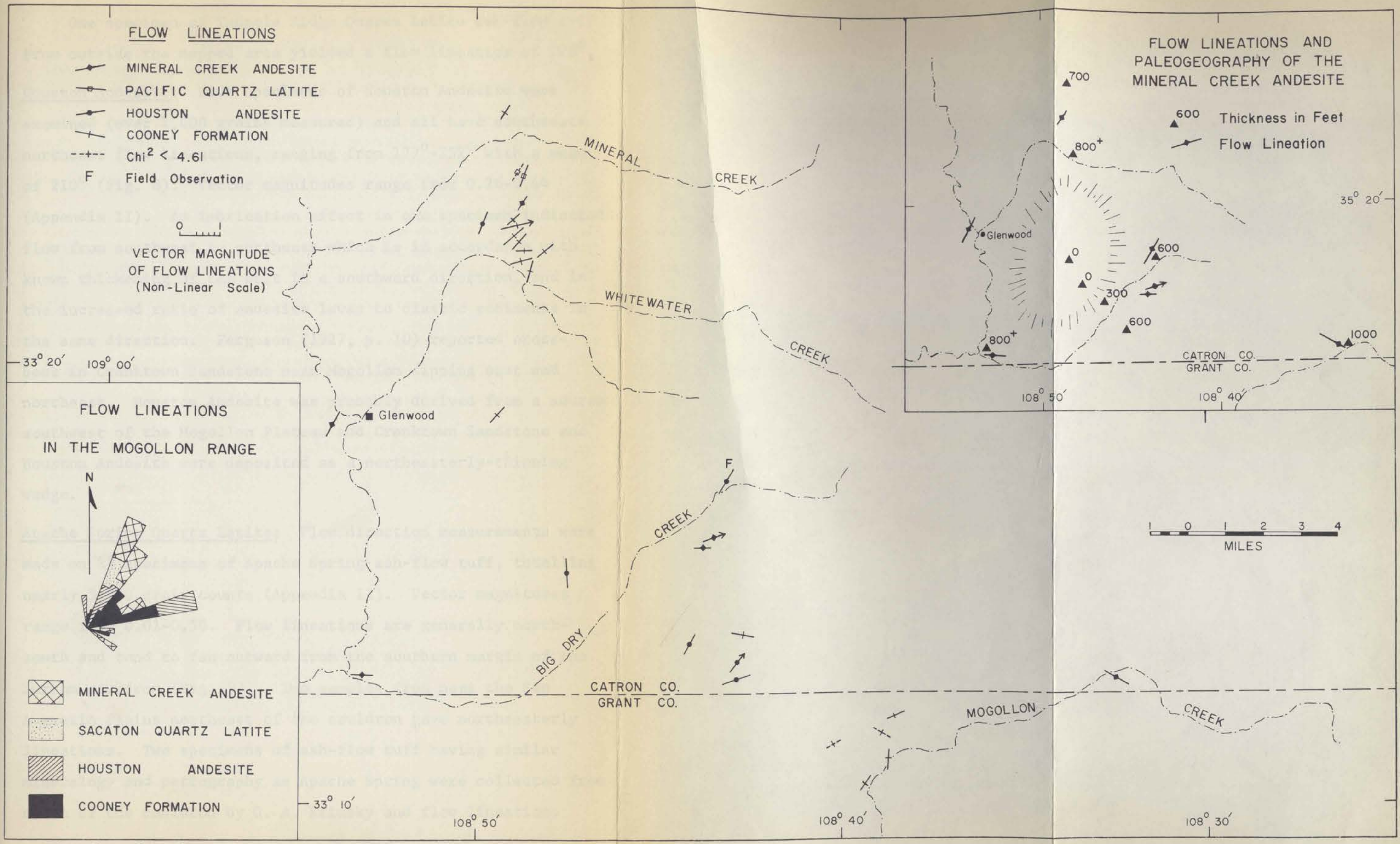

Fig. 8. Flow direction map of the Lower Volcanic Group.

One specimen of Tadpole Ridge Quartz Latite ash-flow tuff from outside the mapped area yielded a flow lineation of 228°.

Houston Andesite: Five specimens of Houston Andesite were examined (over 1,000 grains measured) and all have southwest-northeast flow lineations, ranging from 177°-252° with a mean of 210° (Fig. 8). Vector magnitudes range from 0.26-0.44 (Appendix II). An imbrication effect in one specimen indicated flow from southwest to northeast which is in accordance with known thickening of the unit in a southward direction, and in the increased ratio of andesite lavas to clastic sediments in the same direction. Ferguson (1927, p. 10) reported cross-beds in Cranktown Sandstone near Mogollon dipping east and northeast. Houston Andesite was probably derived from a source southwest of the Mogollon Plateau and Cranktown Sandstone and Houston Andesite were deposited as a northeasterly-thinning wedge.

Apache Spring Quartz Latite: Flow direction measurements were made on 21 specimens of Apache Spring ash-flow tuff, totalling nearly 3,200 grain counts (Appendix II). Vector magnitudes range from 0.01-0.50. Flow lineations are generally north-south and tend to fan outward from the southern margin of the Bursum cauldron (Fig. 9). Two samples from near the San Augustin Plains northeast of the cauldron gave northeasterly lineations. Two specimens of ash-flow tuff having similar mineralogy and petrography as Apache Spring were collected from north of the cauldron by G. A. Krimsky and flow lineations

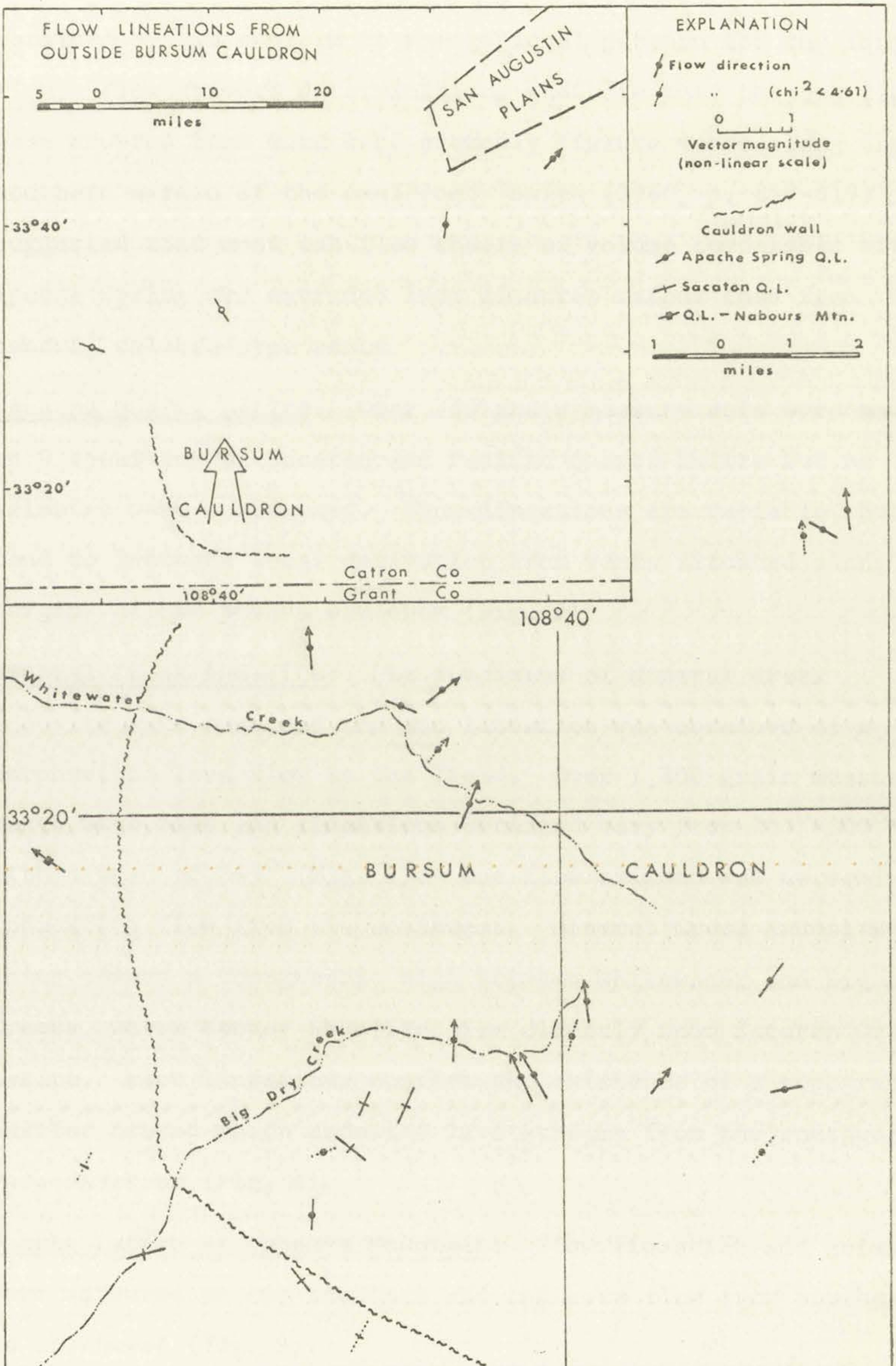

Fig. 9. Flow direction map of the Apache Spring and Sacaton Quartz Latites.

obtained by him conform to the regional pattern for the formation. Flow azimuth determinations indicate that the ash flows were erupted from what were probably fissure vents along the southern margin of the cauldron. Smith (1960, p. 817-819) suggested that most ash-flow sheets of volume comparable with Apache Spring are extruded from fissures rather than from central caldera-type vents.

Sacaton Quartz Latite: Over 750 grain measurements were made on 9 specimens of Sacaton and Pacific Quartz Latite but no azimuths were determined. Flow lineations are variable, but tend to indicate local derivation from vents situated along margins of the Bursum cauldron (Fig. 9).

Mineral Creek Andesite: Six specimens of Mineral Creek Andesite were examined and one lineation was obtained of a porphyritic lava flow in the field. Over 1,200 grain measurements were made and lineations obtained vary from 204°-300° with a mean of 245° (Fig. 8). One flow azimuth was determined, indicating flow from the southwest. Mineral Creek Andesite thins toward a topographic high between Whitewater and Big Dry Creeks, where Fanney Rhyolite lies directly upon Sacaton Quartz Latite. Flow lineations confirm the existence of a topographic barrier around which andesite lava streams from the southwest were diverted (Fig. 8).

Quartz Latite at Nabours Mountain: Flow lineation and azimuth were measured on one specimen and indicate flow from southeast to northwest (Fig. 9).

Bloodgood Canyon Rhyolite: Nearly 1,500 grain measurements were made on 12 specimens of Bloodgood Canyon Rhyolite from the Gila Cliff Dwellings cauldron (Appendix II). Vector magnitudes are low, ranging from 0.08-0.44. Flow lineations show only locally persistent trends and no definite conclusions can be reached regarding location of the eruptive vent, although a source in the southwest corner of the cauldron seems likely (Fig. 10). Northerly flow lineations near the western margin of the cauldron possibly result from topographic control exerted by the cauldron wall. An azimuth was determined for one specimen, showing that flow was from west to east.

Deadwood Gulch Rhyolite: Flow lineations of 6 specimens of Deadwood Gulch Rhyolite and 2 tuffaceous sandstone cross-beds are plotted on Fig. 2. Vector magnitudes are generally low (Appendix II). Flow orientations for Deadwood Gulch Rhyolite vary widely from one part of the mapped area to another, but are roughly radial to the Dry Creek and Hell's Hole basins. They are tentatively interpreted as indicating flow into the basins from surrounding highlands. No indications were obtained regarding locations of eruptive vents.

Mogollon Andesite: Flow directions of 2 samples of Mogollon Andesite suggest eruption from more than one volcanic vent (Fig. 3), including the Willow Mountain and Glenwood Brushy basaltic centers. Correspondence of extrusive vents for Mogollon Andesite and the Bearwallow Mountain Formation supports the interpretation that Mogollon Andesite is a local basal member of the Bearwallow Mountain Formation.

[illegible] Canyon Rhyolite: Nearly 1,300 grain measurements were made on 12 specimens of Dogwood Canyon Rhyolite from the [illegible] (Appendix II). Vector magnitudes are low, ranging from [illegible] [illegible] can be [illegible] regarding location of the eruptive vent. [illegible] of the [illegible] [illegible] directions near the western [illegible] possibly result from [illegible], are [illegible] by the caldera wall. An [illegible] inter- [illegible] for one specimen, showing that flow was from west to east.

[illegible] Rhyolite: Flow directions of 8 specimens [illegible] Rhyolite and 2 [illegible] are plotted on Fig. 2. Vector magnitudes are generally low [illegible] very widely from one part of the mapped area to another, but are roughly radial in the dry Creek and [illegible] [illegible] indicating flow [illegible] from surrounding [illegible]. No indication was obtained regarding location of eruptive vents.

[illegible] Rhyolite: Flow directions of 7 samples of rhyolite [illegible] suggest eruption from more than one volcanic vent (Fig. 3), including the [illegible] and [illegible] [illegible]. [illegible] of [illegible] [illegible] and the [illegible]

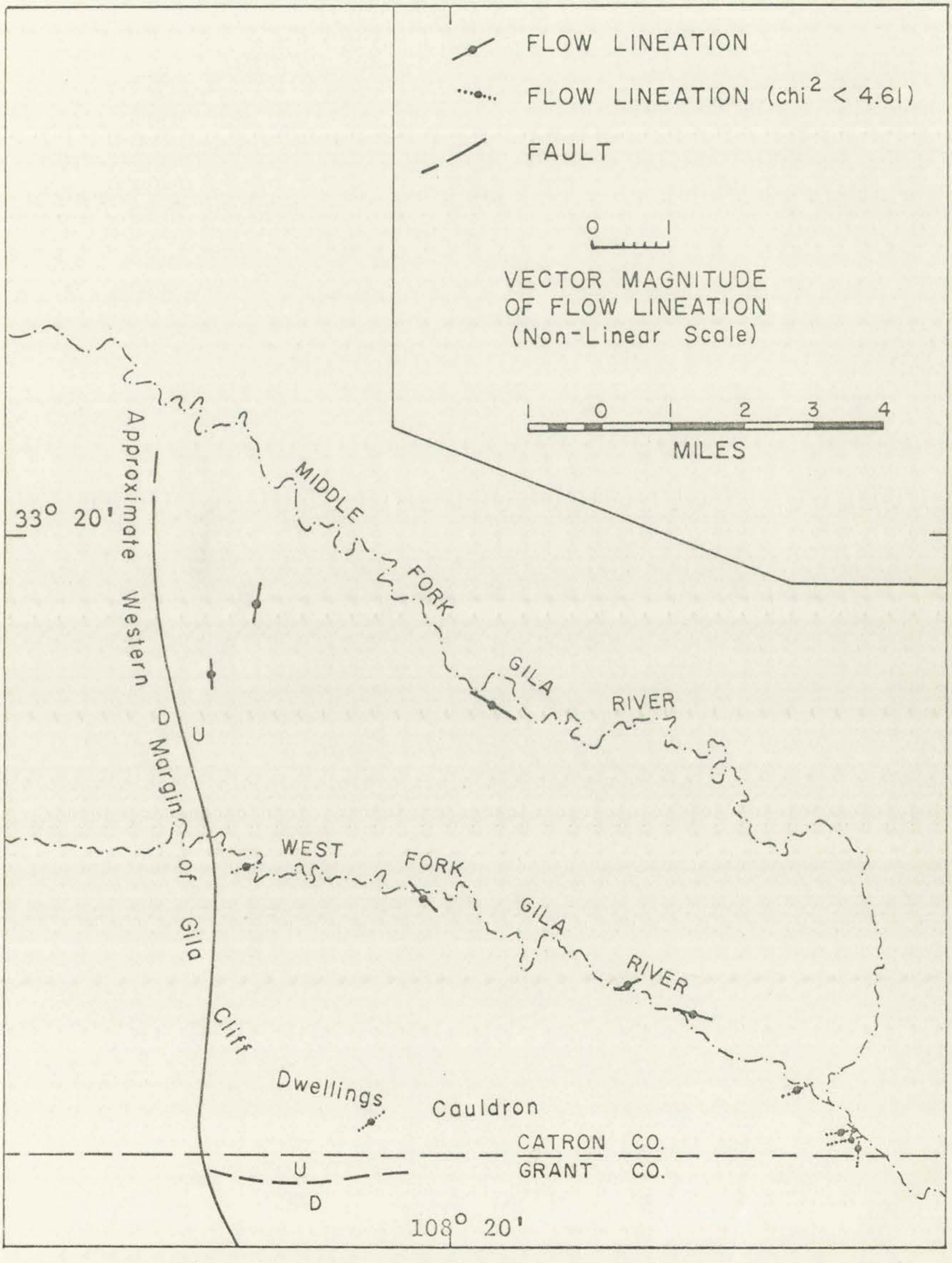

Fig. 10. Flow direction map of the Bloodgood Canyon Rhyolite in the Gila Cliff Dwellings cauldron.

Bearwallow Mountain Formation: Flow lineation analyses were made on 20 specimens from the Bearwallow Mountain Formation (Appendix II). Vector magnitudes are high, ranging from 0.08-0.85 with a mean of 0.37. Flow azimuths were determined on a few samples. Five known centers for the Bearwallow Mountain Formation are plotted, together with measured flow orientations of the lavas (Fig. 3). The Glenwood Brushy center apparently formed the source for much of the basaltic andesite in the San Francisco Valley. Two flow patterns can be distinguished around the Willow Mountain caldera. Orthopyroxene-clinopyroxene andesites have northeasterly flow orientations that are in part radial to the caldera, but may also reflect topographic control exerted by the northeast-trending Dry Creek basin. Hornblende-orthopyroxene latites from the same area, and also from the outlier on the northern end of the Diablo Mountains, have a northwesterly flow orientation and may have flowed along a structural depression from a source northwest of the mapped area. Olivine-clinopyroxene basaltic andesites east of Mogollon Baldy have a complex flow pattern reflecting the topographic influence of the ancestral Jerky and Diablo Mountains. The lavas were probably derived from the Mogollon Baldy center and flowed in an easterly direction with a consistent tendency to swing southward. On the flanks of the Jerky and Diablo Mountains the lava flows were sharply deflected by barriers of flow-banded rhyolite over which, in the case of the Jerky Mountains, they ultimately overflowed. Three flow lineations from

south of Black Mountain caldera display a radial pattern from that center.

SUMMARY AND CONCLUSIONS

Volcanic rocks from the mapped area exhibit distinct flow patterns related to postulated vents and to the regional tectonic evolution of the area. Ash-flow tuffs from the Cooney Formation and lavas from Houston and Mineral Creek Andesites display northeasterly flow lineations and probably flowed to the northeast from a source southwest of the Mogollon Plateau. Early topographic expression of the western rim of the Mogollon Plateau, in the form of extrusive domes of Sacaton Quartz Latite, is reflected by the distribution and flow pattern of the overlying Mineral Creek Andesite. Ash-flow tuffs of Apache Spring Quartz Latite flowed northward from fissure vents along the southern margin of the developing Bursum cauldron. Similarly, Bloodgood Canyon ash-flow tuffs poured out of the Gila Cliff Dwellings cauldron and covered wide areas. Following grand-scale eruption of the two major ash-flow sheets, flow patterns for younger rocks show the influence of more localized and restricted structural elements. Following a period of erosion, Deadwood Gulch Rhyolite appears to have filled relatively small structural basins superimposed upon the larger volcano-tectonic complex. Lava flows of Mogollon Andesite and the Bearwallow Mountain Formation are related to specific eruptive centers superimposed upon older rocks.

The results demonstrate the validity of using microscopic fluidal textures to determine vents and flow patterns of ancient volcanic rocks. In this first attempt to apply the techniques of Smith (1967) to a complex area of previously unknown geology, 98 microscopic analyses were made, with a total of 16,403 individual grain measurements (Table 11), and all but 19 specimens yielded significant flow orientations above the 90 percent confidence level. Basaltic andesites generally yielded much higher Chi-square and vector magnitude values than ash-flow tuffs, with Deadwood Gulch and Bloodgood Canyon Rhyolites being especially low in this respect. Deadwood Gulch consists in part of waterlain and ash-fall tuffs which account for its low mean vector magnitude.

Significant differences in vector magnitudes were found to exist between Apache Spring and Bloodgood Canyon ash-flow tuffs, with Apache Spring displaying more strongly developed flow lineations than Bloodgood Canyon Rhyolite. Consideration of the manner of emplacement of ash-flow sheets provides a possible explanation for this phenomenon. Eruption of ash-flow tuffs as <u>nueès ardentes</u> and their subsequent downslope flow is considered by most authors to be a turbulent process giving rise to a non-sorted deposit with random orientation of component particles. R. L. Smith (1960, p. 807), however, noted that some welded tuffs display preferred orientation of stretched pumice fragments which he suggested may indicate "...mass flowage during or after welding." Similarly, Schmincke and Swanson (1967, p. 657) described ash-flow tuffs

Table 11. Summary of flow orientation data for volcanic rocks in the mapped area

	Total samples	No. significant (90% confidence level)	Average Chi-square	Average vector magnitude	Total grain counts
Bearwallow Mountain Formation	20	19	73.92	0.37	4,348
Mogollon Andesite	2	2	133.58	0.57	403
Deadwood Gulch Rhyolite	6	4	6.56	0.15	739
Bloodgood Canyon Rhyolite	12	6	7.48	0.17	1,429
Quartz Latite at Nabours Mountain	1	1	26.53	0.26	200
Mineral Creek Andesite	6	6	42.83	0.30	1,237
Sacaton Quartz Latite	9	6	10.77	0.23	753
Apache Spring Quartz Latite	21	16	20.93	0.22	3,176
Houston Andesite	5	5	71.32	0.39	1,061
Tadpole Ridge Quartz Latite	1	1	11.16	0.21	129
Cooney Formation	15	13	18.05	0.23	2,928
Total	98				16,403
+ field measurements	4	-	-	-	-

from Gran Canaria that show distinct preferred orientation, possibly due to "...mass laminar flowage of each ash flow when it was in a viscous, fluid-like state." They suggested that "...the laminar flowage must have occurred late in the movement of the flow, just prior to final rest." E. I. Smith (1967) called upon late-stage laminar flowage to account for primary flow lineation in the Bandelier Rhyolite.

Differences in the degree of preferred orientation between Apache Spring and Bloodgood Canyon ash-flow tuffs possibly reflect differences in viscosities between the glass phases during late stage flow. According to Barth (1952, p. 132) viscosity of silicate melts increases with increasing Si and Al, but is lowered by the addition of increasing amounts of Fe. The atomic ratio Fe/(Si + Al), therefore, gives an indication of the viscosity of the glass, with viscosity decreasing as the ratio increases. The calc-alkalic Apache Spring Quartz Latite has Fe/(Si + Al) ratios of 0.027-0.029 whereas Bloodgood Canyon Rhyolite, with significantly lower preferred orientation, has lower Fe/(Si + Al) ratios of 0.015-0.017 (Table 12). Nockolds' (1954) average calc-alkali rhyolite has an atomic ratio of 0.018 whereas Schmincke and Swanson (1967) reported ratios of 0.032-0.072 for peralkalic welded tuffs on Gran Canaria that display extremely strong flow lineation.

The viscosity of volcanic glass at any given temperature can also be estimated by using the ratio R = (Si + Al)/O (Shaw, 1965, p. 121-122), the viscosity decreasing with

Table 12. Relationship between the degree of preferred orientation and viscosity in the Apache Spring and Bloodgood Canyon ash-flow tuffs.

	Vector Magnitude	Fe/(Si+Al)	R=(Si+Al)/O	Viscosity at 800°C (poises)
Apache Spring Quartz Latite	0.22	0.027-0.029	0.47-0.48	10^7-$10^{7.7}$
Bloodgood Canyon Rhyolite	0.17	0.015-0.017	0.49	10^9
Gran Canaria rhyolites*	strong orientation	0.032-0.072	0.46-0.48	$10^{6.1}$-$10^{7.7}$
Nockholds' average calc-alkali rhyolite	-	0.018	0.49	10^9

*from Schmincke and Swanson (1967)

decreasing values for R. In Apache Spring Quartz Latite, $R = 0.47\text{-}0.48$, corresponding to a viscosity at 800°C of $10^7\text{-}10^{7.7}$ poises, whereas for Bloodgood Canyon Rhyolite, $R = 0.49$, corresponding to a viscosity of 10^9 poises, more than an order of magnitude higher (Table 12). Lower glass viscosity of Apache Spring Quartz Latite probably enabled late-stage laminar flowage to occur more easily and effectively, resulting in stronger preferred orientation than is the case for Bloodgood Canyon Rhyolite. Correlation between vector magnitude (or the degree of preferred orientation) and the $Fe/(Si + Al)$ and $(Si + Al)/O$ ratios supports the conclusion that viscosity of the glass is an essential factor determining the degree of late-stage laminar flowage in welded tuffs, which in turn determines the degree of preferred orientation of component particles. Volatile content of the glass is an additional factor but the presence of extensive vapor-phase crystallization in both Apache Spring and Bloodgood Canyon suggests that differences in volatile content were of secondary importance.

[illegible] Apache Spring Tuff, Warren latite, [illegible], corresponding to a viscosity at 800°C of [illegible] Bloodgood Canyon Rhyolite, [illegible], corresponding to a viscosity at 800°C [illegible] than [illegible] of magnitude higher [illegible]. Lower vis- [illegible] Apache Spring Tuff [illegible] latite probably ensured [illegible] rapidly and [illegible] of preferred orientation than in the case for [illegible] Canyon Rhyolite. Correlation between [illegible] and the degree of preferred orienta- tion, and the [illegible] supports the conclusion that viscosity of the magma is an essential factor determining the degree of [illegible], which in turn determines the degree of preferred orientation of phenocryst particles. Volatile content of the [illegible] the presence of [illegible] crystallization in both Apache Spring and Bloodgood Canyon suggests that differences in volatile content were of secondary importance.

ZIRCON ANALYSES

GENERAL STATEMENT

The significance of morphological characters of zircons as an aid to petrogenetic interpretation is well documented in the literature. Several features such as color, habit, size, and roundness of terminations may be used to describe zircon populations, but these are at best semi-quantitative and subject to operator bias. To overcome these handicaps, the method of statistical analysis of lengths and breadths of a representative number of crystals per sample has been applied with considerable success by Poldervaart (1955; 1956), Eckelmann and Kulp (1956), Larsen and Poldervaart (1957), Alper and Poldervaart (1957), and others. This statistical method is based on the assumption that zircons are early products of crystallization in granitic magmas and that habits (morphology) of zircon crystals are a function of the physico-chemical environment during crystallization. Zircons crystallizing in granitic magmas under different physico-chemical conditions, therefore, may be expected to display different morphological parameters that are subject to analysis by statistical means. Interpreted with caution, zircon studies of this type can aid in solving problems of petrogenesis and consanguinity between felsic rocks.

In the present study, 13 analyses of zircon populations were made in an attempt to determine relationships between

rhyolitic rock types in the mapped area and to "fingerprint" rocks derived from different magma sources. In general, the results obtained support the conclusions drawn from field and petrologic data.

LABORATORY PROCEDURE

Rocks were crushed to 80-mesh and fine rock dust was decanted. Heavy minerals were separated with bromoform and magnetite was removed with a hand magnet. Other magnetic minerals were extracted from the heavy fraction with a Frantz isodynamic separator and the residue, chiefly zircon and apatite, was mounted on glass microscope slides. Two hundred doubly-terminated zircon crystals per specimen were measured, using a mechanical stage to ensure random selection of grains. Data were reduced with a Fortran IV computer program (Appendix III).

Reduced major axes represent mean growth trends of zircon populations (Larsen and Poldervaart, 1957) and their slopes can be compared by applying the z-test. Zircons crystallizing under different physico-chemical conditions commonly have different growth trends and this statistical test detects significant variations between them. Taking the level of confidence at $z \geqq 1.96$ z may be calculated:

$$z = \frac{(Sy/Sx)_1 - (Sy/Sx)_2}{\sqrt{(SE^2)_1 - (SE^2)_2}}$$

where Sy = standard deviation of breadth

Sx = " " " length

SE = standard error of slope of reduced major axis.

(Alper and Poldervaart, 1957, p. 955).

CRYSTAL MORPHOLOGY

Microscopic examination of zircons from the volcanic units failed to differentiate between the different populations on purely qualitative grounds. Almost all crystals are doubly terminated and sharply euhedral; very few have rounded crystal edges. Twinned crystals and grains with prismatic outgrowths are rare. Elongated prismatic crystals with length/breadth ratios of 2.0 - 3.0 are common. Crystal forms are combined first-order prisms and pyramids, as well as more complex habits which combine first- and second-order prisms and pyramids. With increasing suppression of prism faces, crystals become short and stubby, with length/breadth ratios of 1.0 - 2.0. These football-shaped grains tend to be highly faceted. Colorless zircons predominate over pale brown or yellow crystals and inclusions of minute zircons or of opaque material are present in many crystals.

STATISTICAL ANALYSIS

Nine specimens of ash-flow tuffs and flow-banded rhyolites from the Middle Volcanic Group were analyzed, but

consistently significant differences were not found. Four specimens of the Lower Volcanic Group, including three of Cooney ash-flow tuff in Whitewater Creek and one of Kneeling Nun Rhyolite were analyzed and compared with the mean growth trend (MGT) of the Middle Volcanic Group (Table 13).

Middle Volcanic Group: Mean lengths and breadths of zircons are similar and mean elongation ratios vary from 1.73-2.17, averaging 1.88. Mean diameters of crystals ($\overline{s}$) vary from 0.049-0.101 mm and average 0.074 mm. Comparison of slopes of reduced major axes with the mean growth trend by means of the z-test showed significant differences in four samples. One of these (#3) is the quartz latite at Nabours Mountain. Two others (#4 and #5) were taken from the basal part of the Apache Spring ash-flow sheet and may be contaminated by xenoliths. The fourth (#9) is from a rhyolite dike from the front of the Mogollon Range.

Lower Volcanic Group: Three specimens of ash-flow tuff from the Cooney Formation in Whitewater Creek were analyzed. Elongation ratios in Cooney ash-flow tuffs vary from 1.78-2.06, averaging 1.92. The mean size of zircons is 0.070 mm, similar to the Middle Volcanic Group. Comparison of slopes of reduced major axes with the mean growth trend of the Middle Volcanic Group indicated significant differences to exist in two samples (Table 13).

One specimen of Kneeling Nun Rhyolite from the Mimbres Valley province yielded zircons similar in size and shape to

Table 13. Statistical parameters of zircon crystals from rhyolitic rocks in the mapped area.

	1	2	3	4	5	6	7	8	9	10	11	12	13
$\bar{x}$ (mm)	0.107	0.066	0.147	0.122	0.095	0.102	0.079	0.086	0.105	0.087	0.074	0.128	0.122
$\bar{y}$ (mm)	0.057	0.037	0.070	0.063	0.056	0.058	0.045	0.049	0.055	0.043	0.042	0.067	0.063
$\bar{e}$	1.928	1.785	2.178	1.961	1.732	1.804	1.757	1.810	1.952	2.060	1.781	1.928	1.966
$\bar{s}$ (mm)	0.078	0.049	0.101	0.087	0.073	0.077	0.059	0.064	0.076	0.061	0.056	0.092	0.087
Sx (mm)	0.039	0.029	0.071	0.058	0.029	0.038	0.032	0.034	0.029	0.042	0.029	0.063	0.068
Sy (mm)	0.018	0.015	0.032	0.026	0.018	0.021	0.015	0.020	0.015	0.017	0.015	0.026	0.030
r	0.703	0.808	0.821	0.888	0.814	0.827	0.752	0.802	0.660	0.741	0.844	0.696	0.872
slope	0.462	0.516	0.442	0.452	0.608	0.556	0.466	0.578	0.516	0.415	0.524	0.408	0.451
SE	0.023	0.022	0.018	0.015	0.025	0.022	0.022	0.024	0.027	0.020	0.020	0.021	0.016
regression lines y=	0.462x +0.007	0.516x +0.004	0.442 +0.005	0.452x +0.008	0.608x +0.002	0.556 +0.001	0.466 +0.009	0.578 +0.001	0.516 +0.001	0.415 +0.007	0.524 +0.003	0.408 +0.015	0.451 +0.008
No. of crystals counted	200	200	200	200	200	200	200	200	200	200	200	200	200
z (MGT)	1.53	0.17	2.44	2.20	2.92	1.46	1.44	2.07	0.14	3.24	0.45	3.38	2.19

1 - Jerky Mountain Rhyolite
2 - Bloodgood Canyon Rhyolite
3 - Quartz latite at Nabours Mountain
4, 5, 6, 7 - Apache Spring Quartz Latite
8, 9 - Fanney Rhyolite
10, 11, 12 - Cooney Formation
13 - Kneeling Nun Rhyolite

$\bar{x}$ - mean length
$\bar{y}$ - mean breadth
$\bar{e}$ - mean elongation
$\bar{s}$ - mean diameter
Sx - standard deviation of length
Sy - standard deviation of breadth
r - coefficient of correlation
SE - standard error of slope

those of the previously described formations. Comparison of the slope of the reduced major axis with the mean growth trend of the Middle Volcanic Group produced a value of $z = 2.19$, suggesting that significant differences exist between them.

SUMMARY AND CONCLUSIONS

Results of these zircon analyses are not conclusive, although trends established indicate petrogenetic relationships in agreement with evidence obtained from other laboratory and field studies:

(1) Zircons from Apache Spring and Bloodgood Canyon ash-flow tuffs, and Fanney and Jerky Mountain flow-banded rhyolites failed to exhibit consistently significant differences. These results support the interpretation that the four rock types are genetically related to one another and form part of a continuous magma series.

(2) Although data are scanty, zircons from the compositionally-zoned Apache Spring ash-flow sheet show progressive increase in elongation from bottom to top ($\bar{e} = 1.73$-1.80) which may be due to more rapid rates of gravitative settling of elongated crystals or to different crystallization habits of zircon under different physico-chemical conditions in the magma chamber.

(3) Zircons from the Cooney Formation are, in general, significantly different from those of the Middle Volcanic Group, and this is tentatively interpreted as indicating that the two volcanic groups are genetically unrelated.

(4) Zircons from Kneeling Nun Rhyolite are significantly different from those of the Middle Volcanic Group, indicating that Kneeling Nun Rhyolite also is genetically unrelated to the Middle Volcanic Group.

PETROLOGY AND PETROGENESIS

GENERAL STATEMENT

Three volcanic groups have been distinguished in the mapped area. The Lower Volcanic Group includes Whitewater Creek and Cooney ash-flow tuffs, and lavas from the Houston, Mineral Creek, and Last Chance Andesites. The andesites interfinger with felsic rocks assigned to the Middle Volcanic Group but are genetically unrelated to them. Flow direction studies indicate a source southwest of the Mogollon Plateau for members of the Lower Volcanic Group.

The Middle Volcanic Group comprises Apache Spring and Bloodgood Canyon ash-flow tuffs, Fanney and Jerky Mountain flow-banded rhyolites, Sacaton Quartz Latite, and the quartz latite at Nabours Mountain. These rocks are superimposed upon Datil (restricted sense) (Elston, 1968) and form the framework of the Mogollon Plateau volcanic complex.

Separated by an erosional unconformity from rocks of the Middle Volcanic Group are tuffs and lavas belonging to Deadwood Gulch Rhyolite, the latite at Willow Creek, and the quartz latite at Turkeyfeather Creek, as well as basaltic to latitic lavas of the Double Spring and Mogollon Andesites, and the Bearwallow Mountain Formation. These units probably represent volcanic associations distinct from the Middle Volcanic Group and have been assigned to the Upper Volcanic Group.

Chemical data for volcanic rocks are sparse and are

restricted to the Bearwallow Mountain Formation and the Middle Volcanic Group. Little information is available for the Lower Volcanic Group or felsic rocks of the Upper Volcanic Group, so conclusions regarding their relationship with the Middle Volcanic Group remain tentative.

LOWER VOLCANIC GROUP

Included within this group are lavas and ash-flow tuffs ranging in composition from andesite to rhyolite. Little is known regarding their chemistry or petrogenesis although two partial chemical analyses given by Ferguson (1927) are reproduced in Table 2. Both specimens are from the Mogollon mining district and the analyses should be regarded with caution owing to pervasive hydrothermal alteration that in places produced sericite and calcite. Andesite lavas make up a large proportion of the Lower Volcanic Group and many ash-flow tuffs within the Cooney Formation have dacitic affinities. Available evidence is compatible with the interpretation that the Lower Volcanic Group evolved from a dioritic parent magma by processes of crystal fractionation and assimilation.

MIDDLE VOLCANIC GROUP

The overall petrologic trend of the Middle Volcanic Group is toward an increasingly silicic residue, although vertical compositional zoning of ash-flow sheets introduces complexities to this scheme. The following conclusions are tentatively put

forward, but further work in other parts of the Mogollon Plateau will probably modify and expand this interpretation. Chemical analyses of 6 specimens from this group are given in Table 5.

Vertical compositional zoning of Apache Spring Quartz Latite is strongly developed and is reflected in the mineralogy of the rock (Fig. 11). Modal analyses of a vertical section from Whitewater Creek are given (Table 4) and chemical analyses from the top and bottom of the section are included in Table 5, nos. 1 and 2. The phenocryst content of the rock varies systematically from 20 percent at the base to 50 percent near the top, then decreases slightly in the upper 500 feet of the section. The relative proportion of quartz to total phenocryst content (expressed as percent) decreases upward in the section from over 20 percent at the base to less than 10 percent at the top, although values in the lower part of the section tend to be erratic. Biotite is present throughout the section but, near the top, clinopyroxene phenocrysts appear. Hornblende occurs sporadically in a zone intermediate between the biotite and clinopyroxene-biotite mineralogic zones. Plagioclase varies from oligoclase at the base of the section to andesine at the top, although zoning of individual phenocrysts includes nearly this entire range. Compositions of alkali feldspar also show systematic variation from approximately Or_{80} at the base to Or_{50} at the top of the section.

Chemically, Apache Spring varies from rhyolite at the base to quartz latite at the top with a decrease in silica content

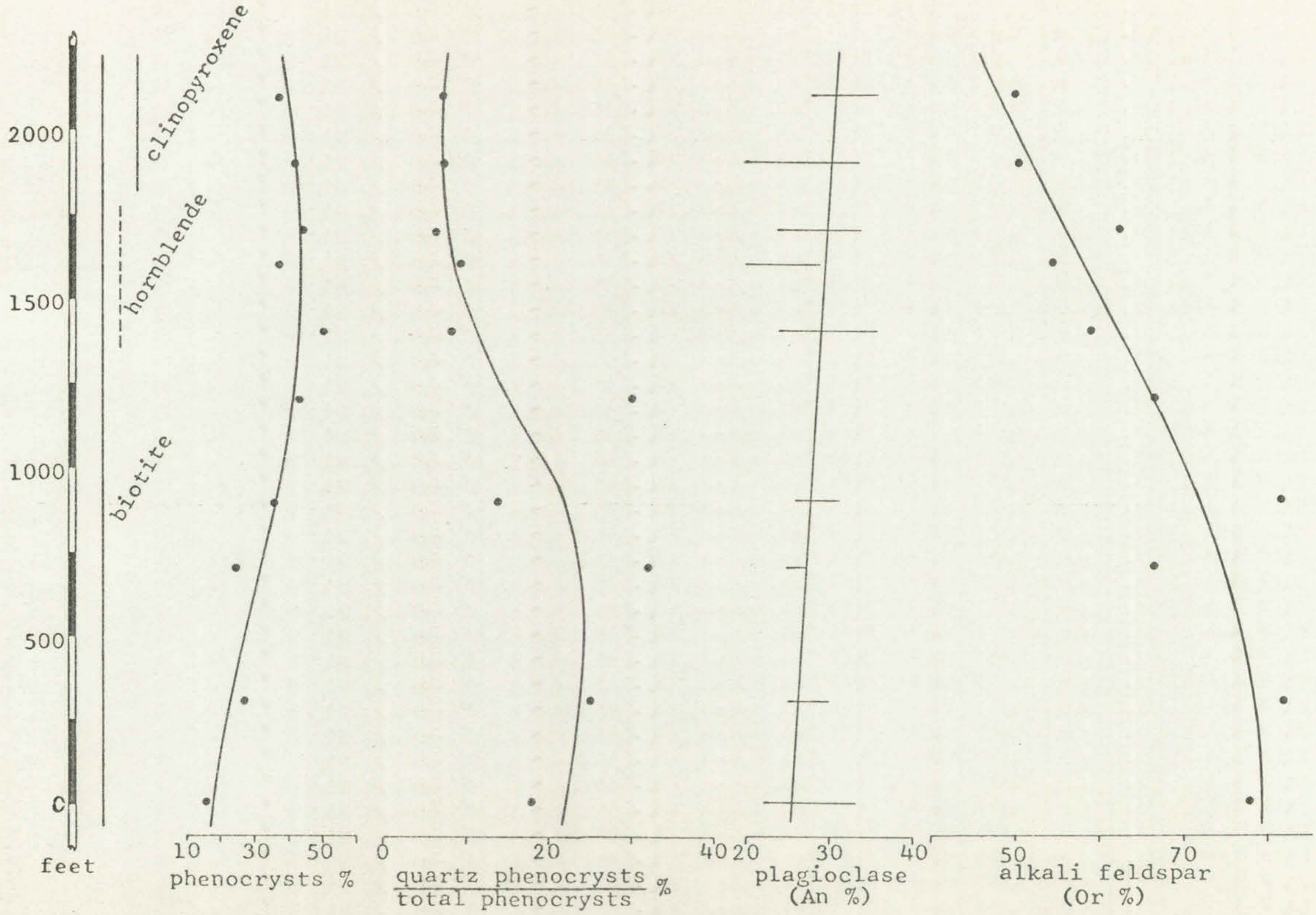

Fig. 11. Vertical compositional zoning in the Apache Spring ash-flow sheet.

from 73.6-69.1 percent (Table 5). Similarly FeO and Fe_2O_3 decrease upward, but TiO_2, Al_2O_3, MnO, MgO, CaO, Na_2O, and K_2O all increase. Upward decrease in silica is reflected by decrease in the abundance of quartz phenocrysts whereas increase of MgO and CaO results in the appearance of clinopyroxene and the increased An-content of plagioclase near the top of the section. Apache Spring is more alkalic at the top of the section, expressed by the alk/al ratio which increases from 0.86 at the base to 0.91 at the top. The Fe_2O_3/FeO ratio, regarded by Kennedy (1948) as a measure of the volatile content of the magma at the time of crystallization, increases toward the top of the formation, but this may be a result of post-depositional oxidation at the top of the ash-flow sheet during vapor-phase crystallization.

Vertical zonation of the Apache Spring ash-flow sheet from rhyolite to quartz latite is consistent with the concept of repeated eruption from a zoned magma chamber, with the resulting ash-flow sheet presenting an inverted image of the parent magma (Giles, 1967). Fractional crystallization was probably controlled by variations in physico-chemical conditions, especially volatile content, at different levels in the magma chamber. High phenocryst content in lower parts of the magma chamber may have resulted from gravitative crystal settling, but probably also reflects lower volatile content at the bottom of the chamber, resulting in higher crystallization temperatures and hence more rapid crystallization rates than those prevailing in the volatile-rich upper

parts of the magma. Temperature gradients were probably less important. Increased volatile content favored crystallization of biotite and hornblende rather than pyroxene in upper parts of the chamber. Although the total alkali content of Apache Spring decreases slightly upward, the K_2O/Na_2O ratio increases significantly, possibly accounting for the increased K-content in alkali feldspar from the top of the magma chamber. Gravitative crystal settling probably played a part in compositional zoning of the magma, but gas transfer was probably the dominant agent in differentiation. Upward moving volatiles (especially H_2O) may have carried silica and iron, concentrating these elements in upper parts of the chamber and leaving behind the more refractory materials. Post-depositional vapor-phase activity was probably responsible for upward leaching of alkalis from the base of the ash-flow sheet.

Compositional zoning is poorly developed in Bloodgood Canyon Rhyolite and, despite its thickness, the ash-flow sheet is noteworthy for its mineralogical and chemical homogeneity. Modal data for a vertical sequence taken in Middle Fork Gila River, just north of the mapped area, are given in Table 7, and chemical analyses from the top and bottom of the section are given in Table 5, nos. 4 and 5. Mineralogically, the only significant compositional variation is the presence of hornblende at the top of the section. Xenoliths are rare except for a poorly welded zone at the base. Chemically the formation shows slight, but probably significant, differentiation trends. SiO_2 and Na_2O decrease very slightly parts of the magma. Temperature gradients were probably less important. Increased volatile content favored crystallization of biotite and hornblende rather than pyroxene in upper parts of the chamber. Although the total alkali content of Apache Spring decreases slightly upward, the K_2O/Na_2O ratio increases significantly, possibly accounting for the increased K-content in alkali feldspar from the top of the magma chamber. Gravitative crystal settling probably played a part in compositional zoning of the magma, but gas transfer was probably the dominant agent in differentiation. Upward moving volatiles (especially H_2O) may have carried silica and iron, concentrating these elements in upper parts of the chamber and leaving behind the more refractory materials. Post-depositional vapor-phase activity was probably responsible for upward leaching of alkalis from the base of the ash-flow sheet.

Compositional zoning is poorly developed in Bloodgood Canyon Rhyolite and, despite its thickness, the ash-flow sheet is noteworthy for its mineralogical and chemical homogeneity. Modal data for a vertical sequence taken in Middle Fork Gila River, just north of the mapped area, are given in Table 7, and chemical analyses from the top and bottom of the section are given in Table 5, nos. 4 and 5. Mineralogically, the only significant compositional variation is the presence of hornblende at the top of the section. Xenoliths are rare except for a poorly welded zone at the base. Chemically the formation shows slight, but probably significant differentiation trends. SiO_2 and Na_2O decrease very slightly toward the top of the sequence whereas FeO and, to a lesser extent, MgO and K_2O increase upward. These trends reflect weak compositional differentiation in a manner similar to Apache Spring Quartz Latite, with the top of the ash-flow sheet being slightly less felsic than the base.

The association of rhyolitic lava flows and ash-flow tuffs is known from many volcanic complexes and the lavas are commonly interpreted as defluidized residue from a zoned magma chamber (Ratté and Steven, 1964). Similar relationships probably exist between Apache Spring ash-flow tuff, and lava flows of Sacaton Quartz Latite and quartz latite at Nabours Mountain. Data on these lava flows are sparse and chemical analyses are lacking. Sacaton Quartz Latite, however, is crystal-rich and lithologically very similar to Apache Spring Quartz Latite. Absence of quartz phenocrysts in some flows may reflect a further stage of differentiation in a quartz-poor zone near the bottom of the original magma chamber. Younger quartz latite lava flows at Nabours Mountain contain unusual reaction pairs of biotite rimmed with hornblende and augite. This suggests abrupt decrease in vapor pressure during final crystallization in the magma chamber, possibly resulting from eruption of the volatile-rich fraction as Apache Spring ash-flow tuff. Consequently, Sacaton Quartz Latite and the lava flows at Nabours Mountain probably represent the defluidized residue of Apache Spring magma, and are intimately associated with the development of the Bursum cauldron.

Fanney and Jerky Mountain Rhyolites, on the other hand,

form the structural framework of the Mogollon Plateau volcano-tectonic complex and are not the defluidized residue of ash-flow tuffs. Trends of compositional zoning of Apache Spring and Bloodgood Canyon ash flows are not continuous with Fanney and Jerky Mountain lava flows, there being a discordant break between them. This is brought out by mineralogical changes between the units (Fig. 12). Abundance of phenocrysts in the lavas increases progressively upward from approximately 4 percent in Fanney to about 8 percent in Jerky Mountain Rhyolite, whereas phenocryst contents of Apache Spring and Bloodgood Canyon ash-flow tuffs are significantly higher. Similarly, sanidine compositions vary from approximately Or_{55} in Fanney to Or_{43} in Jerky Mountain Rhyolites whereas, in Apache Spring ash-flow tuff, it ranges from Or_{80} at the base to Or_{50} at the top. Sanidine in Bloodgood Canyon is likewise more potassic than in Jerky Mountain Rhyolite. Similarly, Fanney Rhyolite contains phenocrysts of oligoclase (An_{20}-An_{25}) whereas in Apache Spring they vary from oligoclase (An_{26}) at the base to andesine (An_{32}) at the top. Plagioclase is absent in Bloodgood Canyon and Jerky Mountain Rhyolites. Carmichael (1963) showed that plagioclase is resorbed by alkali-rich magma during late stages of differentiation, with resultant crystallization of high-Na sanidine or anorthoclase and quartz.

Similar relationships can be demonstrated between the chemistry of the rhyolite lavas and ash-flow tuffs (Fig. 13). Silica increases progressively with time yet decreases toward the top of each zoned ash-flow sheet, and Al_2O_3, MgO, and CaO into the structural framework of the Mogollon Plateau volcano-tectonic complex and are not the voluminous remnants of ash-flow units. Groups of compositional ranges of Apache Spring and Bloodgood Canyon ash-flow tuffs are not continuous with Jerky Mountain lava flows, there being a distinct break between them. This is brought out by mineralogical changes between the units (Fig. 19). Abundance of phenocrysts in the lavas increases progressively upward from approximately 2 percent in [illegible] to about 8 percent in Jerky Mountain rhyolite, whereas phenocryst contents of Apache Spring and Bloodgood Canyon ash-flow units are significantly higher. Similarly, feldspar compositions vary from approximately $Or_{[illegible]}$ in [illegible] to $Or_{[illegible]}$ in Jerky Mountain Rhyolites whereas, in Apache Spring ash-flow tuff, it ranges from $Or_{[illegible]}$ at the base to $Or_{[illegible]}$ at the top; feldspar in Bloodgood Canyon is likewise more potassic than in Jerky Mountain Rhyolite. Similarly, [illegible] rhyolites contains phenocrysts of oligoclase ($An_{[illegible]}$-$An_{[illegible]}$) whereas in Apache Spring they vary from oligoclase ($An_{[illegible]}$) at the base to andesine ($An_{[illegible]}$) at the top. Plagioclase is absent in Bloodgood Canyon and Jerky Mountain Rhyolites. Carmichael (1963) argues that plagioclase is resorbed by alkali-rich magmas during late stages of differentiation, with resultant crystallization of high-Or sanidine or anorthoclase and quartz.

Similar relationships can be demonstrated between the chemistry of the rhyolite lavas and ash-flow units (Fig. 11). [illegible] increases progressively with [illegible] toward the top of each [illegible] ash-flow sheet, and K_2O, Na_2O, and [illegible]

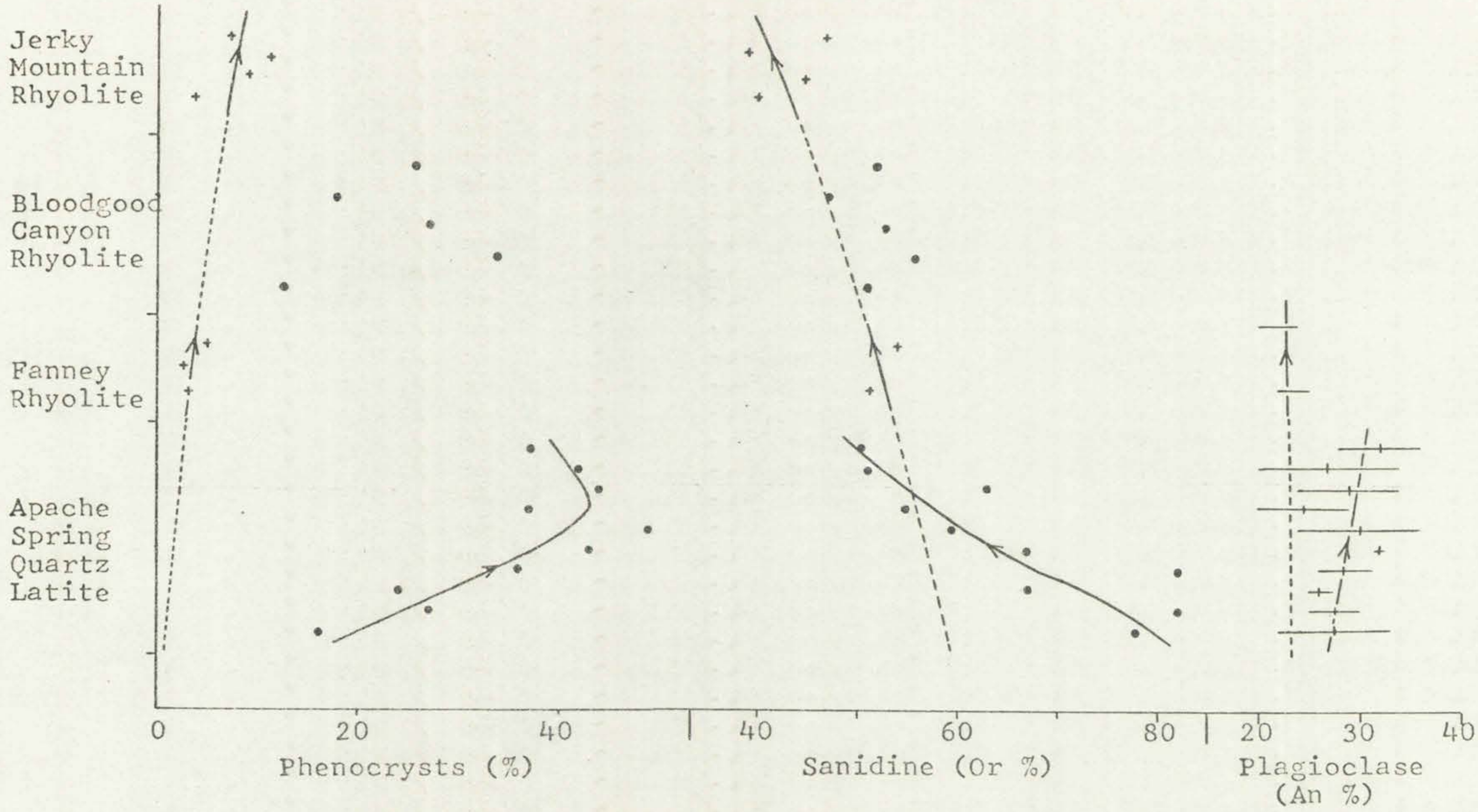

Fig. 12. Variation trends in ash flows and lava flows of the Middle Volcanic Group plotted against an arbitrary time scale.

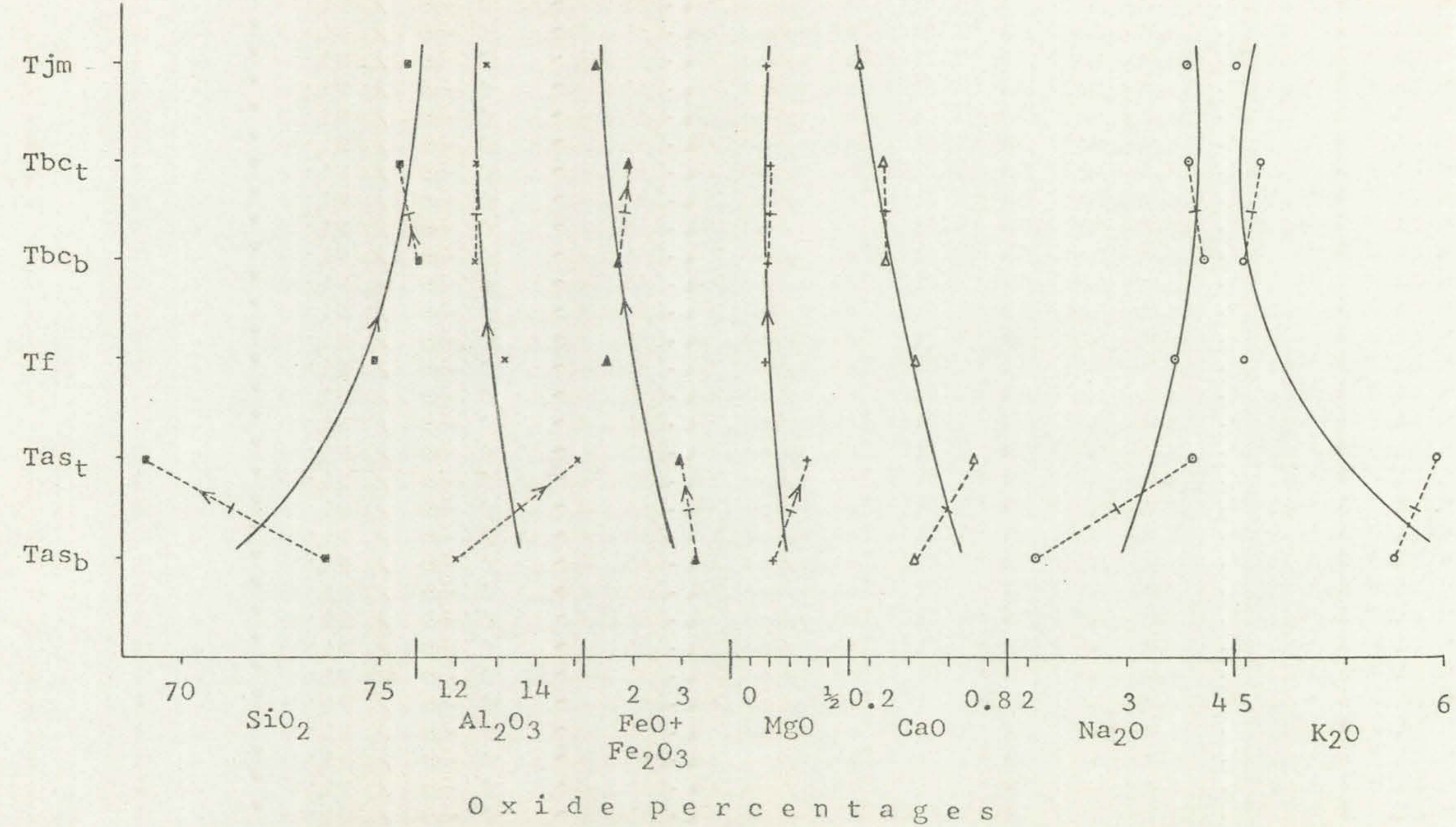

Tjm-Jerky Mountain Rhyolite; Tbc-Bloodgood Canyon Rhyolite (t)-top (b)-base; Tf - Fanney Rhyolite; Tas-Apache Spring Quartz Latite (t)-top (b)-base.

Fig. 13. Chemical variation trends in the Middle Volcanic Group, plotted against an arbitrary time scale.

all decrease slightly with time but increase toward the top of the ash flows. The alkalis also show discordant trends. Total iron is higher in the ash flows than in the lavas, possibly due to its concentration in the volatile-rich fractions of the magma by gas transfer (Stanton, 1967).

Despite local variations there can be little doubt that the Middle Volcanic Group represents a continuous differentiation series becoming progressively more felsic with time. The rocks are cogenetic and were probably derived from a batholithic parent magma that underwent fractional crystallization, the approximate course of differentiation being indicated by the compositions of Fanney and Jerky Mountain Rhyolites. Volatile-rich fractions that became concentrated at the top of the magma chamber formed smaller secondary chambers or cupolas that became separated from the bulk of the granitic magma. Differentiation and crystal growth were enhanced within these secondary, gas-rich chambers, resulting in strongly zoned magmas that burst out of their subterranean confines in the form of _nueés ardentes_, depositing Apache Spring and Bloodgood Canyon ash-flow tuffs. Each volatile-rich secondary magma retained the composition of the parent body at that stage of development, but strong differentiation in the secondary chambers resulted in the overprint of new variation trends different to those of the parent magma. Average composition of each ash-flow sheet falls close to the differentiation trend of the Middle Volcanic Group, indicating that compositional zoning of the ash flows was a secondary phenomenon all decrease slightly with time but increase toward the top of the ash flows. The alkalis also show discordant trends. Total iron is higher in the ash flows than in the lavas, possibly due to its concentration in the volatile-rich fractions of the magma by gas transfer (Stevens, 1952).

Despite local variations there can be little doubt that the Middle Volcanic Group represents a continuous differentiation series becoming progressively more felsic with time. The rocks are cogenetic and were probably derived from a [illegible] parent magma that underwent fractional crystallization, the predominant source of differentiation being indicated by the compositions of [illegible] and [illegible] Mountain Rhyolites. Volatile-rich fractions that became concentrated at the top of the magma chamber formed smaller secondary chambers or cupolas that became separated from the bulk of the parent magma. Differentiation and crystal growth were enhanced within these secondary, gas-rich chambers, resulting in strongly zoned magmas that burst out of their subterranean confines in the form of nuée ardentes, depositing Apache Spring and El [illegible] Canyon ash-flow tuffs. Each volatile-rich secondary magma retained the composition of the parent body at that stage of development, but strong differentiation in the secondary chambers resulted in the reversing of any variation trends inherent to those of the parent magma. Average compositions of each ash-flow sheet falls close to the differentiation trend of the Middle Volcanic Group, indicating that compositional zoning of the ash flows was a secondary phenomenon.

superimposed upon the differentiating parent batholith.

UPPER VOLCANIC GROUP

Rocks within this group fall into two separate suites - felsic and mafic - that probably originated independantly of one another. Included within the felsic suite in the mapped area are Deadwood Gulch Rhyolite, and the quartz latite at Turkeyfeather Creek. The mafic suite includes the Bearwallow Mountain Formation, Mogollon Andesite, and Double Spring Andesite. Chemical data are scanty and cover only the Bearwallow Mountain Formation.

Felsic Suite: Only two representatives of this suite are known from the mapped area and no chemical data are available. Vents for these units have not been located and little is known regarding their petrologic relationship to the voluminous post-Jerky Mountain felsic rocks in the northern part of the Mogollon Plateau. They lie unconformably upon rocks of the Middle Volcanic Group and are probably not part of the same differentiation sequence. Deadwood Gulch Rhyolite is more felsic than the older quartz latite at Turkeyfeather Creek and may be a more silicic differentiate of a common granodioritic parent magma. Quartz, ubiquitous in Deadwood Gulch Rhyolite, occurs only intermittently as phenocrysts in the quartz latite, whereas clinopyroxene is invariably present in the quartz latite but was not found in Deadwood Gulch Rhyolite.

Mafic Suite: Discussion of the mafic suite is restricted by

lack of data to the Bearwallow Mountain Formation. Only one thin section of Double Spring Andesite was examined and it is petrographically similar to Type I basaltic andesite of the Bearwallow Mountain Formation. Mogollon Andesite corresponds to Types I and II of the Bearwallow Mountain Formation.

A mineralogical variation diagram for five petrographic classes recognized within the Bearwallow Mountain Formation is presented (Fig. 14) while modal and chemical analyses of representative specimens are given in Tables 9 and 5 respectively. Three Bearwallow Mountain analyses were plotted on a chemical variation diagram (Fig. 15).

The Bearwallow Mountain Formation is calc-alkalic with a Peacock Index of 58 and a differentiation trend toward progressive enrichment of silica and alkalis with no significant increase in iron (Fig. 16). Although rare xenocrysts of quartz occur there is no evidence of large-scale assimilation, and fractional crystallization of basaltic magma is considered adequate to account for observed variation trends, although late-stage concentration of alkalis may have been enhanced by some process such as gas transfer. Relative volumes of the five petrographic types are difficult to determine but Types I, II, and III considerably exceed Types IV and V, and Types I and II are especially voluminous. Types I, II, and III are older than Types IV and V. Basaltic andesite with normative quartz and modal olivine (Type I) is probably closest to the composition of the parent magma which differentiated to produce small amounts of late-stage latitic residue (Types IV and V).

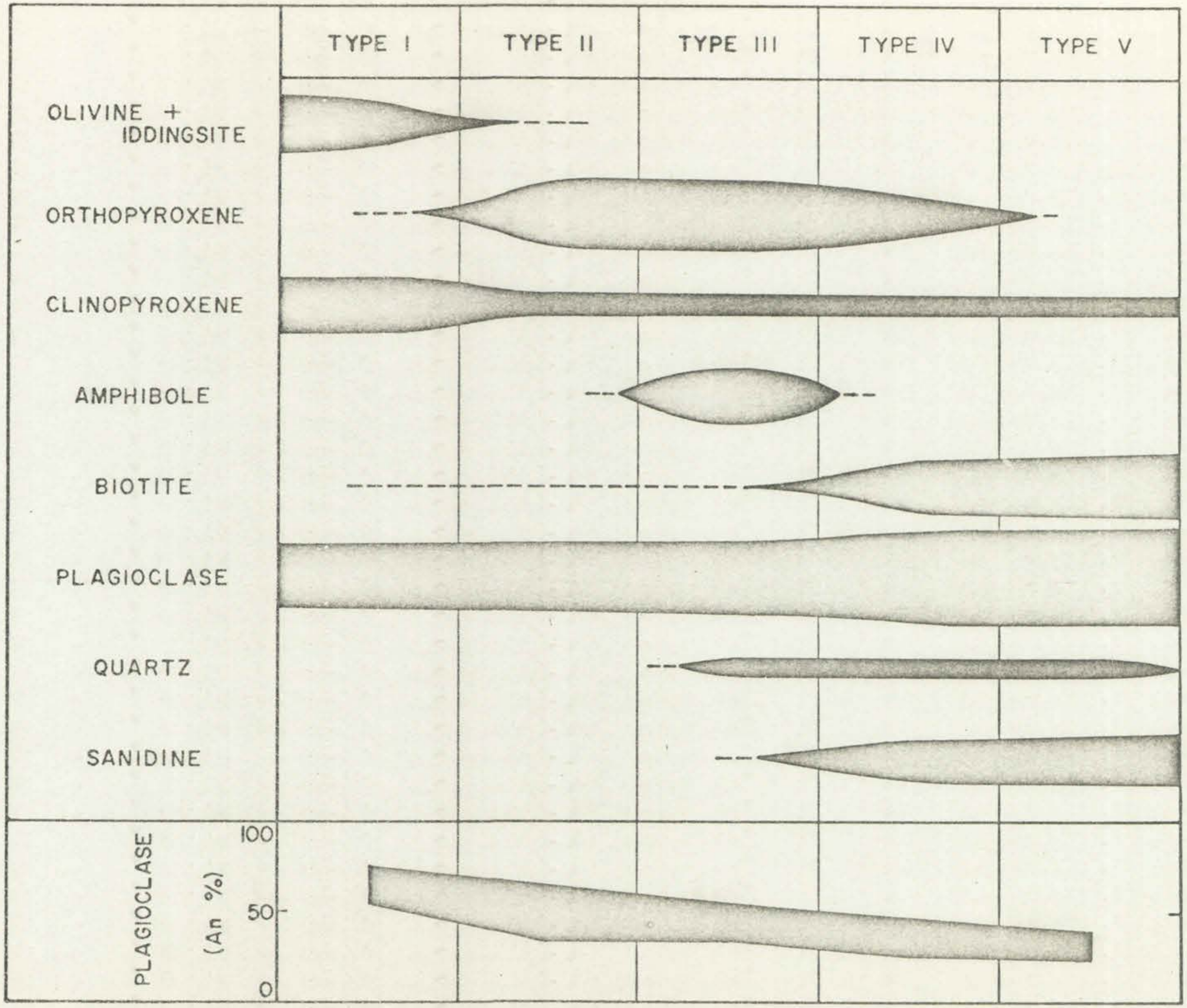

Fig. 14. Mineralogical variation diagram for the Bearwallow Mountain Formation.

Plagioclase crystallized continuously, becoming increasingly albite-rich in response to steadily increasing Na content of the magma (Fig. 14). Ferromagnesian minerals crystallized simultaneously with plagioclase, beginning in early stages with olivine and clinopyroxene. According to Sun (1957) alteration of olivine to iddingsite is a deuteric effect. Poldervaart and Hess (1951) showed that olivine reacts with silica-saturated melt to form orthopyroxene which continues to crystallize side by side with clinopyroxene. Two-pyroxene andesites of this type are represented by the Type II rocks (Fig. 14). Increasing silica, water and alkalis in the melt finally caused precipitation of hydrous oxyhornblende, the characteristic mineral of Type III latite, and by this stage the melt was depleted in MgO, total Fe, and CaO. Continued crystallization of orthopyroxene and clinopyroxene depleted the magma further in these elements whereas crystallization of albite-rich plagioclase resulted in preferential enrichment of the magma in K_2O (possibly assisted by gas transfer). The increased relative proportion of K_2O caused biotite to precipitate in place of hornblende and the residue crystallized largely as alkali feldspar and quartz.

REGIONAL PETROLOGIC TRENDS

The work of N. L. Bowen popularized the concept of differentiation of basaltic magma to produce rhyolitic residue, and the close association of andesitic and rhyolitic volcanic

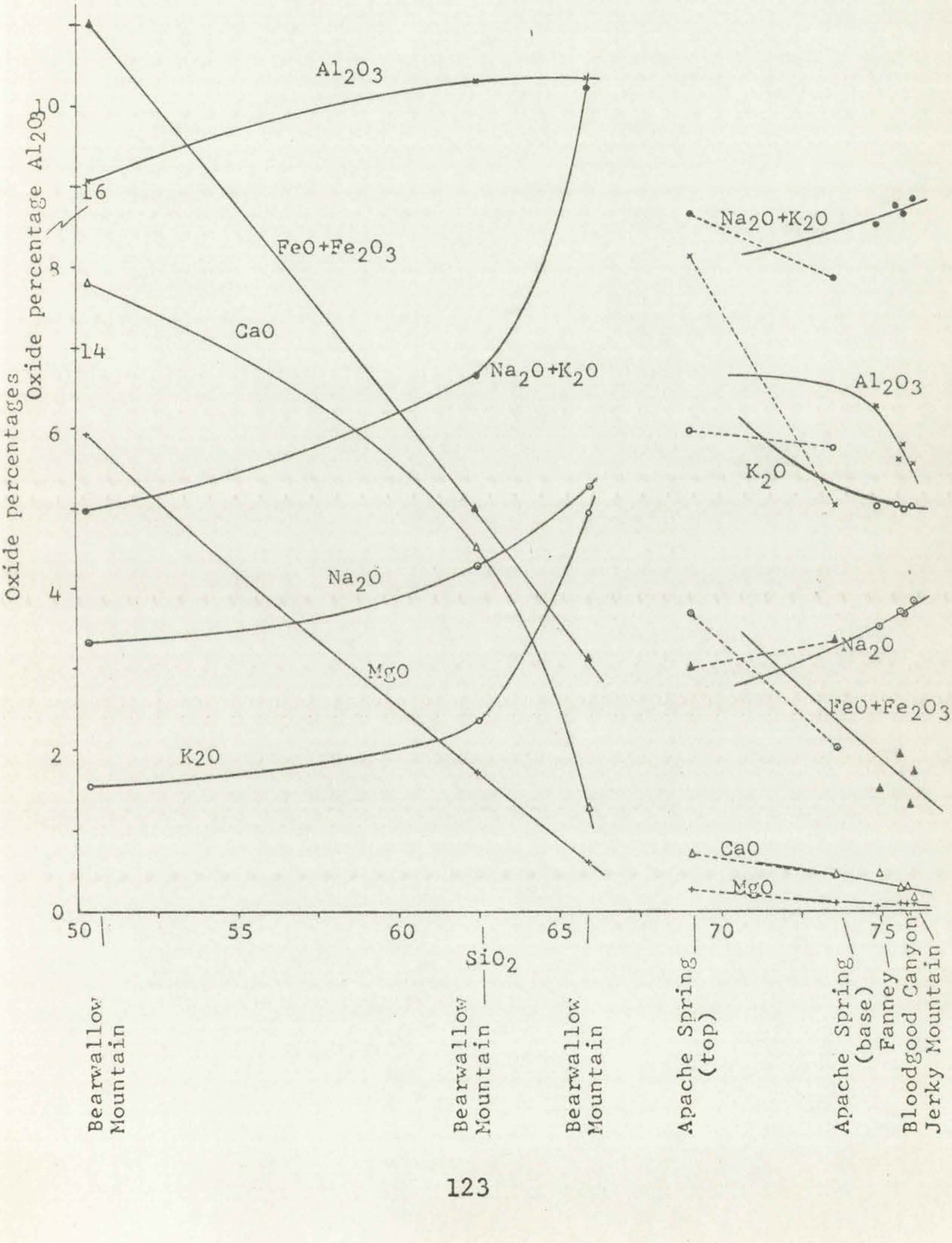

Fig. 15. Chemical variation diagram of volcanic rocks from the Mogollon Plateau.

rocks in the western United States has added further impetus to this school of thought. In the Mogollon Plateau volcanic province, however, there is evidence in favor of at least two separate magmas, one basaltic and the other rhyolitic.

Variation curves of the Bearwallow Mountain Formation and the Middle Volcanic Group are sharply discordant at approximately 67 percent SiO_2, similar to the break between intermediate and acidic rocks in the Mimbres Valley province (Elston, 1957, p. 53). I consider this discontinuity between the two suites to reflect fundamental differences in their differentiation paths, with the mafic rocks moving toward a highly alkalic end-product whereas the felsic suite trends toward a slightly more alkalic, but very silica-rich residue. This is well illustrated by the variation curve of K_2O which, in the mafic suite, increases sharply in the later stages of differentiation whereas it decreases slightly with increasing silica content in the Middle Volcanic Group (Fig. 15).

When the same rocks are plotted on a differentiation diagram (SiO_2/normative Q + Or + Ab) a similar relationship is observed (Fig. 17). The curve representing the mafic suite is less steep than that of the Middle Volcanic Group and is sharply discontinuous with it. This is significantly different to the differentiation pattern of volcanic rocks associated with the Creede caldera in Colorado which show continuous variation from 65-75 percent SiO_2 (Rattè and Steven, 1964).

Fourteen analyses of mafic and intermediate rocks (containing less than 66 percent SiO_2) from the Mogollon

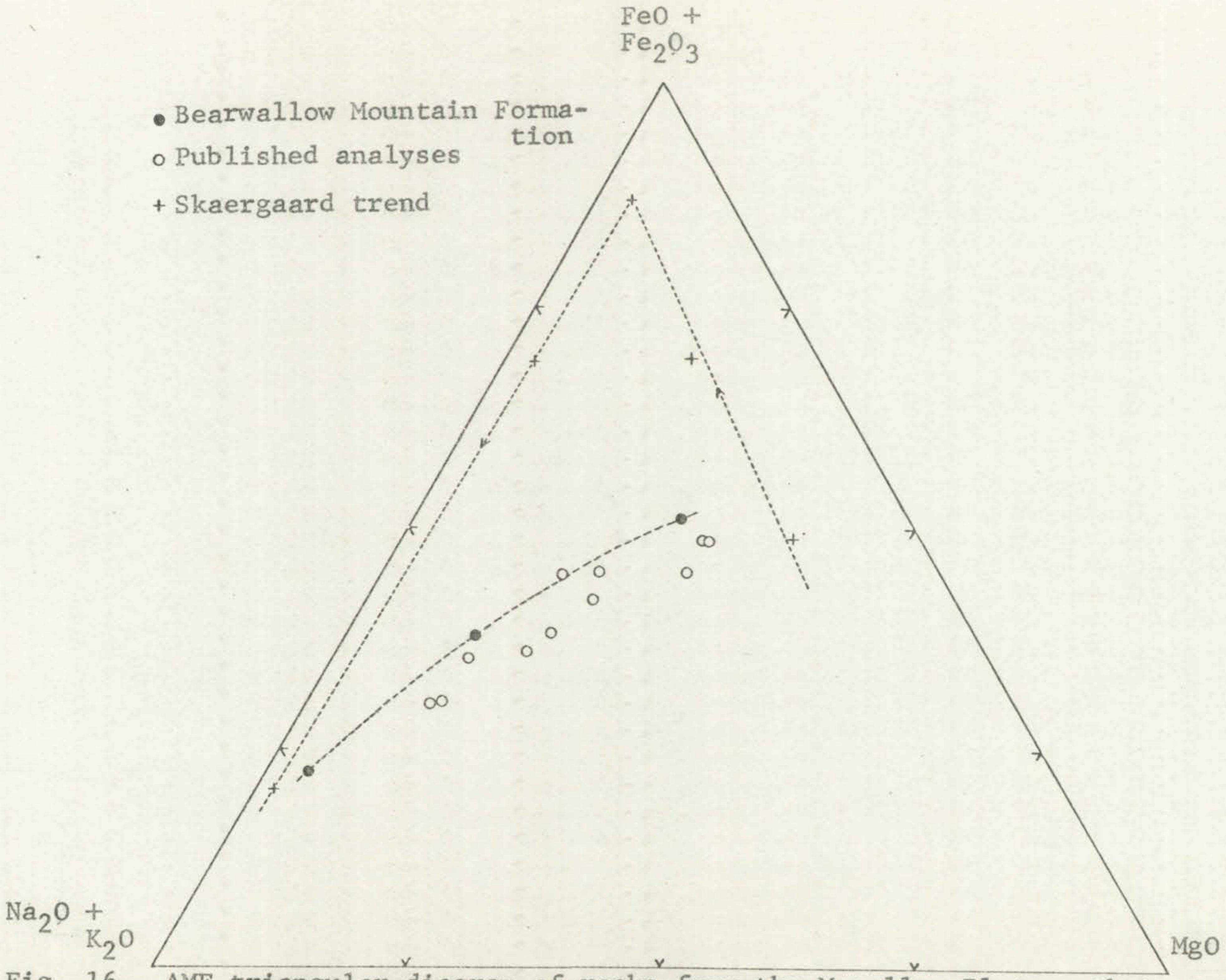

Fig. 16. AMF triangular diagram of rocks from the Mogollon Plateau that contain less than 66 percent SiO_2.

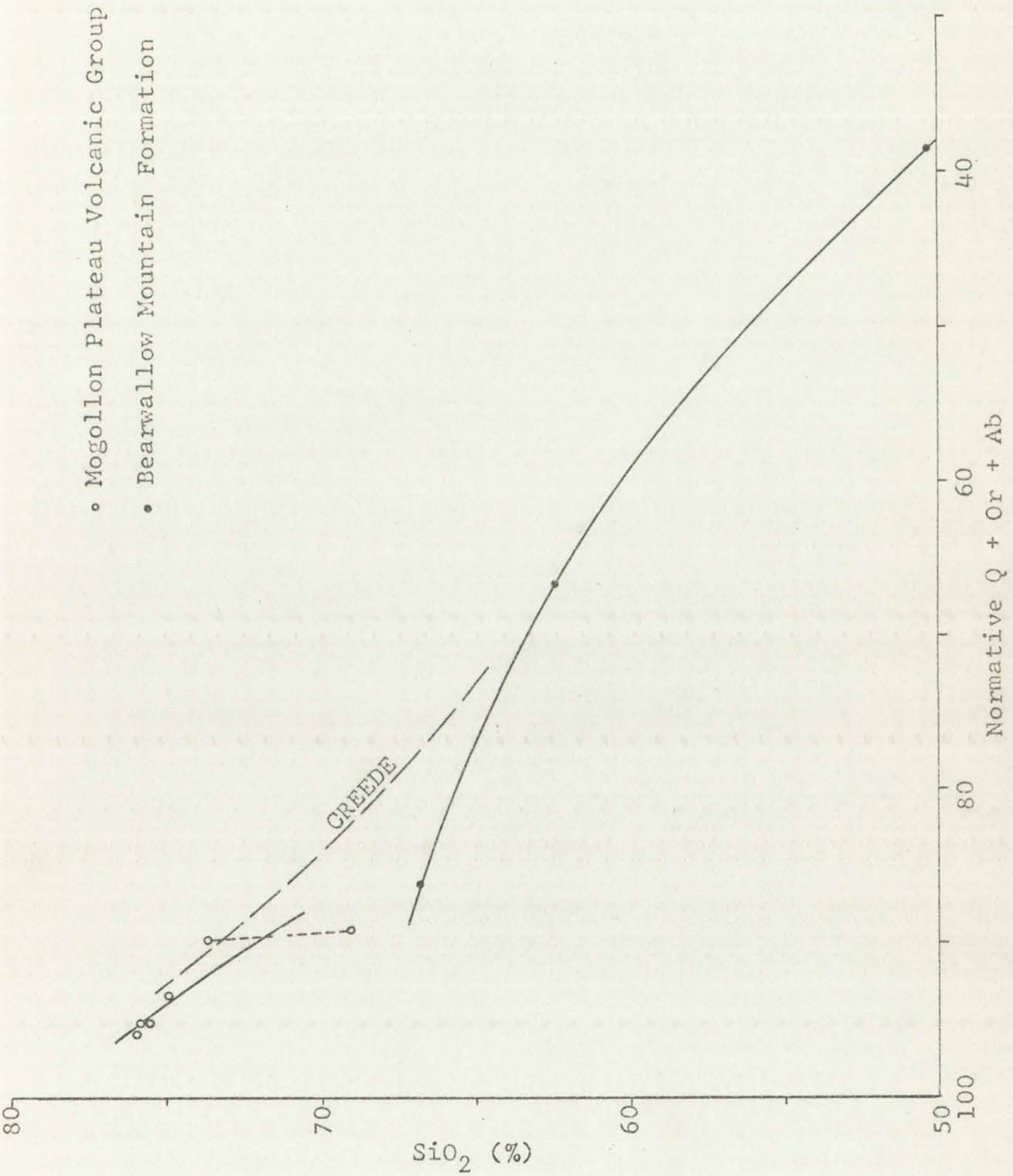

Fig. 17. Differentiation diagram of rocks of the Middle Volcanic Group and the Bearwallow Mountain Formation.

Plateau and its environs have been plotted on a triangular diagram ((Na_2O + K_2O) : MgO : (FeO + Fe_2O_3)) (Fig. 16). They display a calc-alkalic trend toward enrichment in alkalis with no noticeable increase in iron. The calc-alkalic trend is possibly due to crystallization of basaltic magma under constant P_{O_2} in an open system (Osborn, 1959). Free migration of volatiles (especially H_2O) in the upper mantle, coupled with high heat flow, satisfies the requirements for the observed trend of crystallization-differentiation.

Chemical analyses of the Middle Volcanic Group and felsic rocks from the Mimbres Valley province have been plotted on a CaO : (Na_2O + K_2O) : (FeO + Fe_2O_3 + MgO) triangular diagram (Fig. 18). The Mimbres Valley rocks are significantly richer in CaO and plot in a separate field from the Middle Volcanic Group. This is consistent with the interpretation that the Mimbres Valley rocks were derived by differentiation from an andesitic parent magma (Elston, 1957) whereas I consider the Middle Volcanic Group to have descended from a rhyolitic parent.

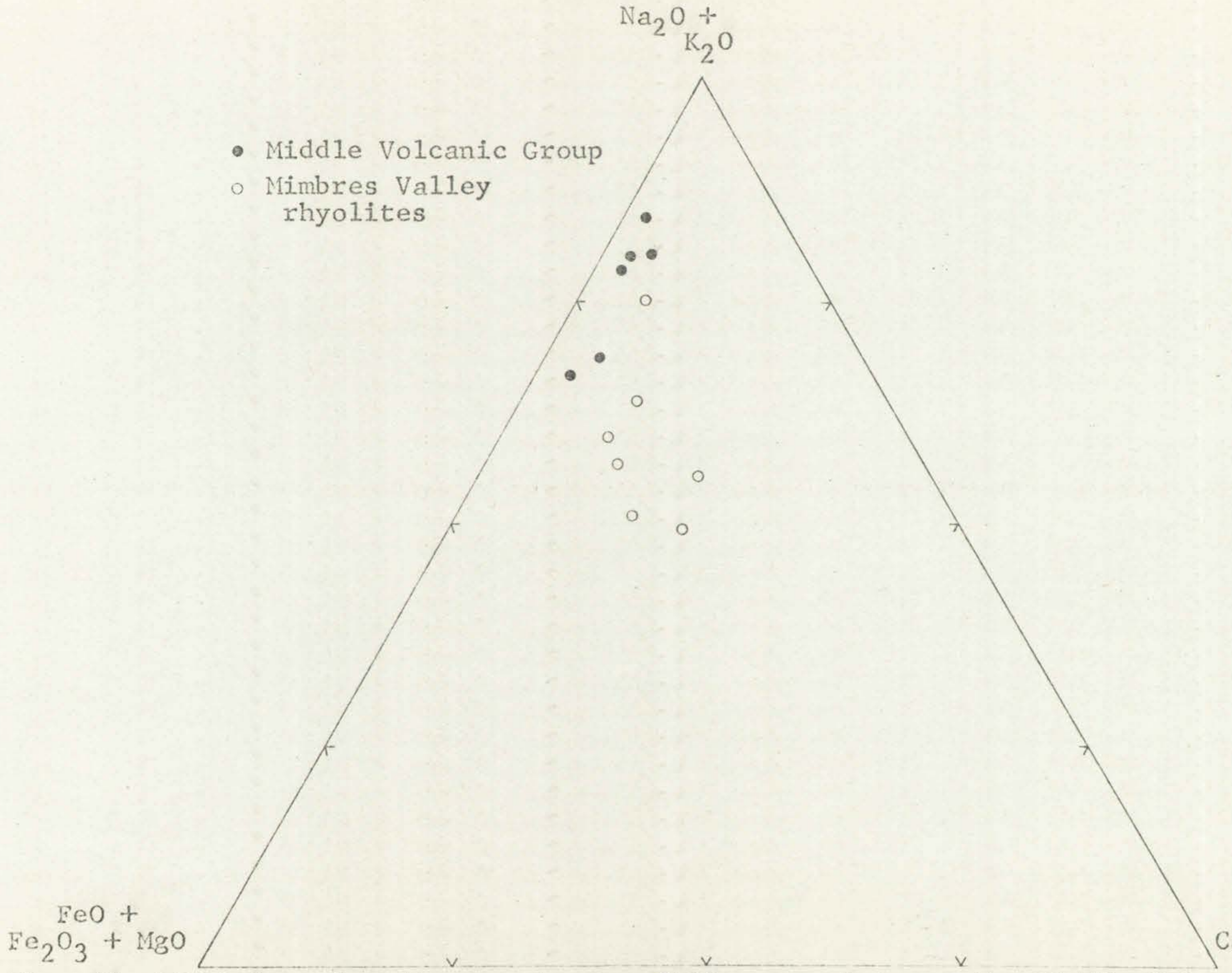

Fig. 18. ACF triangular diagram showing differences between the Middle Volcanic Group and felsic rocks from the Mimbres Valley province.

VOLCANO-TECTONIC EVOLUTION OF THE MOGOLLON PLATEAU

The Mogollon Plateau complex is an excellent example of calc-alkalic volcanism associated with a large volcano-tectonic depression which, unlike the San Juan Mountains in Colorado, has been recognized and interpreted as a unified structure since volcanological investigations on the complex began in 1963 (Elston, 1965a; Elston, Coney, and Rhodes, 1968). Following are some general observations and speculative conclusions regarding the geologic evolution of the western part of the structure:

(1) The Mogollon Plateau complex is superimposed upon a basement of older rocks (Datil, restricted sense) derived from widely separated source areas and belonging to at least three distinct petrologic provinces. Little is known of the volcano-tectonic structures related to these older rocks, and part of the vent of only one major ash-flow sheet, the Kneeling Nun Rhyolite, has been found (Kuellmer, 1954). Detailed petrologic work on the Mimbres Valley province has shown the volcanics to have been derived by differentiation from an andesitic parent magma (Elston, 1957).

(2) Direction of flow and stratigraphic thinning of the Lower Volcanic Group toward the Mogollon Plateau suggest that the area may have been a structural and topographic high. Thick accumulations of older andesite in areas peripheral to the Mogollon Plateau suggest the possible existence of large

andesitic volcanoes that collapsed into subsiding structural basins (Elston, 1960b).

(3) Volatile constituents were concentrated at the top of a rising granitic batholith and ultimately became separated as a separate phase when concentration of volatiles exceeded solubility in the magma. The volatile-rich fraction separated into a smaller cupola and, when gas pressure within the chamber exceeded lithostatic load, the magma was rapidly discharged as *nueès ardentes*, concurrently with volcano-tectonic collapse of the cupola roof. This activity gave rise to the Apache Spring ash-flow sheet within the Bursum cauldron. Defluidized residue of this magma was finally extruded as quartz latite lava flows (Sacaton Quartz Latite and the quartz latite at Nabours Mountain). Fracturing along the margins of the deep-seated batholith resulted in extrusion of crystal-poor viscous rhyolite lava, giving rise to Fanney Rhyolite. The vent of Apache Spring ash-flow tuffs, as determined by flow direction studies, is located along the southern margin of the Bursum cauldron and is not coincident with vents of Fanney Rhyolite west of the Bursum cauldron.

(4) Extrusion of the Bloodgood Canyon and Jerky Mountain Rhyolites probably occurred in a similar manner, the former accompanied by volcano-tectonic collapse of the Gila Cliff Dwellings cauldron. The almost complete lack of compositional zoning in Bloodgood Canyon Rhyolite suggests that it had reached its thermal and compositional trough, preventing

further crystallization-differentiation. Jerky Mountain Rhyolite was extruded along fissures outlining the margins of a diminished batholith, giving rise to a second concentric ring of flow-banded lava inside the outer band of Fanney Rhyolite.

(5) Following extrusion of Jerky Mountain Rhyolite a period of erosion ensued, giving rise to a regional unconformity. Subsidence of the central basin commenced, accompanied by faulting and development of radial sags and spurs which were filled with Deadwood Gulch Rhyolite. Volcanism in the Mogollon Plateau culminated in the extrusion of dark-colored rocks, ranging in composition from basaltic andesite to latite. Some rhyolite domes may have protruded as arcuate ridges above the basaltic plains.

(6) The post-volcanic history of the Mogollon Plateau complex is largely one of tensional faulting, erosion, and sedimentation, and continued sagging of the central basin in post-Gila time. Preservation of the complex as a physiographic entity is due in part to its relatively young age and also to the fact post-Bearwallow Mountain faulting to a large extent followed pre-existing structural trends.

APPENDIX I

Fortran IV program for flow lineation analysis (Smith, 1967).

```
/ID
/JOB TIME=02,GO
/FTC NAME=FLOLIN,LIST
      DIMENSION O(18),TH(18),X(18)
  100 FORMAT(18F3.0,12X,A4,A2)
      WRITE(6,104)
  104 FORMAT('1     VEC M    VEC S    VAR VM    SD VM     CHI 2
     1 CHI OR       VAR CH   SD CH    IDENT')
    9 READ(5,100)O,ID1,ID2
      IF(O(1)-999.)10,11,10
   10 XX=0.0
      DO 2 I=1,18
      TH(I)=XX/57.29577951
    2 XX=XX+10.0
      R=0.0
      DO 3 I=1,18
    3 R=R+O(I)
      RR=R/18.0
      DO 4 I=1,18
    4 X(I)=(O(I)-RR)/SQRT(RR)
      SUM1=0.0
      SUM2=0.0
      SUM3=0.0
      SUM4=0.0
      DO 1 I=1,18
      TH2=TH(I)*2.0
      SUM1=SUM1+(X(I)*COS(TH2))
      SUM2=SUM2+(COS(TH2)**2)
      SUM3=SUM3+(X(I)*SIN(TH2))
    1 SUM4=SUM4+(SIN(TH2)**2)
      C=SUM1/2.994
      S=SUM3/2.994
      SC=S/C
      THX=.5*ATAN(SC)*57.29577951+5.0
      IF(THX)15,16,16
   15 THX=180.0+THX
      THZ=THX-90.0
      GO TO 20
   16 THZ=THX+90.0
   20 X2=C*C+S*S
      Z=0.0
      DO 7 I=1,18
      TH(I)=Z/57.29577951
    7 Z=Z+20.0
      SUMS=0.0
      SUMC=0.0
      DO 8 I=1,18
```

```
      BVX=TH(I)
      SUMS=SUMS+SIN(BVX)*O(I)
    8 SUMC=SUMC+COS(BVX)*O(I)
      XY=SUMS/SUMC
      ALF=.5*ATAN(XY)*57.29577951
      IF(ALF)13,14,14
   13 ALF=180.0+ALF
      ALX=ALF-90.0
      GO TO 21
   14 ALX=ALF+90.0
   21 Q1=SUMS**2+SUMC**2
      Q2=SQRT(Q1)/R
      Z=5.0
      DO 5 I=1,18
      TH(I)=Z
    5 Z=Z+10.0
      SUMV=0.0
      SUMVX=0.0
      DO 6 I=1,18
      SUMVX=SUMVX+O(I)*((TH(I)-ALX)**2)
    6 SUMV=SUMV+O(I)*((TH(I)-ALF)**2)
      S2=SUMV/(R-1.0)
      S2X=SUMVX/(R-1.0)
      S=SQRT(S2)
      SX=SQRT(S2X)
      SCH=0.0
      SCHX=0.0
      DO 12 I=1,18
      SCHX=SCHX+O(I)*((TH(I)-THZ)**2)
   12 SCH=SCH+O(I)*((TH(I)-THX)**2)
      CHV=SCH/(R-1.0)
      CHVX=SCHX/(R-1.0)
      CHSD=SQRT(CHV)
      CHSDX=SQRT(CHVX)
  105 FORMAT(2X,F7.2,2X,F7.2,2X,F9.0,2X,F7.2,2X,F8.3,2X,F6.1,
     12X,F7.1,2x,F6.2,5X,A4,A2)
      WRITE(6,105)ALF,Q2,S2,S,X2,THX,CHV,CHSD,ID1,ID2
  106 FORMAT(2X,F7.2,11X,F9.0,2X,F7.2,12X,F6.1,2X,F7.1,2X,F6.2)
      WRITE(6,106)ALX,S2X,SX,THZ,CHVX,CHSDX
      GO TO 9
   11 CONTINUE
      CALL EXIT
      END
/DATA
```

APPENDIX II

Statistical values for flow lineation measurements of volcanic rocks

	Grains counted	Vector mean	Vector magnitude	Tukey Chi-square	Azimuth
Cooney Formation	108	198°	0.25	13.87	-
	230	223°	0.36	60.42	-
	242	256°	0.36	61.97	-
	87	249°	0.30	15.49	-
	166	270°	0.14	6.70	-
	74	222°	0.23	7.70	-
	521	229°	0.07	5.24	-
	30	259°	0.61	22.62	f
	158	214°	0.18	9.80	-
	233	184°	0.19	16.77	-
	292	215°	0.10	6.06	-
	148	280°	0.32	30.14	-
	225	248°	0.13	8.02	-
	220	242°	0.08	2.92*	-
	194	300°	0.09	2.99*	-
	field observation	230°	-	-	f
Tadpole Ridge Quartz Latite	129	223°	0.21	11.16	-
Houston Andesite	200	177°	0.44	78.09	-
	200	201°	0.26	27.20	-
	200	200°	0.35	50.14	-
	233	218°	0.39	70.63	i
	228	252°	0.53	130.52	-
Apache Spring Quartz Latite	127	169°	0.23	13.94	b, s
	115	183°	0.38	32.92	e
	148	260°	0.17	8.82	-
	150	202°	0.41	50.47	f, b, s
	153	216°	0.25	19.78	-
	134	149°	0.50	67.31	e, b
	181	156°	0.40	58.53	b
	158	219°	0.18	9.99	p, e, b
	141	188°	0.15	6.57	-
	170	231°	0.29	28.17	p
	178	111°	0.14	6.97	-
	184	171°	0.37	50.40	b, s
	201	120°	0.16	10.61	-
	199	176°	0.35	49.03	p, s

APPENDIX II (contd.)

	Grains counted	Vector mean	Vector magnitude	Tukey Chi-square	Azimuth
Apache Spring Quartz Latite (contd.)	151	223°	0.16	8.17	-
	204	185°	0.16	9.91	-
	90	218°	0.01	0.03*	p
	147	196°	0.07	1.25*	-
	172	167°	0.08	2.13*	b, s
	59	250°	0.12	1.65*	-
	104	223°	0.11	2.79*	-
Quartz Latite at Nabours Mountain	200	126°	0.26	26.53	s
Sacaton Quartz Latite	57	308°	0.28	8.87	-
	158	207°	0.20	13.18	-
	30	206°	0.30	5.42	-
	121	141°	0.14	5.03	-
	83	256°	0.39	24.76	-
	50	189°	0.20	3.83*	-
	55	209°	0.10	1.08*	-
Pacific Quartz Latite	138	203°	0.35	33.87	-
	61	214°	0.09	0.91*	-
Mineral Creek Andesite	171	269°	0.18	11.50	-
	163	247°	0.33	36.69	b
	232	204°	0.49	113.11	-
	200	209°	0.12	5.52	-
	226	274°	0.24	26.76	-
	245	300°	0.46	103.42	-
	field observation	210°	-	-	-
Bloodgood Canyon Rhyolite	144	106°	0.21	13.09	-
	140	137°	0.27	21.20	-
	147	180°	0.14	5.44	-
	57	122°	0.44	21.67	-
	90	190°	0.21	8.29	-
	124	250°	0.17	7.33	-
	85	250°	0.10	1.85*	-
	83	259°	0.12	2.27*	-
	97	274°	0.07	0.87*	-
	141	260°	0.08	1.61*	p, s
	121	249°	0.12	3.39*	-
	200	234°	0.08	2.80*	-

APPENDIX II (contd.)

	Grains counted	Vector mean	Vector magnitude	Tukey Chi-square	Azimuth
Deadwood Gulch Rhyolite	150	112°	0.25	19.04	-
	73	212°	0.21	6.18	-
	156	211°	0.14	6.18	-
	119	251°	0.14	4.65	f
	92	237°	0.06	0.60*	-
	149	143°	0.10	2.72*	-
	field observation	110°	-	-	-
	"	120°	-	-	-
Mogollon Andesite	203	104°	0.44	78.33	b
	200	213°	0.69	188.83	b
Bearwallow Mountain Formation	180	268°	0.79	226.52	b
	211	240°	0.53	117.88	-
	200	231°	0.55	120.12	-
	209	135°	0.85	305.45	b
	239	143°	0.36	60.49	-
	269	263°	0.15	12.40	-
	238	264°	0.19	17.08	-
	273	266°	0.18	18.04	-
	245	143°	0.39	76.22	-
	175	108°	0.40	55.64	-
	263	244°	0.13	9.08	-
	215	213°	0.30	39.64	-
	211	134°	0.27	31.24	-
	204	212°	0.39	61.66	-
	211	184°	0.19	15.43	-
	200	232°	0.71	202.03	s
	204	226°	0.18	13.06	-
	197	127°	0.31	38.43	-
	189	209°	0.38	55.48	-
	215	150°	0.08	2.52*	-

Azimuth criteria:
f - fork-shaped shards
i - imbrication effect
b - block effect
p - penetration effect
s - spindle-shaped objects
e - eddy effect
- - not determined
* - significance below 90% confidence level

APPENDIX III

Fortran IV program for statistical analysis of zircons.

```
/ID
/JOB TIME=02,GO
/FTC NAME=ZIRCON,LIST
      DIMENSION NL(100),NB(100),NS(100),NE(100),NV(100)
      DIMENSION X(4),Y(4)
   50 N=
      C=
      WRITE(6,1)N,C
    1 FORMAT(1X,'N=',I3,3X,'C=',F7.3)
      HL1=0.000
      HL2=0.020
      HL3=0.560
      HE1=1.00
      HE2=0.20
      HE3=6.00
      HV1=0.00000
      HV2=0.00010
      HV3=0.00500
    2 FORMAT(2F6.3,5X,2F6.3,5X,2F6.3,5X,2F6.3)
      DO 20 JJ=1,100
      NL(JJ)=0
      NB(JJ)=0
      NS(JJ)=0
      NE(JJ)=0
   20 NV(JJ)=0
      SUMX=0.
      SUMY=0.
      SUME=0.
      SUMS=0.
      SUMV=0.
      SUMXX=0.
      SUMYY=0.
      SUMXY=0.
      FN=N
      DO 6 K=1,N,4
      READ(5,2)X(1),Y(1),X(2),Y(2),X(3),Y(3),X(4),Y(4)
      IF(N-K-3)4,3,3
    3 M=4
      GO TO 5
    4 M=N-K+1
    5 DO 6 J=1,M
      X(J)=X(J)/C
      Y(J)=Y(J)/C
      E=X(J)/Y(J)
      S=SQRT(X(J)*Y(J))
      V=X(J)*Y(J)*Y(J)
      JJ=(X(J)-HL1)/HL2+1.0
      NL(JJ)=NL(JJ)+1
```

```
    JJ=(Y(J)-HL1)/HL2+1.0
    NB(JJ)=NB(JJ)+1
    JJ=(S-HL1)/HL2+1.0
    NS(JJ)=NS(JJ)+1
    JJ=(E-HE1)/HE2+1.0
    NE(JJ)=NE(JJ)+1
    JJ=(V-HV1)/HV2+1.0
    NV(JJ)=NV(JJ)+1
    SUMX=SUMX+X(J)
    SUMY=SUMY+Y(J)
    SUME=SUME+E
    SUMS=SUMS+S
    SUMV=SUMV+V
    SUMXX=SUMXX+X(J)*X(J)
    SUMYY=SUMYY+Y(J)*Y(J)
  6 SUMXY=SUMXY+X(J)*Y(J)
    XBAR=SUMX/FN
    YBAR=SUMY/FN
    EBAR=SUME/FN
    SBAR=SUMS/FN
    VBAR=SUMV/FN
    WRITE(6,7)XBAR,YBAR,EBAR
  7 FORMAT(1X,'XBAR=',F7.5,3X,'YBAR=',F7.5,3X,'EBAR=',F7.5)
    WRITE(6,15)SBAR,VBAR
 15 FORMAT(1X,'SBAR=',F7.5,3X,'VBAR=',F7.5)
    RATIO=XBAR/YBAR
    SX=SQRT(SUMXX/FN-XBAR*XBAR)
    SY=SQRT(SUMYY/FN-YBAR*YBAR)
    WRITE(6,8)RATIO,SX,SY
  8 FORMAT(1X,'RATIO=',F7.5,3X,'SX=',F7.5,3X,'SY=',F7.5)
    RD=SQRT((FN*SUMXX-SUMX*SUMX)*(FN*SUMYY-SUMY*SUMY))
    R=(FN*SUMXY-SUMX*SUMY)/RD
    SLOPE=SY/SX
    RECIP=1.0/SLOPE
    WRITE(6,9)R,SLOPE,RECIP
  9 FORMAT(1X,'R=',F7.5,3X,'SLOPE=',F7.5,3X,'RECIP=',F7.4)
    SE=SLOPE*SQRT((1.0-R*R)/FN)
    DS=2.0*(1.0-R)*(SX*SX+SY*SY)/(XBAR*XBAR+YBAR*YBAR)
    D=100.*SQRT(DS)
    WRITE(6,10)SE,D
 10 FORMAT(1X,'ST ERROR SLOPE=',F7.5,3X,'D=',F6.2)
    A=SLOPE
    B=YBAR-A*XBAR
    WRITE(6,11)A,B
 11 FORMAT(1X,'REG LINE Y=',F7.5,'X + ',F7.5)
    WRITE(6,21)
 21 FORMAT(1X,'ELONGATION HISTOGRAM')
    JJ=1
    H1=HE1
 23 H2=H1+HE2
    HN=NE(JJ)
    PERC=HN/FN*100.
    WRITE(6,22)H1,H2,HN,PERC
```

```
   22 FORMAT(1X,F5.2,3X,F5.2,3X,F6.0,3X,F6.3)
      JJ=JJ+1
      H1=H1+HE2
      IF(H1-HE3)23,24,24
   24 CONTINUE
      WRITE(6,25)
   25 FORMAT(1X,'LENGTH AND BREADTH HISTOGRAMS')
      JJ=1
      H1=HL1
   27 H2=H1+HL2
      HNL=NL(JJ)
      PERCL=HNL/FN*100.
      HNB=NB(JJ)
      PERCB=HNB/FN*100.
      HNS=NS(JJ)
      PERCS=HNS/FN*100.
      WRITE(6,26)H1,H2,HNL,PERCL,HNB,PERCB,HNS,PERCS
   26 FORMAT(1X,2F8.3,F8.0,F8.2,10X,F8.0,F8.2,10X,F8.0,F8.2)
      JJ=JJ+1
      H1=H1+HL2
      IF(H1-HL3)27,28,28
   28 CONTINUE
      WRITE(6,30)
   30 FORMAT(1X,'VOLUME HISTOGRAM')
      JJ=1
      H1=HV1
   31 H2=H1+HV2
      HNV=NV(JJ)
      PERCV=HNV/FN*100.
      WRITE(6,32)H1,H2,HNV,PERCV
   32 FORMAT(1X,F7.5,3X,F7.5,3X,F6.0,3X,F6.3)
      JJ=JJ+1
      H1=H1+HV2
      IF(H1-HV3)31,34,34
   34 CONTINUE
      CALL EXIT
      END
/DATA
```

REFERENCES

Alper, A. M. and Poldervaart, A., 1957, Zircons from the Animas stock and associated rocks, New Mexico: Econ. Geol., v. 52, p. 952-971.

Barth, T. F. W., 1952, Theoretical Petrology: John Wiley and Sons, Inc., New York, 387 p.

Carmichael, I. S. E., 1963, The crystallization of feldspar in volcanic acid liquids: Quart. J. Geol. Soc. London, v. 119, p. 95-131.

Christiansen, R. L. and Lipman, P. W., 1966, Emplacement and thermal history of a rhyolite lava flow near Fortymile Canyon, southern Nevada: Bull. Geol. Soc. Amer., v. 77, p. 671-684.

Cummings, D., 1964, Eddies as indicators of local flow directions in rhyolite: U. S. Geol. Surv. Prof. Paper 475-D, p. D70-D72.

Dallmus, K. F., 1958, Mechanics of basin evolution and its relation to the habitat of oil in the basin: in "Habitat of Oil" (ed. L. G. Weeks), Amer. Assoc. Petrol. Geol. Symposium, p. 883-931.

Dane, C. H. and Bachman, G. O., 1965, Geologic map of New Mexico: U. S. Geol. Surv., 2 sheets.

Eckelmann, F. D. and Kulp, J. L., 1956, The sedimentary origin and stratigraphic equivalence of the so-called Cranberry and Henderson granites in western North Carolina: Amer. J. Sci., v. 254, p. 288-315.

Elston, W. E., 1957, Geology and mineral resources of Dwyer quadrangle, Grant, Luna and Sierra Counties, New Mexico: New Mexico Bur. Mines. Min. Res. Bull. 38, 86 p.

_______, 1958, Burro uplift, northeastern limit of sedimentary basin of southwestern New Mexico and southeastern Arizona: Bull. Amer. Assoc. Petrol. Geol., v. 42, p. 2514-2516.

_______, 1960a, Reconnaissance geologic map of Virden thirty-minute quadrangle: New Mexico Bur. Mines Min. Res. Geol. Map 15.

_______, 1960b, Some aspects of volcanism and mineralization in southwestern New Mexico: Roswell Geol. Soc. Guidebook 11 to Hatchet Mountains, p. 57-59.

REFERENCES

[illegible], 1971?, [illegible] from the [illegible] ranges, New Mexico: [illegible]

Barth, T. F. W., 1962, Theoretical Petrology: John Wiley and Sons, Inc., New York, 416 p.

Carmichael, I. S. E., 1963, The crystallization of feldspar in volcanic acid liquids: Quart. J. Geol. Soc. London, v. 119, p. 95-131.

Christiansen, R. L. and Lipman, P. W., 1966, Emplacement and thermal history of a rhyolite lava flow near Fortymile Canyon, southern Nevada: Geol. Soc. Amer. Bull., v. 77, p. 671-684.

Cummings, D., [illegible]

[illegible], 1958, [illegible] in the basins in "Habitat of Oil" (ed. L. G. Weeks), Amer. Assoc. Petrol. Geol. Symposium, p. [illegible]

Dane, C. H. and Bachman, G. O., 1965, Geologic map of New Mexico: U. S. Geol. Survey, 2 sheets.

[illegible], 1956, The sedimentary origin and stratigraphic equivalence of the so-called Cranberry and Henderson granites in western North Carolina: Amer. J. Sci., v. 254, p. [illegible]

Elston, W. E., 1957, Geology and mineral resources of Dwyer quadrangle, Grant, Luna, and Sierra Counties, New Mexico: New Mexico Bur. Mines Mineral Res. Bull. 38, 86 p.

______ 1968, [illegible] of southwestern New Mexico and southeastern Arizona: Amer. Assoc. Petrol. Geol. Bull., v. 52, p. [illegible]

______ 1970, [illegible]

______ [illegible]

Elston, W. E., 1965a, Rhyolite ash-flow plateaus, ring-dike complexes, calderas, lopoliths, and moon craters: Ann. New York Acad. Sci., v. 123, p. 817-842.

_______, 1965b, Volcanic rocks of the Mimbres and upper Gila drainages, New Mexico: New Mexico Geol. Soc. Guidebook 16 (Southwestern New Mexico II), p. 167-179.

_______, 1965c, The Mogollon Plateau volcanic province: possible connection with ring-dike complexes and lunar craters (abs): New Mexico Geol. Soc. Guidebook 16 (Southwestern New Mexico II), p. 239.

_______, 1968, Terminology and distribution of ash flows of the Mogollon-Silver City-Lordsburg region, New Mexico: Arizona Geol. Soc. Guidebook III to Southern Arizona, p. 231-240.

Elston, W. E., Bikerman, M., and Damon, P. E., 1968, Significance of new K-Ar dates from southwestern New Mexico: in "Correlation and chronology of ore deposits and volcanic rocks", U. S. Atomic Energy Comm. Ann. Prog. 600-689-100, AT(11-1)-689, Geochronology Labs., Univ. Arizona, p. AIV-1-AIV-20.

Elston, W. E., Coney, P. J., and Rhodes, R. C., 1968, A progress report on the Mogollon Plateau volcanic province, southwestern New Mexico: Quart. Colorado School Mines, v. 63, no. 3, p. 261-287.

Farkas, S. E., 1969, Geology of the southern San Mateo Mountains, Socorro and Sierra Counties, New Mexico: Ph.D. dissertation, Univ. New Mexico (unpublished), 137 p.

Ferguson, H. G., 1927, Geology and ore deposits of the Mogollon mining district, New Mexico: U. S. Geol. Surv. Bull. 787, 100 p.

Furlow, J. W., 1965, Geology of the San Mateo Peak area, Socorro County, New Mexico: M.S. thesis, Univ. New Mexico (unpublished), 83 p.

Gilbert, G. K., 1875, Report on the geology of portions of New Mexico and Arizona examined in 1873: U. S. Geol. and Geog. Surv. West of 100th Meridian, v. 3, pt. 5, p. 515-516.

Giles, D. L., 1967, A petrochemical study of compositionally zoned ash-flow tuffs: Ph.D. dissertation, Univ. New Mexico (unpublished), 184 p.

Gillerman, E., 1964, Mineral deposits of western Grant County, New Mexico: New Mexico Bur. Mines Min. Res. Bull. 83, 213 p.

Givens, D. B., 1957, Geology of Dog Springs quadrangle: New Mexico Bur. Mines Min. Res. Bull. 58, 40 p.

Heindl, L. A., 1952, Gila Conglomerate: Arizona Geol. Soc. Guidebook to Southern Arizona, p. 113-116.

_______, 1962, Should the term "Gila Conglomerate" be abandoned?: Arizona Geol. Soc. Digest, v. 5, p. 73-88.

Jicha, H. L. Jr., 1954, Geology and mineral resources of Lake Valley quadrangle, Grant, Luna, and Sierra Counties, New Mexico: New Mexico Bur. Mines Min. Res. Bull. 37, 93 p.

Jones, W. R., Hernon, R. M., and Moore, S. L., 1967, General geology of Santa Rita quadrangle, Grant County, New Mexico: U. S. Geol. Surv. Prof. Paper 555, 144 p.

Kelley, V. C., 1955, Regional tectonics of south-central New Mexico: New Mexico Geol. Soc. Guidebook 6 (South-central New Mexico), p. 96-104.

Kennedy, G. C., 1948, Equilibrium between volatiles and iron oxides in igneous rocks: Amer. J. Sci., v. 246, p. 529-549.

Kuellmer, F. J., 1954, Geologic section of the Black Range at Kingston, New Mexico: New Mexico Bur. Mines Min. Res. Bull. 33, 100 p.

Larsen, L. H. and Poldervaart, Arie, 1957, Measurement and distribution of zircons in some granitic rocks of magmatic origin: Min. Mag., v. 31, p. 544-564.

Nockolds, S. R., 1954, Average chemical compositions of some igneous rocks: Bull. Geol. Soc. Amer., v. 65, p. 1007-1032.

Osborn, E. F., 1959, Role of oxygen pressure in the crystallization and differentiation of basaltic magma: Amer. J. Sci., v. 257, p. 609-647.

Poldervaart, Arie, 1955, Zircons in rocks: I. Sedimentary rocks: Amer. J. Sci., v. 253, p. 433-461.

_______, 1956, Zircons in rocks: II. Igneous rocks: Amer. J. Sci., v. 254, p. 521-554.

Poldervaart, Arie and Hess, H. H., 1951, Pyroxenes in the crystallization of basaltic magma: J. Geol., v. 59, p. 472-489.

Ratté, J. C. and Steven, T. A., 1964, Magmatic differentiation in a volcanic sequence related to the Creede caldera, Colorado: U. S. Geol. Surv. Prof. Paper 475-D, p. D49-D53.

Ratté, J. C., Landis, E. R., Gaskill, D. L., and Raabe, R. G., 1969, Mineral resources of the Blue Range Primitive Area, Greenlee County, Arizona, and Catron County, New Mexico: U. S. Geol. Surv. Bull. 1261-E, 91 p.

Rhodes, R. C., 1968, Summary of the geology of the Mogollon Range, southwestern New Mexico: Arizona Geol. Soc. Guidebook III to Southern Arizona, p. 260-261.

Rittmann, A. and El-Hinnawi, E. E., 1961, The application of the zonal method for the distinction between low- and high-temperature plagioclase feldspars: Schweiz. Miner. Petrogr. Mitt., v. 41, p. 41-48.

Ross, C. S. and Smith, R. L., 1960, Ash-flow tuffs: their origin, geologic relations, and identification: U. S. Geol. Surv. Prof. Paper 366, 81 p.

Schmincke, H-U., 1967, Flow directions in Columbia River Basalt flows and paleocurrents of interbedded sedimentary rocks, south-central Washington: Geol. Rundsch., v. 56, p. 992-1020.

_______ and Swanson, D. A., 1967, Laminar viscous flowage structures in welded ash-flow tuffs from Gran Canaria, Canary Islands: J. Geol., v. 75, p. 641-664.

Shaw, H. R., 1965, Comments on viscosity, crystal settling, and convection in granitic magmas: Amer. J. Sci., v. 263, p. 120-152.

Smith, E. I., 1967, Criteria for the determination of flow direction in volcanic rocks: M.S. thesis, Univ. New Mexico (unpublished), 118 p.

_______ and Elston, W. E., 1967, Determination of flow direction of rhyolitic ash-flow tuffs and andesitic lavas from fluidal textures (abs): Geol. Soc. Amer., Program, 80th Ann. Meeting, New Orleans, Louisiana, p. 207.

Smith, R. L., 1960, Ash flows: Bull. Geol. Soc. Amer., v. 71, p. 795-843.

Stanton, R. L., 1967, A numerical approach to the andesite problem, I, II and III: Proc. Kon. Nederlandse Akad. Wetensch., ser. B, v. 70, p. 176-216.

Stearns, C. E., 1962, Geology of the north half of the Pelona quadrangle, Catron County, New Mexico: New Mexico Bur. Mines Min. Res. Bull. 78, 46 p.

Steven, T. A., 1968, Critical review of the San Juan peneplain, southwestern Colorado: U. S. Geol. Surv. Prof. Paper 594-I, 19 p.

Sun, M. S., 1957, The nature of iddingsite in some basaltic rocks of New Mexico: Amer. Min., v. 42, p. 525-533.

Szabo, E., 1968, Pennsylvanian paleotectonics of the Paradox region in parts of Utah, Arizona, New Mexico and Colorado: Ph.D. dissertation, Univ. New Mexico (unpublished), 144 p.

Tonking, W. H., 1957, Geology of Puertecito quadrangle, Socorro County, New Mexico: New Mexico Bur. Mines Min. Res. Bull. 41, 67 p.

Trauger, F. D., 1965, Geologic structure pattern of Grant County, New Mexico: New Mexico Geol. Soc. Guidebook 16 (Southwestern New Mexico II), p. 184-187.

Tuttle, O. F. and Bowen, N. L., 1958, Origin of granite in the light of experimental studies in the system $NaAlSi_3O_8$-$KAlSi_3O_8$-SiO_2-H_2O: Geol. Soc. Amer. Mem. 74, 153 p.

Van Bemmelen, R. W., 1961, Volcanology and geology of ignimbrites in Indonesia, north Italy, and the U. S. A.: Geol. Mijnb., 40c jaargang, p. 399-411.

Wargo, J. G., 1959a, Geology of the Schoolhouse Mountain quadrangle, Grant County, New Mexico: Ph.D. dissertation, Univ. Arizona (unpublished), 187 p.

_______, 1959b, Sequence of volcanic rocks in southwestern New Mexico (abs): Bull. Geol. Soc. Amer., v. 70, p. 1754.

Waters, A. C., 1960, Determining direction of flow in basalts: Amer. J. Sci., Bradley Vol., 258-A, p. 350-366.

Weber, R. H. and Willard, M. E., 1959a, Reconnaissance geologic map of Mogollon thirty-minute quadrangle: New Mexico Bur. Mines Min. Res. Geol. Map 10.

Wengerd, S. A., 1962, Pennsylvanian sedimentation in Paradox basin, Four Corners region: in "Pennsylvanian System in United States", Amer. Assoc. Petrol. Geol. Symposium, p. 264-330.

Willard, M. E., Weber, R. H. and Kuellmer, F. J., 1961, Reconnaissance geologic map of Alum Mountain thirty-minute quadrangle: New Mexico Bur. Mines Min. Res. Geol. Map 13.

Wisser, E., 1960, Relation of ore deposition to doming in the North American Cordillera: Geol. Soc. Amer. Mem. 77, 117 p.

Plate 2. Aerial view looking east down West Fork Gila River toward the central Gila Basin with the Black Range on the skyline. West Fork Gila River and its tributaries have incised several hundred feet below the pediment surface that slopes toward the center of the basin.

Plate 3. Volcanic mudflow in Big Dry Creek forming part of the avalanche deposits around the margin of the Bursum cauldron. Angular fragments of andesite and rhyolite are present in a matrix of Apache Spring Quartz Latite.

Plate 4. Photomicrograph of graphically intergrown quartz and alkali feldspar in a phenocryst in Apache Spring Quartz Latite. Groundmass is very slightly devitrified (X-nicols, x25).

Plate 5. Photomicrograph of Fanney Rhyolite showing phenocryst of plagioclase rimmed with alkali feldspar and set in a devitrified, spherulitic groundmass (X-nicols, x25).

Plate 6. Vertically flow-banded Fanney Rhyolite near Mogollon.

Plate 7. Cliffs of Bloodgood Canyon Rhyolite in West Fork Gila River, within the Gila Cliff Dwellings cauldron. At least three cooling units can be seen in the section of ash-flow tuff at this locality.

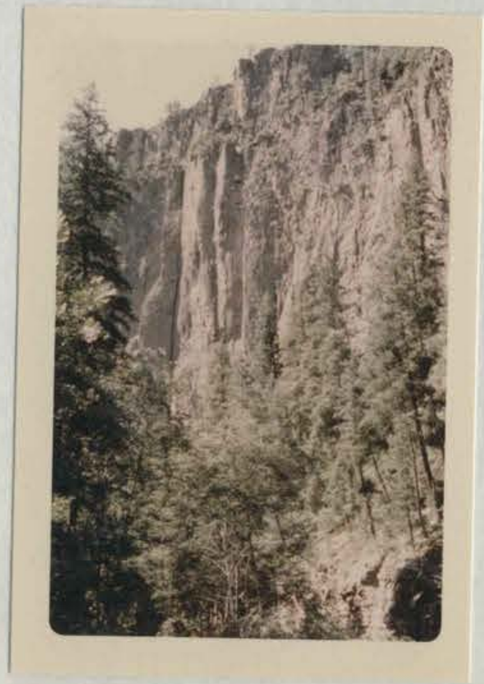

Plate 8. Photomicrograph of oriented thin section of Type I olivine-clinopyroxene basaltic andesite from the Bearwallow Mountain Formation. An olivine phenocryst, rimmed with iddingsite (black) is set in a medium-grained groundmass of plagioclase laths. This specimen yielded a significant preferred orientation (Tukey Chi-square 55.64, vector magnitude 0.40) (X-nicols, x25).

Plate 9. Photomicrograph of oriented thin section of Type II orthopyroxene-clinopyroxene andesite from the Bearwallow Mountain Formation showing porphyritic texture and strong flow lineation. Phenocrysts are of plagioclase and pyroxene (X-nicols, x25).

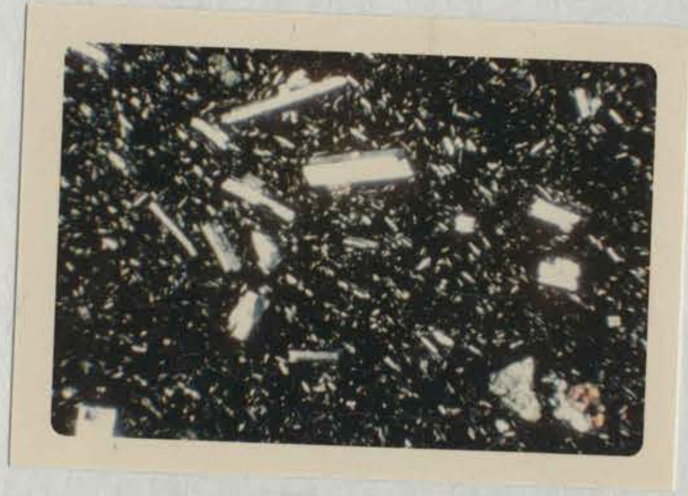

Plate 10. Photomicrograph of oriented thin section of Type III oxyhornblende-orthopyroxene latite from the Bearwallow Mountain Formation showing phenocrysts of oxyhornblende and plagioclase in an aphanitic groundmass. This specimen yielded strong preferred orientation (Tukey Chi-square 60.49, vector magnitude 0.36) (plane light, x25).

Plate 11. Photomicrograph of Type V biotite-clinopyroxene quartz latite from the Bearwallow Mountain Formation showing large phenocrysts of biotite and plagioclase in an aphanitic groundmass (X-nicols, x25).